TABLE I Elastic shear moduli

Metal	Transformation	M_s, °K	Reference	C_{44} x 10^{11}	$(C_{11}-C_{12})/2$, dynes/cm^2	T, °K	C/C′	Reference
Li	bcc–hcp	78	3, 5	1·08	0·116	78	9·3	6
Na	bcc–hcp	36	4	0·491	0·065	210	7·6	7
β-Sn	tet.–dc	286	—	2·20	0·645	300	3·4	8
γ-Fe	fcc–bcc	1 183	—	(9·7)	(1·15)	300	(8·5)	(see text)
Au–47·5%Cd	bcc–ortho.	323	10, 11	4·24	0·62	323	14·0	9
Au–50%Cd	bcc–ortho.	303	—	4·4	0·35	303	11·6	9
Fe–30%Ni	fcc–bcc	243	—	11·3	2·9	293	3·9	12
				(11·6)	(3·2)	293	(3·6)	*
Fe–18%Cr–12%Ni	fcc–bcc + hcp	215	2, 13	12·9	3·5	293	3·7	14

*Paramagnetic extrapolation

there is some question concerning their magnitude at the transformation temperature (1183°K). Also, γ-iron is paramagnetic at the transformation temperature and the iron–nickel alloys are ferromagnetic at the temperature of measurement. However, data are available for Fe–30%Ni over a range of temperature, including the paramagnetic state.[12] Extrapolation of these data to room temperature decreases the anisotropy ratio in Figure 2 from 3·9 to about 3·6, and correspondingly reduces the (extrapolated) anisotropy of γ-iron to perhaps 5 or 6. Nevertheless, in spite of the uncertainties, it appears that the anisotropy of γ-iron may be significantly large and the corresponding vibration amplitudes may make an appreciable contribution to the entropy and the stability of γ-iron at the high temperature where it appears. Certainly more extensive measurements should be made to evaluate the constants as a function of temperature (and composition) in both phases.

The temperature dependence of anisotropy is available for lithium,[17] sodium,[7] β-tin,[8] gold–cadmium,[9] and Fe–30%Ni.[12] Approaching the transformation from a high temperature (Figure 3) the anisotropy of lithium, sodium, gold–cadmium, and iron–nickel increases; the anisotropy of β-tin decreases. In the absence of a complete analysis of the relevant thermodynamic quantities for each phase it can only be observed, at this time, that in β-tin both anisotropy and temperature increase in the same direction and both, therefore, contribute directly to the stability of the high-temperature phase (β) relative to the diamond cubic structure stable below 286°K.

In the case of lithium and sodium the large absolute magnitude of the anisotropy of the bcc phase is evidently such that it more than compensates for the low temperature (about $\frac{1}{4}$ of the Debye temperature in both lithium and sodium) at which the transformation occurs.

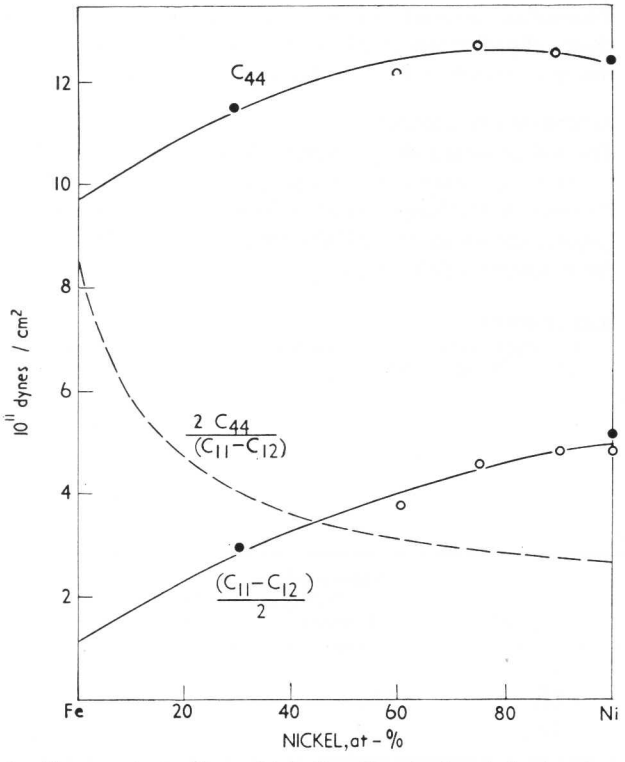

2 *Shear constants of iron–nickel alloys,*[16] *and extrapolation to γ-iron*

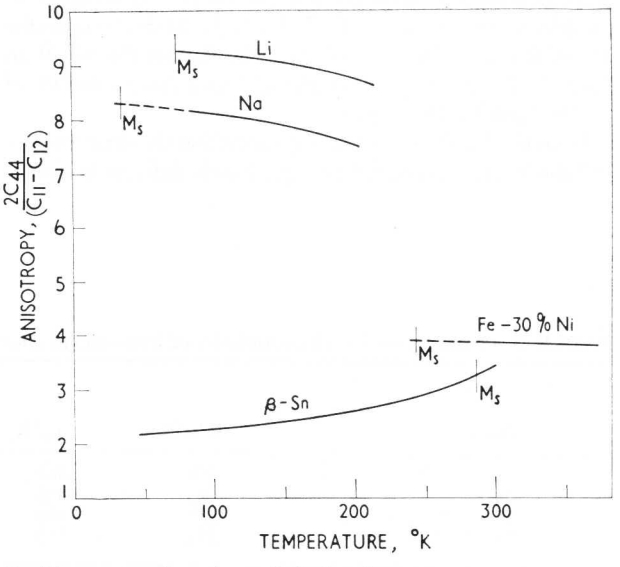

3 *Temperature dependence of elastic anisotropy*

TRANSFORMATION TEMPERATURE

In general, the transformation in the solid state does not occur at the equilibrium temperature T_0 at which the free energy of the two phases is equal, but at some lower temperature M_S. The extent of supercooling ($T_0 - M_S$) is determined by the requirement that the increasing free energy difference between the two phases must be at least equal to the sum of the energy associated with the elastic strain of the matrix in which the new phase is formed and the energy associated with the interface between the old and the new phases. If the change in specific volume is large, the volume change in the transformation of β-tin is 21·4%, and the work of plastic deformation will also have to be obtained from the free energy, requiring additional supercooling.

The applicability of these principles to the martensite transformation in iron–nickel alloys has been tested by Goldman and Robertson.[2,18] The elastic moduli (Young's modulus and the shear modulus) of polycrystalline austenite and martensite were measured[18] by resonant frequency methods (composite oscillator) in four different alloys which were chosen to represent a wide range of alloy behaviour with respect to the composition dependence of the transformation. That is, using Fe–30%Ni as a point of departure, cobalt raises the transformation temperature, carbon lowers it, and chromium both lowers the temperature and produces two transformation products (bcc and hcp). Furthermore, iron–nickel and iron–nickel–cobalt are ferromagnetic before and after transformation; iron–nickel–carbon and iron–nickel–chromium are paramagnetic before and ferromagnetic after transformation.

The M_S temperature was obtained by differential thermal analysis and change in resonant frequency with temperature. The equilibrium temperature T_0 was obtained from the relationship[19] $T_0 = \frac{1}{2}(A_S + M_S)$. The A_S temperature of the reverse transformation from martensite to austenite was obtained by high-temperature X-ray observation of the change in diffracted intensity from martensite.

The nickel content in each alloy was adjusted to bring the M_S temperature into the same range, below room temperature. To make comparisons between different alloys it is necessary to consider that the addition of 5·7%Co to Fe–31·3%Ni raises the M_S of this alloy by 70 degK; 0·26%C lowers the M_S of an Fe–21·5%Ni alloy by 150 degK; 15·1%Cr lowers the M_S of Fe–11·7%Ni by 450 degK.[15]

From the data in Table II it is apparent that the shear moduli, and also Young's moduli,[18] are significantly different in each of the four alloys. Measurements of the moduli in the ferromagnetic austenites in a saturating magnetic field of 1 600 oersteds demonstrated that the differences in moduli are not due to magneto-elastic effects of domain rotation but instead reflect real differences in cohesive properties of the four austenites.

For the purpose of the present discussion it is clear that the extent of supercooling ($T_0 - M_S$) required for the transformation process to begin increases as the moduli increase. This result is, of course, completely consistent with the idea that the matrix of austenite imposes an elastic (and plastic) restraint on the transformation which is overcome by a corresponding increase in the driving force, the free energy, which increases as the temperature falls below the equilibrium temperature.

The effect of adding cobalt to iron–nickel is especially notable since it is the one addition known to raise the M_S.[20] It now appears that the addition of cobalt also produces a significant decrease in the moduli and a corresponding decrease in the elastic restraint.

CONCLUSIONS

Considering the martensite transformation as a problem in lattice stability, it appears that elastic moduli may be used as a bridge between the (atomistic) cohesive properties of a metal lattice and the macroscopic thermodynamic quantities which determine the temperature and composition dependence of the transformation. At present very little is known about the crystal moduli of transforming phases but it seems possible to obtain the relevant information by an appropriate choice of alloys.

Knowledge of both the moduli and the thermodynamic quantities for a limited number of systems would provide the information necessary to construct a more comprehensive theory of such transformations, which would permit extrapolation and prediction of properties of new and untested alloys.

ACKNOWLEDGMENT

The author would like to express his thanks to the Fulbright Commission for the award of a Senior Research Fellowship, to Professor A. H. Cottrell for an invitation to spend a year in his Department at Cambridge University, and to Churchill College for an Overseas Fellowship.

REFERENCES

1. C. ZENER: 'Elasticity and anelasticity of metals,' 37; 1948, University of Chicago Press.

TABLE II Transformation characteristics of iron–nickel alloys[18]

Alloy	M_S,°K	T_0,°K	$(T_0 - M_S)$	Shear moduli x 10^{11} dynes/cm^2 at M_S Austenite	Martensite*
Fe–31·3%Ni–5·7%Co	258	463	205	5·2	5·0
Fe–30%Ni	243	453	210	6·5	5·5
Fe–25·1%Ni–0·26%C	217	488	271	7·5	6·5
Fe–11·7%Ni–15·1%Cr	215	533	318	8·4	—

*Modulus of martensite calculated from measured values of resonant frequency of austenite and the two-phase structures containing both austenite and martensite

2. A. J. GOLDMAN and W. D. ROBERTSON: *Acta Met.*, 1965, **13,** 391–401.
3. C. S. BARRETT: *Phys. Rev.*, 1947, **72,** 245.
4. C. S. BARRETT: *Acta Cryst.*, 1956, **9,** 671–677.
5. C. S. BARRETT: *J. Inst. Metals*, 1955–56, **84,** 43–46.
6. H. C. NASH and C. S. SMITH: *J. Phys. Chem. Solids*, 1958, **9,** 113–118.
7. S. L. QUIMBY and S. SIEGEL: *Phys. Rev.*, 1938, **54,** 293–299.
8. J. A. RAYNE and B. S. CHANDRASEKHAR: *ibid.*, 1960, **120,** 1658–1663.
9. S. ZIRINSKY: *Acta Met.*, 1956, **4,** 164–171.
10. L. C. CHANG and T. A. READ: *Trans. AIME*, 1951, **191,** 47–52.
11. L. C. CHANG: *Acta Cryst.*, 1951, **4,** 320–324.
12. G. A. ALERS *et al.*: *J. Phys. Chem. Solids*, 1960, **13,** 40–55.
13. J. F. BREEDIS and W. D. ROBERTSON: *Acta Met.*, 1962, **10,** 1077–1088.
14. G. BRADFIELD: *JISI*, 1964, **202,** 616.
15. L. KAUFMAN and M. COHEN: *Trans. AIME*, 1956, **206,** 1393–1401.
16. J. SAKURAI *et al.*: *J. Phys. Soc. Japan*, 1964, **19,** 308–310.
17. H. C. NASH and C. S. SMITH: *J. Phys. Chem. Solids*, 1958, **9,** 113–118.
18. A. J. GOLDMAN and W. D. ROBERTSON: *Acta Met.*, 1964, **12,** 1265–1275.
19. L. KAUFMAN and M. COHEN: 'Progress in metal physics' VII, 165–246; 1958, London, Pergamon.
20. R. B. G. YEO: *Trans. AIME*, 1963, **227,** 884–890.

H.K.D.H. Bhadeshia

Isothermal martensite kinetics in iron alloys

V. Raghavan, B.Sc., M.Met., Ph.D., and A. R. Entwisle, M.A., Ph.D.

SYNOPSIS

A brief survey of transformation kinetics in iron base alloys is given. Experimental work on the isothermal transformation behaviour of iron alloys containing 25·9%Ni and 2% Mn is described, with particular reference to the effect of austenite grain size. The early stages of transformation can be readily interpreted and lead to the conclusion that the nuclei responsible for transformation are uniformly distributed in the alloy, irrespective of grain size.

A phenomenological theory is introduced, based on the assumption that when a martensite plate forms, embryos are created in the surrounding austenite. These can then be thermally activated to give further transformation. This accounts satisfactorily for the main features of the observed transformation kinetics. 2637

INTRODUCTION

THE MARTENSITE TRANSFORMATION in iron base alloys shows three different types of kinetic behaviour.

Low-alloy steels with M_S above 100°C usually show 'athermal' behaviour, i.e. when austenite is quenched into a constant temperature bath transformation ceases within a very short time. The amount of transformation is essentially only a function of the temperature (neglecting stabilization effects). The transformation curves, Figure 1*a*, are similar for a wide range of steels.[1,2]

In iron alloys with M_S below room temperature two further types of behaviour are observed. Iron–nickel[3] and iron–nickel–carbon alloys,[4] for example, show discontinuous transformation curves, in which transformation is initiated by a 'burst' (Figure 1*b*). Other alloys, particularly iron–nickel–manganese alloys,[5,6] show completely isothermal transformation curves (Figure 1*c*). There is also abundant evidence that isothermal transformation is often associated with athermal and burst transformation in alloys with low M_S temperatures.

The understanding of these basic types is limited, being largely confined to the start of transformation M_S rather than the progress of the reaction after transformation has been initiated.[7] For example, with athermal kinetics, the effect of different alloying elements on M_S can be understood in terms of changes in the driving force for transformation. There is as yet no satisfactory method for predicting the slope of the transformation curve in the linear region, nor is it clear whether the gradual beginning of transformation is a significant feature. In burst transformations increasing nickel enhances the phenomenon in iron–nickel–carbon alloys, and chromium and manganese seem to have some inhibiting effect. There is no quantitative model which enables the size of the burst to be estimated. Similarly, for isothermal transformation, the early stages have been studied[6] but the progress of transformation has yet to be accounted for.

It is now generally accepted that martensite is nucleated heterogeneously, i.e. that the virgin austenite contains embryos which become operative and grow into macroscopic plates when the driving force is sufficiently large. For isothermal transformation some information about these pre-existing embryos has been obtained from a study of the earliest stages of transformation, and a quantitative model has been developed.

Shih *et al.*[6] determined the incubation period τ_i for the formation of 0·2% martensite in an alloy containing 23·2%Ni and 3·62%Mn as a function of temperature. They considered that the plates forming at the beginning of transformation derived from the most potent of the pre-existing embryos, requiring an activation energy ΔW for their operation. For a population n_i per cm³ of these embryos, the nucleation rate $\dot{N}$/cm³. s was expressed as

$$\dot{N} = n_i \nu \exp -(\Delta W/RT) \quad \ldots\ldots (1)$$

where ν is the lattice vibration frequency. Assuming that there were no autocatalytic effects during the incubation period

$$\dot{N}\tau_i v = 0{\cdot}002 \quad \ldots\ldots (2)$$

where v is the volume of a plate formed in the early stages. As a working hypothesis, n_i was taken to be 10^5/cm³ and values of ΔW calculated. ΔW was found to decrease steadily as the temperature of transformation was lowered.

Kaufman and Cohen[7] have developed the model of Knapp and Dehlinger[8] for an embryo, which they considered to be an

Both authors were at the Department of Metallurgy, University of Sheffield, when this work was carried out. Dr Raghavan is now at the Indian Institute of Technology, Kanpur U.P., India. (MG/Conf/73/65). UDC No. 669.15:669.112.227.346.2

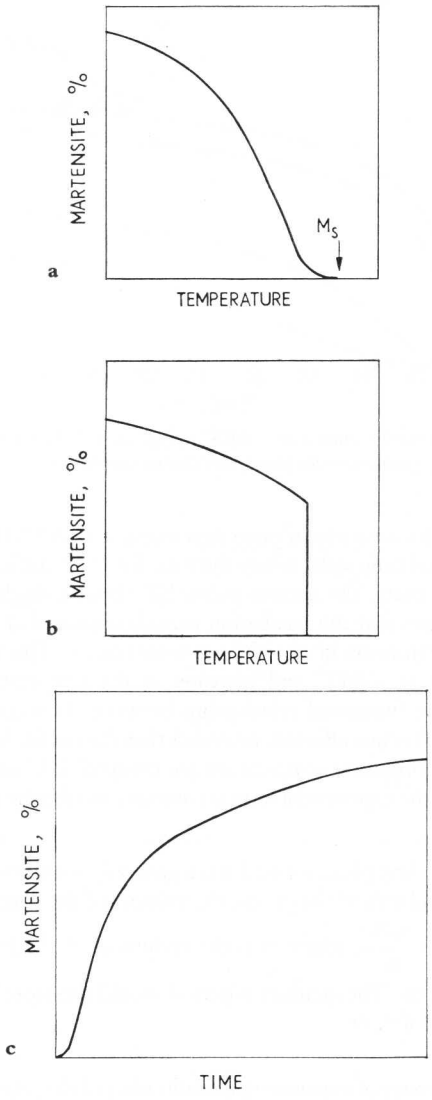

a athermal **b** burst **c** isothermal

1 *Schematic transformation curves*

oblate spheriod of martensite with an array of screw dislocation loops in the interface. They were able to show that the activation energy for the growth of such an embryo is

$$\Delta W = 4\times 10^{-2}\left(\frac{\sigma}{A}\right)^{\frac{1}{2}}\left(3\sigma r_e^{3/2}+\Delta f\left(\frac{\sigma}{A}\right)^{\frac{1}{2}} r_e^2\right) \text{ ergs}$$

where σ is the surface energy of the austenite/martensite interface, r_e is the radius of the embryo, A is a parameter related to the strain energy associated with the embryo and estimated to be $2{\cdot}1\times 10^{10}$ ergs/cm^3, and Δf is the free energy change accompanying the formation of unit volume of martensite.

Satisfactory agreement with the experimental values of ΔW was obtained for $r_e = 180$ Å and $\sigma = 160$ ergs/cm^2. The essential feature of this relationship is that the experimentally observed activation energies are proportional to the driving force. (Since Δf is negative ΔW decreases as the driving force increases, i.e. as temperature falls.) This has been confirmed[9] for a number of alloys with compositions close to that of those investigated by Shih *et al.*

The transformation accelerates because it is autocatalytic. It is presumed that when martensite plates form they create new embryos which are then available for further transformation. As the reaction proceeds the martensite plates formed at each successive stage are smaller (due to the partitioning of the austenite) and the number of embryos required to be activated to form unit volume of martensite increases. Thus it is not only necessary for any theory of the transformation to provide a copious supply of embryos, but it is also necessary to make allowance for the decreasing volume of transformation per embryo activated. A simple partitioning theory has been developed,[10] although it has not yet been confirmed by experiment.

Attempts have been made to rationalize martensite kinetics by assuming that athermal transformation is merely a rapid isothermal transformation.[11,12] This also accounts for those alloys in which an apparently athermal increment of transformation is immediately followed by an isothermal increment. Bursts are presumed to be the extreme form of autocatalysis in which the newly created embryos are immediately activated.

It has not yet proved possible to develop this hypothesis quantitatively, but if it has any real physical basis a more detailed study of isothermal transformation kinetics is necessary before any general quantitative theory can be formulated.

In the work described in this paper the effect of austenite grain size on isothermal transformation kinetics is studied, and a simple phenomenological theory is presented to account for the transformation curves observed.

Experimental

An iron–nickel–manganese alloy was melted in an induction furnace and cast as a 6 lb ingot. The chemical analysis was: 25·90%Ni, 1·94%Mn, 0·04%Si, 0·009%S, 0·013%P, 0·025% C, and 0·004%N. The ingot was forged and then hot rolled to $\frac{1}{2}$in diameter. After homogenization for 64 h at 1200°C the rods were cold swaged to 0·055in with various intermediate annealing treatments. In all cases the final amount of cold work was sufficient to cause recrystallization of the material during the austenitizing treatment used immediately before testing. Different grain sizes were established by using different prior thermal and mechanical histories for the specimens, but the final austenitizing treatment was maintained constant for any one group of tests. The range of grain diameters was relatively small (0·01–0·1 mm), but it seemed desirable to compare results only from specimens with the same final austenitizing treatment. The transformation behaviour was found to be very sensitive to grain size, and the range of sizes obtained gave rates of transformation within convenient limits for observation.

The progress of the isothermal martensite transformation was followed with a Kelvin double bridge by observing changes in resistance of the specimens maintained at constant sub-zero temperatures. Specimens $2\frac{1}{2}$in. long and 0·055in diameter were used, with electrical leads of 0·02in diameter nickel wire. The leads were spot welded onto the specimens and the composite specimens were electropolished and then sealed in evacuated silica tubes for the final austenitizing treatment. After this heat treatment the silica tubes containing the specimens were air cooled, this being sufficient to prevent decomposition of the austenite. After a further electropolishing

treatment, specimens were quenched to the required sub-zero temperature, and resistance was measured as a function of time. The low-temperature baths were usually maintained within 0·2 degC of the required temperatures.

The volume fraction of martensite was determined in several specimens by point counting after the resistivity runs. These values were used to calibrate the resistance changes. It was found that $\Delta R/R$ at 17°C was $\sim 4{\cdot}6\times 10^{-3}$ for 1% transformation. Grain size determinations were carried out on specimens in which transformation was stopped after a few per cent. The mean linear intercept was measured and twin boundaries were included in the counts since they act as barriers to martensite plates. Counts of between 200 and 300 boundary intersections were repeated in two or more areas of the specimens. The grain sizes established were nearly uniform, and variations in the mean linear intercept L in different areas of a specimen were usually within $\pm 5\%$ of the values reported below. All grain sizes are given in terms of the average spherical grain diameter d, which is calculated from the relationship $d = 1{\cdot}6485L$.[13]

An approximate value of the length to thickness ratio of the martensite plates was determined in 11 specimens of different grain sizes, taking an average of about 50 plates in each specimen. All these specimens were transformed about 7% so that the plates could be taken to be among the first formed. The values of the length to thickness ratios measured fell around 15. It was somewhat smaller for the finest grain sizes, although it was difficult to see a clear trend. Making an allowance for the fact that the average values determined from microsections relate to random sections of the plates, it was estimated that the true length to thickness ratio of the first formed plates, i.e. l/t was close to 20. This value was used for all the grain sizes in the range studied.

RESULTS

Groups of specimens were given austenitizing treatments for 5 min at 1000°C, 30 min at 900°C, or 30 min at 800°C, and the transformation behaviour was investigated at —66° and —78·5°C. In addition some further exploration of the temperature dependence was carried out using material with a constant grain size of 0·033 mm (30 min at 900°C). At least three curves were determined for each grain size and testing temperature in all three groups. Typical transformation curves are given in Figures 2 and 3. All these curves showed incubation periods followed by a region in which transformation accelerates rapidly, slowly dying away again at long times. Table I gives the average values of grain size and of incubation period (the time for 0·2% transformation).

To interpret the effect of grain size on incubation period equations (1) and (2) are combined

$$0{\cdot}002 = n_i \tau_i v\nu \exp -(\Delta W/RT) \quad \ldots\ldots (3)$$

This equation assumes that the rate of transformation is constant during the incubation period. In the present experiments the autocatalytic effect becomes significant before the transformation reaches 0·2%. Thus deviations from linearity occur in the earliest stages of transformation accessible to measurement. It was found, however, that the autocatalytic effects were almost identical for the different grain sizes studied. This is shown in Figure 4, where the early stages of transformation

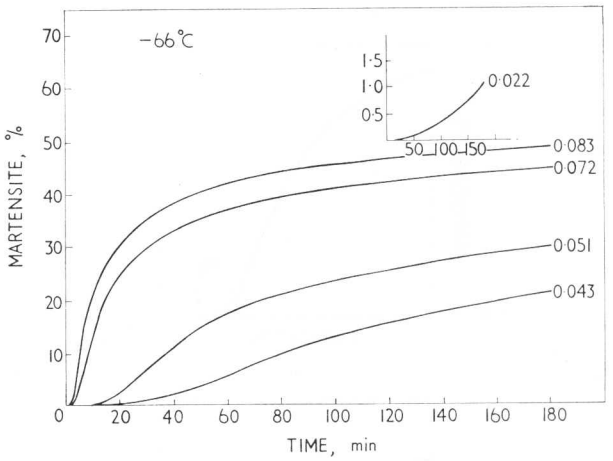

2 *Transformation curves at —66°C; final anneal 30 min 900°C; values of grain diameter (mm) indicated on curves*

are shown for a variety of grain sizes tested at —66°C. By using a normalized time scale, where the time for 1% transformation is taken as unity, the various points fall about a single curve. This indicates that the incubation periods measured at a given test temperature are in error by a constant factor. This factor is about two at —66°C and increases as the temperature decreases. The functional relationship between the variables in equation (3) is not affected, provided that the results from the same transformation temperature are compared. Under these conditions the exponential term is constant, and therefore

$$\tau_i \propto 1/v \quad \ldots\ldots (4)$$

Since the first plates formed were generally found to extend to the boundaries of the grains, the volume of the plate can be expressed as $\frac{\pi d^3 m}{6}$, where m is the reciprocal of the length to thickness ratio. The incubation period should therefore be proportional to d^{-3}, or

$$d \propto \tau_i^{-\frac{1}{3}} \quad \ldots\ldots (5)$$

The five groups of experimental results obeyed the relationship expressed by equation (5). The straight lines fitted by the least

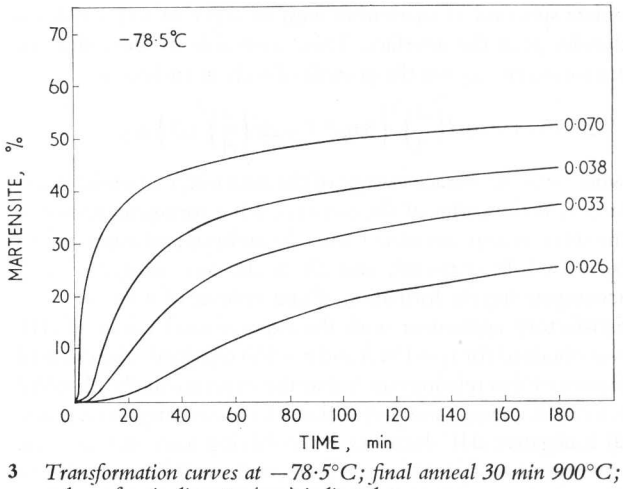

3 *Transformation curves at —78·5°C; final anneal 30 min 900°C; values of grain diameter (mm) indicated on curves*

TABLE I Values of grain size and incubation period related to heat treatment

Final heat treatment	Temperature of test, °C	Average grain diameter, mm	Mean incubation period τ_i, s	$(\tau_i)^{-\frac{1}{3}}$	Slope K, $mm^{-1}\,s^{-\frac{1}{3}}$
900°C 30 min	−66	0·020	8875	0·048	2·92
		0·022	7027	0·052	
		0·033	807	0·107	
		0·042	700	0·113	
		0·051	510	0·125	
		0·072	83	0·229	
		0·0835	69	0·244	
	−78·5	0·026	528	0·124	4·70
		0·033	284	0·152	
		0·038	123	0·201	
		0·070	31	0·318	
1000°C 5 min	−66	0·028	5800	0·056	2·10
		0·032	2875	0·070	
		0·041	1837	0·082	
		0·072	278	0·153	
	−78·5	0·029	777	0·109	4·49
		0·032	492	0·127	
		0·039	119	0·203	
		0·060	54	0·265	
800°C 30 min	−78·5	0·013	10800	0·045	5·69
		0·016	7320	0·052	
		0·020	597	0·119	
		0·024	138	0·194	
		0·035	105	0·212	
		0·059	36	0·303	

squares method all had correlation coefficients greater than 0·95, and in each case the origin was found to lie within the 90% confidence limits of the best fitting line. It is assumed that as the grain diameter tends to zero the incubation period should tend to infinite time. The origin was therefore taken as a fixed point and the best fitting straight line was recalculated to satisfy the condition that it should pass through the origin. These lines are shown together with the experimental points in Figures 5, 6, and 7, and the slopes of the lines K are given in Table I.

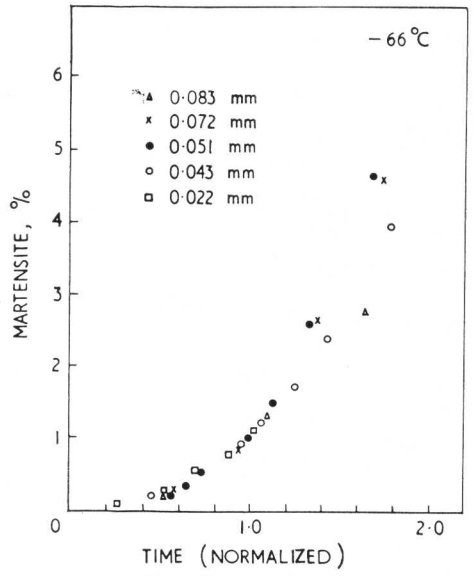

4 *Early stages of transformation at −66°C (normalized time); final anneal 30 min 900°C*

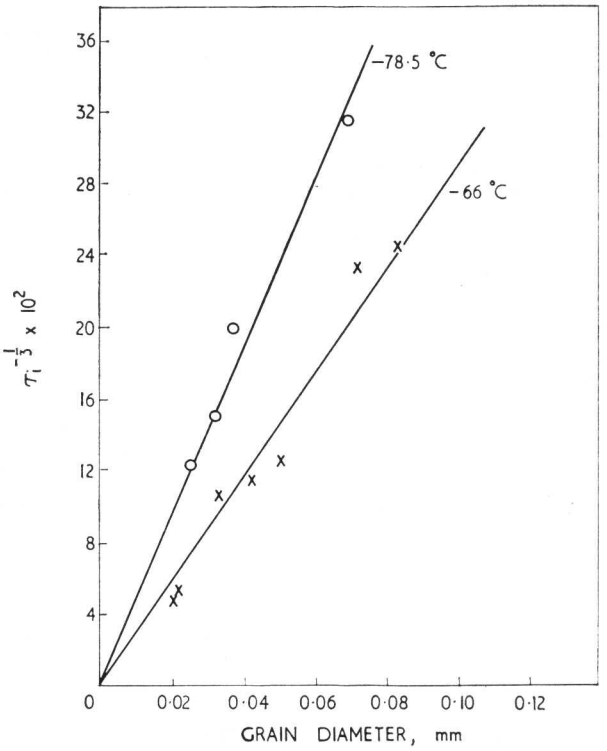

5 *Effect of grain diameter on $\tau_i^{-\frac{1}{3}}$; final anneal 30 min 900°C*

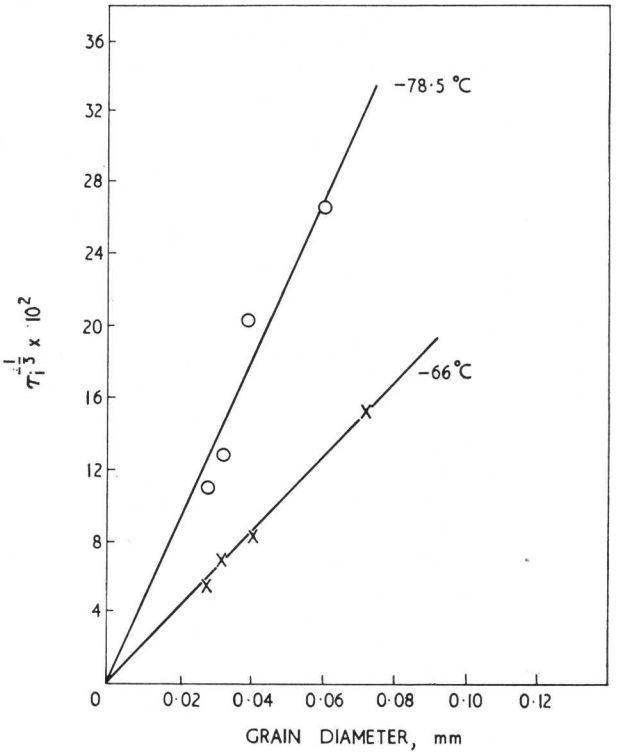

6 *Effect of grain diameter on $\tau_i^{-\frac{1}{3}}$; final anneal 5 min 1000°C*

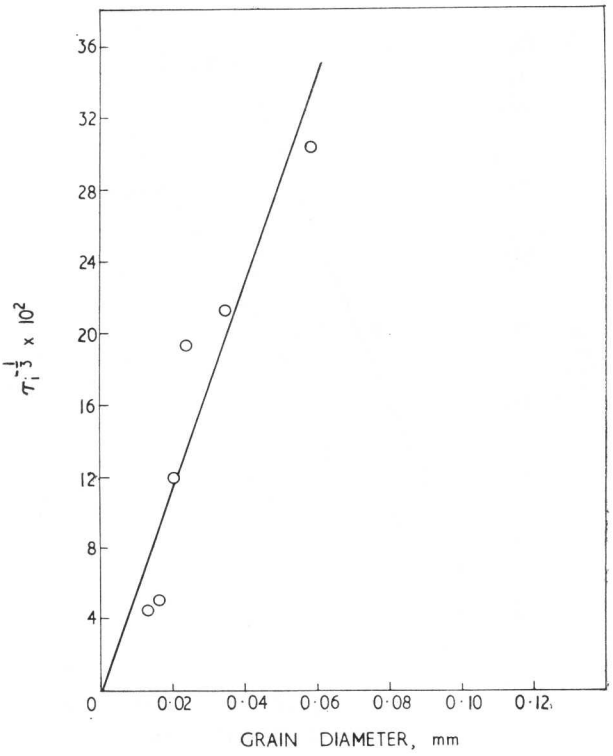

7 *Effect of grain diameter on* $\tau_i^{-\frac{1}{3}}$; *final anneal 30 min 800°C; −78·5°C*

The fact that the predicted relationship is so well confirmed by experiment is a clear indication that the number of pre-existing embryos per unit volume n_i is independent of the grain size. It is evident that the embryos are fairly uniformly distributed within the specimens and that grain boundaries and grain corners are not preferred nucleation sites.

From the gradients of the straight lines, the activation energy ΔW was calculated. For $m = 1/20$, and $\nu = 10^{13}$/s

$K = 5{\cdot}08 \times 10^4 \, [n_i \exp -(\Delta W/RT)]^{\frac{1}{3}}$

The value of n_i used in calculating ΔW was $10^7/\text{cm}^3$, and this value is justified below. The fact that the incubation periods measured were about a factor of 2–3 too low because of autocatalytic effects in the earliest stages hardly influences the value of activation energy. A more detailed discussion of the values of ΔW will be given in a later paper.

At very fine grain sizes (< 0·02 mm) the number of plates required to give 0·2% transformation becomes comparable with the initial population of embryos in the austenite, and a tendency was noted for specimens in this grain size range to give longer incubation periods than expected.

It is also to be noted that, if there is no change in the number of embryos with different austenitizing treatments, the values of K (Table I) should be the same at any one transformation temperature. Small differences in the slopes of the straight lines for different treatments were observed. Any detailed interpretation of this effect is not possible before the effects of austenitizing time and temperature are fully understood. However, it should be noted that the maximum deviation from the mean value of the slope at any one temperature would represent a deviation of about 50% in either of the quantities n_i or $\exp -(\Delta W/RT)$.

Considering the uncertainties involved, and the possible small chemical variations along the length of the forged bar, it does not seem safe to conclude that, for the austenitizing treatments used, there are appreciable changes in the number of most potent embryos.

Progress of transformation

The interpretation of the experimental results given above concentrates on the very early stages of transformation. In this section a phenomenological theory designed to account for the complete transformation curve is outlined.

The essential feature to be incorporated into a theory of the kinetics is the autocatalytic nature of the reaction. When a plate of martensite forms, the surrounding austenite is subject both to elastic and plastic strains. In this stress and plastic strain field it is assumed that new, autocatalytic embryos are created and that these are available for nucleating further transformation. In discussing the early stages of transformation only the most energetic embryos of the untransformed specimen (n_i/cm^3) were considered. It is now assumed that the number of autocatalytic embryos is proportional to the volume of transformation and that they require the same activation energy as the pre-existing embryos.

Considering one cubic centimetre of material at any time t, where the volume fraction of martensite is v, the total number of embryos n_t is given by

$$n_t = n_i + cv - N \qquad (6)$$

where c is the number of autocatalytic embryos produced during the formation of 1 cm³ of martensite and N is the number of plates in the volume of martensite v, i.e. the number of embryos that have been activated. Fisher *et al.*[10] have derived an expression relating the total number of martensite plates to the volume fraction of transformation, assuming a simple partitioning of the austenite by the martensite plates. They showed that

$$N = -\frac{1}{q}\left[\, 1-(1-v)^{\frac{1}{m}} \,\right] \qquad (7)$$

where q is the volume of an austenite grain and m is the thickness to length ratio of the martensite plates. Therefore

$$dv = mq\,(1-v)^{1+\frac{1}{m}}\, dN \qquad (8)$$

Since all embryos are assumed to require the same activation energy ΔW for their operation

$$dN = n_t\, \nu \exp -\left(\frac{\Delta W}{RT}\right).dt \qquad (9)$$

Combining (8) and (9)

$$dv = n_t\, \nu\, mq\,(1-v)^{1+\frac{1}{m}} \exp -\left(\frac{\Delta W}{RT}\right).dt$$

By putting $(1-v) = V$ and substituting for n_t from (6) and (7) this becomes

$$\nu \exp -\left(\frac{\Delta W}{RT}\right).dt = -\frac{1}{m} \cdot \frac{dV}{[1+qc+qn_i-qcV+V-\frac{1}{m}]V^{1+\frac{1}{m}}} \qquad (10)$$

To obtain the volume fraction of martensite as a function of time, this expression is integrated numerically using a digital computer.

When computing transformation curves numerical values must be assigned to the various parameters: q the grain volume is measured directly; m is the shape parameter of the martensite plate, t/l; $\nu \exp -\left(\frac{\Delta W}{RT}\right)$ is a scaling factor and may be determined from the incubation period ($V \rightarrow 1$) or, since some autocatalytic effects were present at 0·2% martensite, curves can be normalized to some convenient time (say that for 1% transformation) and the value of $\nu \exp -\left(\frac{\Delta W}{RT}\right)$ left temporarily unassigned; n_i the number of embryos present in the austenite before transformation begins has previously been taken to be $10^5/cm^3$.[6] This value seems too low in view of the results presented above relating to the effect of grain size on the incubation period. The work of Cech and Turnbull[14] on the transformation behaviour of small particles of an Fe–30%Ni alloy has shown that the probability of transformation in a particle changes markedly as the particle diameter falls from 70 μm to 30μm. Taking a mean value of 50μm and assuming that one embryo is enclosed within such a particle indicates that n_i is about $10^7/cm^3$. The only freely disposable parameter is c, the number of autocatalytically produced embryos per unit volume of transformation to martensite.

Transformation curves were therefore calculated with $m = 1/20$, $n_i = 10^7$, and the appropriate value of q and a range of values of c. These were then normalized to a time corresponding to a fixed amount of transformation and compared with similarly normalized experimental transformation curves. Figure 8 shows a typical example of this procedure, where the time scale is normalized to the time for 4% transformation. The curves for $c = 10^{12}$ and 10^{10} (A and C respectively) are clearly different from the experimental result, but curve B ($c = 5 \times 10^{10}$) agrees closely up to about 4% transformation. Curve D ($c = 5 \times 10^{10}$) is calculated making an empirical correction for the fact that, as transformation proceeds, the smaller martensite plates are relatively thicker than those formed in the early stages. Metallographic observations indicate that taking $\frac{1}{m} = 4 + 16V$ makes a reasonable allowance for this effect, although it is probably not accurate when transformation tends to completion. The correction is negligible below 4% transformation. All further calculated curves include this correction. Satisfactory agreement between the experimental results and the theoretical prediction is obtained up to nearly 10% transformation; thereafter the predicted curve falls below the experimental one.

The shape of the normalized curves is rather sensitive to the value of the autocatalytic parameter c. Figure 9 shows the early stages of transformation corresponding to Figure 8. The experimental results fall between the curves for 5×10^{10} and 10^{11}. In most cases it was possible to assign a value of c to an experimental curve with an uncertainty of a factor of two. Experimental scatter between repeat experiments was the limiting factor controlling the precision of the estimates of c for a given set of experimental conditions.

The most encouraging feature of the model is its ability to account for the effect of grain size. Figure 10 shows the predicted and experimental results for specimens of different grain size tested at −66°C (see also Figure 2). All the theoretical curves have been computed using the same value of the autocatalytic parameter, i.e. $c = 2 \times 10^{10}$, and the same value of the scaling factor, $\nu \exp -\left(\frac{\Delta W}{RT}\right)$. Agreement is satisfactory up to about 10% transformation. Figure 11 gives the situation in more detail, showing the excellent fit in the early part of the transformation. Experimental curves from the other groups of specimens listed in Table I confirm this result; the same kind of agreement with the theoretical prediction is obtained, provided a value of c and of $\nu \exp -\left(\frac{\Delta W}{RT}\right)$ is selected appropriate for the whole group.

The effect of temperature on the transformation curve (at a fixed grain size) can also be encompassed within the theory, but in this case separate values of c and $\nu \exp -\left(\frac{\Delta W}{RT}\right)$ must be used for each curve. Figure 12 shows a set of curves indicating the effect of temperature with a constant grain size.

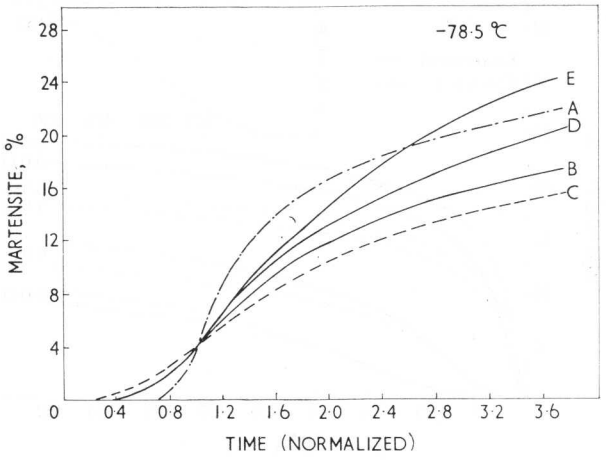

A $c = 10^{12}$; *B* $c = 5 \times 10^5$; *C* $c = 10^{10}$; *D* $c = 5 \times 10^{10}$

8 *Computed transformation curves for various values of autocatalytic parameter* c *with empirical correction for value of* m; *the experimental curve E is for −78·5°C, final anneal 30 min 900°C; all curves normalized taking the time for 4% transformation as unity*

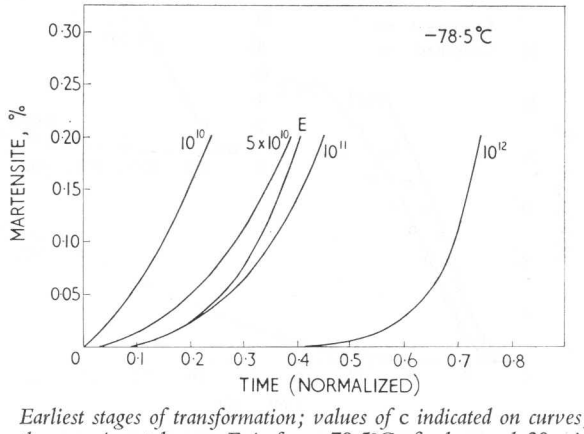

9 *Earliest stages of transformation; values of* c *indicated on curves; the experimental curve* E *is for −78·5°C, final anneal 30 min 900°C; all curves normalized*

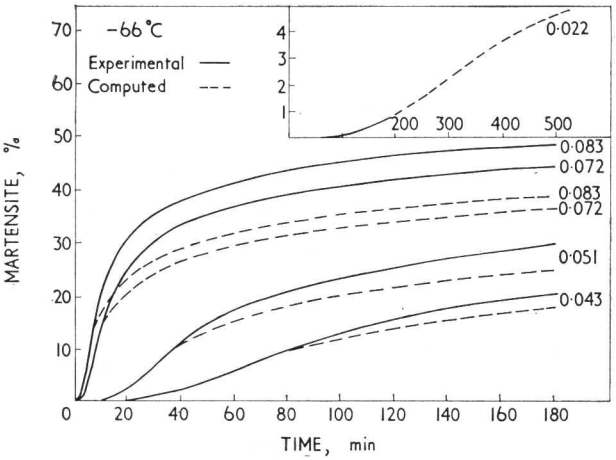

10 *Comparison of experimental transformation curves with those computed for* $c=2\times10^{10}$*; final anneal 30 min 900°C, tested at −66°C; values of grain diameter (mm) indicated on curves*

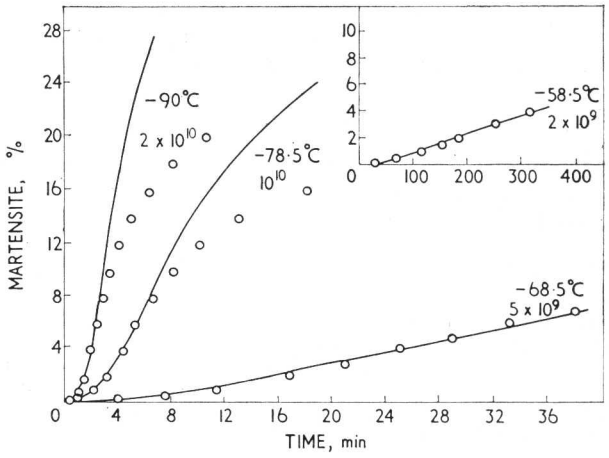

12 *Experimental curves (full lines) at different temperatures; computed values (points) for values of c as indicated; grain diameter 0·033 mm*

The agreement of the calculated transformation curves with the experimental curves and the particularly striking agreement found in the initial stages for a set of grain sizes at a given temperature, together with the systematic trend in the value of c with temperature, lend strong support to the model proposed.

Two features of the results presented earlier in the paper are readily understood in terms of the model. The linear relationship between $\tau_i^{-\frac{1}{3}}$ and the grain diameter d was obeyed even though some autocatalysis was present at 0·2% transformation. This arises because at a given transformation temperature (in this alloy) there is a unique value of the autocatalytic parameter c. This parameter controls the shape of the normalized transformation curves, which are hardly influenced by the grain volume q (provided q is not too small). Thus, as indicated in Figure 4, provided the normalized transformation curves are identical for a given test temperature, the relationship between incubation period and grain size will still be obeyed in the non-linear parts of the curves. It should be noted that for a given group of specimens tested at the same temperature the normalized curves, both experimental and theoretical, were hardly distinguishable below 10% transformation.

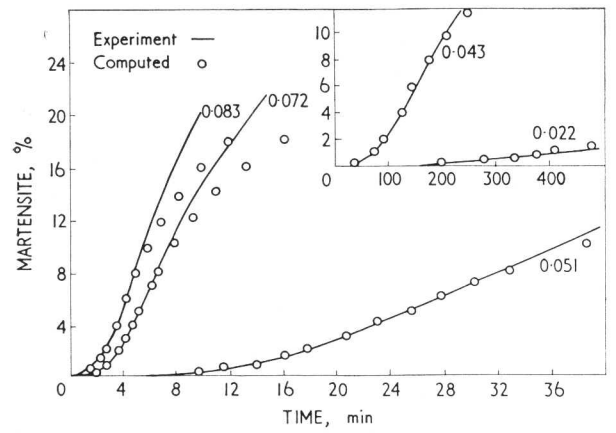

11 *As for Figure 10; the curves are experimental, the points are computed values*

It was also found that for very fine grain sizes ($d<0·02$ mm) the experimental points tend to deviate from the linear relationship between $\tau_i^{-\frac{1}{3}}$ and d. For example, the observed incubation periods at $d=0·013$ mm were found to be a factor of five greater than predicted by equation (5). The computed transformation curves confirm this deviation, which arises essentially because the number of plates required to give 0·2% transformation becomes comparable with n_i.

DISCUSSION

With the theory presented above, it has been possible to account for the isothermal transformation kinetics observed in an iron–nickel–manganese alloy by the use of one freely assignable parameter c. This represents the number of autocatalytic embryos created by the formation of unit volume of martensite. All the other parameters are directly observable (at least in principle). The grain volume q and the plate shape parameter m are readily measured; n_i must lie within the limits set by experiments such as those of Cech and Turnbull and those set by the deviations from the relationship between grain diameter d and incubation period $\tau_i^{-\frac{1}{3}}$; the scaling factor $\nu \exp -\left(\frac{\Delta W}{RT}\right)$ in principle can be determined from the beginning of transformation, and an upper limit to its value can easily be determined.

The autocatalytic parameter c increases steadily as the temperature of transformation decreases, which is consistent with the view that embryos will be more readily created as the driving force for transformation increases. The numerical values of c at −80°C indicate that the first plates forming at a grain diameter of 10^{-2} cm create about 200 embryos per plate. This relatively large number shows that embryo formation is a common occurrence during transformation, and it seems likely that some dislocation mechanism of the type recently suggested by Dash and Brown[15] would be required to account for them.

There is a discrepancy between the values of c used in the curves in Figures 11 and 12. The experimental results from the two groups of specimens are consistent within themselves, but

a rather larger value of c is needed in the tests at −66°C (Figure 11) than that indicated in Figure 12. The two groups of specimens derive from different parts of the original ingot, and it seems likely that the discrepancy derives from small differences in chemical composition.

The main difference between experimental and computed transformation curves occurs when the transformation begins to decelerate. There are several possible reasons for this. The partitioning formula relating volume of transformation to the number of plates has not yet been confirmed experimentally. The assumption that all embryos have the same potency is probably too naive; if a spectrum of activation energies is present the less potent embryos formed in the early stages could make an important contribution to transformation at a later stage. The plate shape parameter m could also affect the shape of the transformation curve if the empirical variation with V is seriously in error.

These points, together with an extension of the present theory which accounts for 'athermal' transformation as a rapid isothermal reaction, will be considered in a further paper.

CONCLUSIONS

1. In the alloy studied the isothermal transformation curves were found to be very sensitive to changes in grain size. The incubation period (for 0·2% transformation) varied inversely with the cube of the grain diameter. This relationship gives a clear indication that the pre-existing embryos in the austenite are uniformly distributed and are not located at special sites in the grain boundaries. The number of these embryos was estimated to be $10^7/cm^3$.

2. The progress of transformation can be quantitatively accounted for by a simple phenomenological theory. It is assumed that, when a martensite plate forms, embryos are created in the surrounding austenite which are then available to be activated to give further transformation.

For a given temperature of transformation there appears to be a unique value of the parameter c, the number of autocatalytic embryos produced per unit volume of transformation. The parameter c increases as the transformation temperature decreases, i.e. the autocatalytic effects increase with increasing driving force.

ACKNOWLEDGMENTS

The authors would like to thank Professor A. G. Quarrell for the provision of laboratory facilities and Mr A. Brownrigg for helpful discussions at various stages in the work. Thanks are also due to the Ministry of Scientific Research and Cultural Affairs, Government of India, and to the Association of Universities of the British Commonwealth, for the provision of a scholarship for one of the authors (V.R.).

References

1. M. Cohen: 'Phase transformations in solids'; 1951, New York, Wiley; London, Chapman and Hall.
2. W. Steven and A. G. Haynes: *JISI*, 1956, **183,** 349–359.
3. E. S. Machlin and M. Cohen: *Trans. AIME*, 1951, **191,** 744.
4. R. Brook and A. R. Entwisle: *JISI*, 1965, **203,** September.
5. G. V. Kurdjumov and O. P. Maksimova: *Doklady AN SSSR*, 1950, **73,** (1), 95.
6. C. H. Shih *et al.*: *Trans. AIME*, 1955, **203,** 183–187.
7. L. Kaufman and M. Cohen: 'Progress in metal physics', **7,** 165; 1958, London, Pergamon.
8. H. Knapp and U. Dehlinger: *Acta Met.*, 1956, **4,** 289–297.
9. A. R. Entwisle: to be published.
10. J. C. Fisher *et al.*: *Trans. AIME*, 1949, **185,** 691–700.
11. J. Philibert and C. Crussard: *JISI*, 1955, **180,** 39–48.
12. G. V. Kurdjumov: *JISI*, 1960, **195,** 26–48.
13. B. S. Lement *et al.*: *Trans. ASM*, 1954, **46,** 851–881.
14. R. E. Cech and D. Turnbull: *Trans. AIME*, 1956, **206,** 124–132.
15. S. Dash and N. Brown: Third European Regional Conference on Electron Microscopy, 179; 1964, Prague, Czechoslovak Academy of Sciences.

Stabilization effect in a high-carbon nickel steel

R. Priestner and S. G. Glover

SYNOPSIS

If the martensitic reaction in a 1·43%C–5%Ni steel with an M_s at room temperature is interrupted by arresting the sub-zero cooling and aging at a slightly elevated temperature, then on subsequent recooling the transformation recommences at a temperature which may either lie below that to which the steel was first cooled, displaying the widely observed stabilization effect, or appreciably above this temperature. The mechanism of the aging process is a reversible one in that the transformation behaviour of a specimen given a succession of aging treatments assumes that characteristic of the latter.

The detailed relationship between aging treatment and subsequent reaction behaviour has been obtained and the type of process which could account for it is discussed. Reference is made to results on the strain aging of high-nickel austenites. 2612

INTRODUCTION

IF the athermal martensite reaction in steels is arrested by interrupting the cooling, then, on the subsequent resumption of cooling, the reaction does not recommence until a temperature appreciably below that of the arrest is reached. This stabilization of the untransformed austenite is of practical interest in tool and bearing steels, the high carbon and alloying element content of which lowers M_S sufficiently to result in a significant amount of retained austenite at room temperature. Only by sub-zero cooling can the optimum hardness and mechanical stability be realized. The stabilization effect is of interest also, however, as a means of altering the course of transformation. Despite great success in understanding other aspects of the martensitic reaction, notably the morphological and crystallographic features, the manner in which the transformation progresses with falling temperature is only vaguely understood.

Stabilization can also affect the isothermal formation of martensite, the rate of reaction at a constant temperature being reduced by interceding an aging treatment at some higher temperature. Philibert[1] made the important observation that the isothermal reaction in an iron–nickel alloy was susceptible to stabilization only if the alloy contained small amounts of carbon or nitrogen. In a later paper,[2] it was shown that in high-carbon chromium steels an isothermal mode of transformation could be revealed by inhibiting the normal athermal reaction by a stabilization treatment. There is no evidence that the mechanism of stabilization is different for the two modes of transformation, which is not surprising since there appears to be no mechanistic distinction between the two types of reaction, the difference in kinetics being ascribed to a variation from one system to another of the temperature dependence of the nucleation rate. For this reason, the present work has been confined to the study of the effect of stabilization on the athermal reaction.

The measure of stabilization is taken to be the temperature interval θ between the temperature to which the specimen is first quenched T_q and that at which transformation recommences, M'_s, on subsequent cooling after aging for a period t_a at T_a. Of the many studies of the phenomenon, a few have isolated the individual effects of variations in T_q, t_a, and T_a on θ. T_q determines the amount of martensite present during the aging treatment which causes stabilization and, despite a few reports to the contrary, θ depends strongly on martensite content so that θ is zero when $T_q = M_S$ and increases as T_q is decreased. The effects of the duration and temperature of aging are complex and it is by studying the variation of θ with t_a at various aging temperatures (T_a) that much can be learnt of the stabilization process. In an unalloyed steel[3] of similar carbon content to the nickel steel used here, θ increased progressively with t_a at $T_a = 26°C$. At higher temperatures θ increased more rapidly with t_a but reached peaks below the 26°C curve and subsequently decreased. The course the transformation took when it recommenced at M_s' also varied with the conditions of aging, bursting being favoured by a low aging temperature and a short time. As first observed by Edmondson[4] in a nickel steel, the stabilization process was reversible in the sense that a sequence of aging treatments resulted in a value of θ and subsequent transformation behaviour characteristic of the final treatment.

Dr Priestner is at the National Physical Laboratory, Teddington, Middlesex, and Dr Glover is at the Department of Physical Metallurgy, Birmingham University. (MG/Conf/74/65). UDC No. 669.15'24–194: 669.112.227.346.2

This description of stabilization appears to be widely applicable to steels and provides a sufficiently clear definition of the problem to permit an attempt at its explanation. An anomaly has been observed,[5] however, in a 1·5%C–5%Ni steel where the effect of what in other steels would be a stabilization treatment leads instead to an enhancement of transformation. Here martensite forms initially as rims on existing plates and later as new plates at a temperature *above* T_q. The present work examines this observation further and relates it to the pattern of stabilization found in other steels.

EXPERIMENTAL

A steel of the following analysis was supplied by the International Nickel Co. Ltd, in the form of 1in diameter forged bar: 1·43%C, 4·85%Ni, 0·48%Si, 0·49%Mn, 0·05%Cr, 0·01%V. It was homogenized, swaged to 0·08in diameter, and cut into specimens 0·16in long weighing about 0·1 g. These were sealed individually in evacuated silicon capsules, austenitized at 1190°C for 20 min, and quenched to 0°, —30°, or —70°C, to form 15%, 30%, and 50% martensite, respectively. The specimens were then reheated and held for 30 s to 3 months at 26°, 50°, 68°, and 100°C, after which they were transferred to a magnetic balance and quickly cooled. From the force exerted on the specimen by the field gradient the martensite content was readily calculated; pure iron provided a standard and the saturation magnetic intensity of the martensite was derived from values listed by Hoselitz.[6] The force, measured by the distortion of a proving ring, was recorded either photographically or, more recently, by means of a transducer, the signal from which was amplified and fed to a chart recorder. Both systems gave an accuracy estimated as 1% martensite and were sensitive to 0·1% changes in martensite content.

RESULTS

To establish the normal progress of transformation, a number of specimens were quenched to 60°C, transferred to the magnetic balance at that temperature, and cooled continuously to —70°C. There was some scatter in the progress curves, the limit of which is indicated by the broken lines in Figure 1. Transformation started with a burst (M_b) varying from 12°C to 17·5°C; the amount of martensite formed in the burst varied between 10% at the upper limit of M_b to 20% at the lower limit. Following the burst there was a temperature interval during which no martensite formed, this plateau extending from M_b to —1°C irrespective of the value of M_b. At —1°C transformation recommenced and the subsequent curve was linear down to —70°C.

The linear part of all curves converged towards a common point. Thus it was possible to construct a 'probable' normal transformation curve for any sample whose martensite content had been determined after quenching to a known temperature, simply by drawing a straight line from —1°C through the coordinates representing the quenched sample and the point of convergence. This proved useful in determining where the transformation curve after stabilization lay with respect to the normal curve.

The mode of transformation after stabilization varied markedly with the aging treatment and the amount of prior martensite. With an initial martensite content of 15% there was a pronounced tendency to bursting (Figure 2), bursts occurring after all aging treatments. An invariable feature of the transformation following stabilization at this martensite level was that the bursts were so large as to bring the martensite content to a value exceeding that indicated by the normal curve. The amount of martensite formed during the burst varied with M_s, increasing as M_s decreased (Figure 2*b*). As θ decreased again after longer aging periods the height of the burst also decreased (Figure 2*c* and *d*). A burst at M_s was often followed by a plateau (Figure 2*c*) but sometimes the transformation curve continued from the top of the burst in a straight line lying above and roughly parallel to the normal curve. After aging for 5 h at 100°C the burst was preceded by a 'tail' of transformation at M_s, which was then above T_q (Figure 2*e*).

With 30% of pre-existing martensite, the tendency to bursting was greatly reduced, as manifested in the occurrence of 'slow' bursts at M_s. In a slow burst a large quantity of martensite is formed within a temperature interval of less than ½ degC, and the martensite content of such samples recovered to above the normal transformation curve (Figure 3*a*). After longer aging

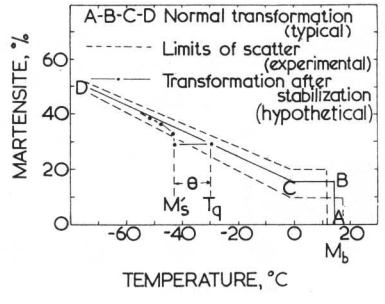

1 *Progress of normal transformation and transformation after stabilization*

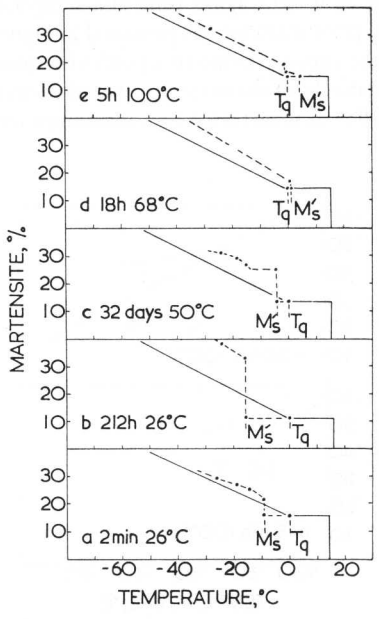

2 *Transformation after stabilization; 15% initial martensite content*

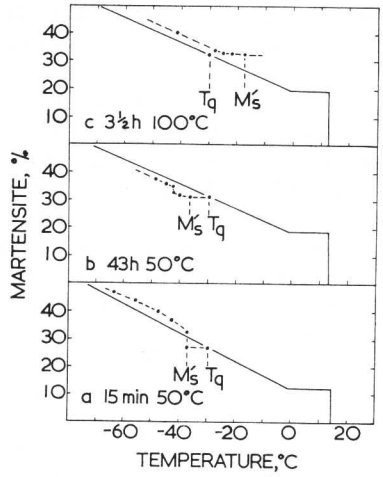

3 *Transformation after stabilization; 30% initial martensite content*

at 50°C, 68°C, and 100°C the bursts were preceded by tails of transformation more readily than at the 15% martensite level, and were reduced in height; the transformation curve then lay below the normal curve (Figure 3*b*). Eventually θ became negative, bursts disappeared, and the transformation curve after stabilization returned to above the normal curve (Figure 3*c*).

Bursts did not occur at all during transformation following aging at the 50% level of prior martensite. However, transformation below Ms was still most rapid after aging at the lower temperatures, when the transformation partially recovered towards the normal curve. After aging at 100°C, however, the curve for subsequent transformation lay essentially parallel to and below the normal curve (Figure 4*a*). For the lower martensite levels, with progressive aging at the high temperatures, transformation eventually recommenced above T_q (Figure 4*b*).

Time and temperature dependence of θ

The variation of θ with aging time and temperature at the three levels of prior martensite is presented in Figures 5–7. It is evident that the curves relating to a particular aging temperature are qualitatively of the same shape at all martensite levels. The value of θ at first increased to a maximum and then, for

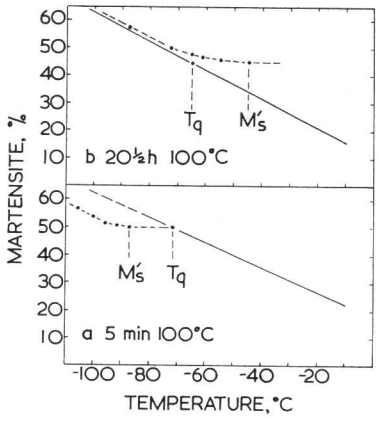

4 *Transformation after stabilization; 50% initial martensite content*

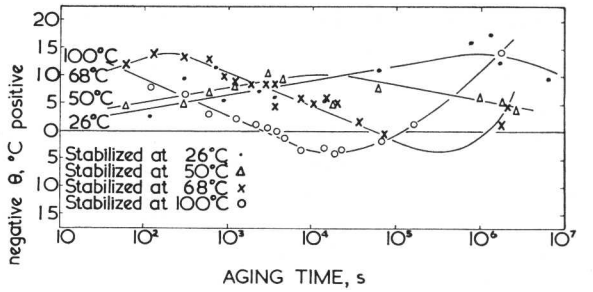

5 *Variation of the degree of stabilization with time of aging; 15% martensite*

temperatures above 50°C, decreased until θ eventually became negative. The curves then passed through a minimum and started to increase again. At 100°C θ reached its maximum value in less than 60 s. The maxima of the 68°C and 50°C curves are at progressively longer times and are well defined at all martensite levels. That of the 26°C curve, on the other hand, is uncertain because of the scatter obtained in the values of θ. However, it appears that after aging for 3 months at 26°C the degree of stabilization is decreasing. The minima of the 100°C and 68°C curves have been established, but longer times are required for the 50°C curves. Presumably θ would show a minimum at 26°C if aging were continued for a sufficient length of time.

The maximum degree of stabilization at a particular martensite level is roughly the same for all aging temperatures, and is the same with 30% of prior martensite as with 15%. At the 50% martensite level the maximum θ is double that at the 30% level. The maximum degree of negative stabilization increases with increasing martensite content, but any variation with temperature is uncertain.

Correlation with the growth of rims

The incidence of negative stabilization is evidently associated with the growth of martensite rims, the earlier observation of which initiated this investigation. After aging a 15% martensitic specimen at 100°C for 1½ h, rims were observed to form at 10–12 degC above the original quenching temperature,[5] whereas the transformation curve after a similar aging treatment indicated that Ms was 4 degC above T_q (Figure 7). This apparent discrepancy is resolved by considering the relative sensitivities of the two methods of observation. Metallographic

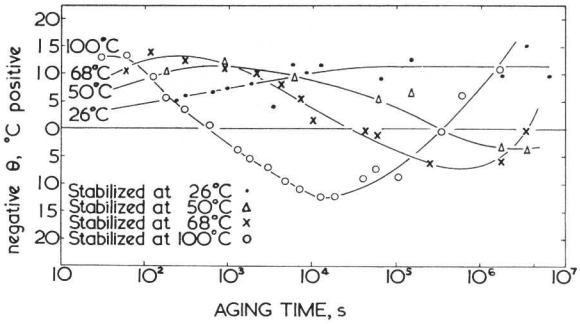

6 *Variation of the degree of stabilization with time of aging; 30% martensite*

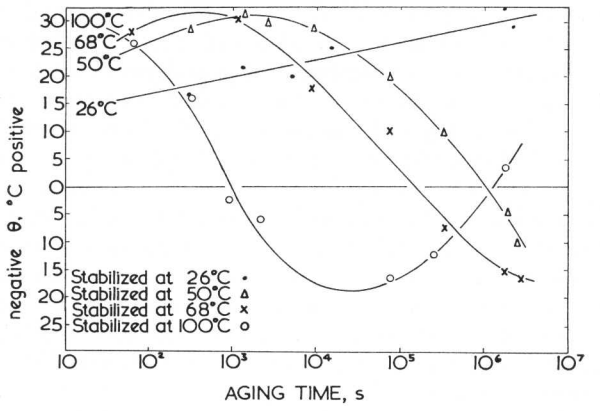

7 *Variation of the degree of stabilization with time of aging; 50% martensite*

measurements indicate that the volume of a martensite rim is, at most, 6–7% of the volume of the parent martensite plate. In order that the magnetic balance, which is sensitive to a change of total martensite content of 0·1%, will detect rims of this size in a sample containing 15% of martensite, it is necessary for every tenth martensite plate to have a rim associated with it. The actual distribution of rims after cooling the above sample to 10 degC above T_q was roughly one to every thirty plates of martensite. By the same argument the increase in the maximum degree of negative stabilization with martensite content, as measured by the magnetic balance, is at least partly due to the increased number of sites available for the formation of rims.

DISCUSSION

An immediate conclusion is that the enhancement of the transformation brought about by certain aging treatments in this particular alloy falls neatly into the general pattern of stabilization kinetics. Thus the curves of Figures 5, 6, and 7 can be regarded as exaggerated forms of the corresponding curves for a plain carbon steel[3] where θ decreases, after passing a peak, but does not become negative. The final increase in θ after aging at the higher temperatures is associated with the formation of bainite during the aging treatment, the bainite growing as an envelope around the martensite plates as previously observed. This is not regarded as a stabilization effect in the accepted sense of the term and so the increasing branch of the θ curve will not be considered further. It is necessary to explain, therefore, the form of θ–time curve in which θ rises to a peak and then falls, eventually becoming negative. Increasing the aging temperature serves primarily to accelerate the process, the peak being attained earlier. The influence of aging conditions on the continuation of the reaction at M_s can be summarized by stating that the amount of martensite formed per unit fall in temperature decreased with increasing prior martensite and with increasing time and aging temperature. In particular, for θ–time curves showing a peak, specimens could be chosen having identical θ values; here, those aged for times less than the peak transformed more rapidly than those aged beyond the peak, in which stabilization was more permanent.

Evidence is accumulating that the martensitic reaction is controlled to a significant extent by the plastic properties of the austenite. Plastic deformation of the fcc phase in iron–nickel alloys depresses M_s for the athermal martensite reaction whether the deformation is produced by an external stress[7] or by previous reaction cycles.[8,9] The latter is known to cause a large increase in yield strength,[9] as will the bulk plastic deformation of a polycrystalline specimen. Although the work hardening of a single crystal deformed in tension may be negligible,[7] its resistance to any subsequent arbitrary deformation will, of course, be increased. Neutron irradiation also lowers M_s in iron–nickel alloys[10] and there would presumably also be a hardening effect here, though no mechanical tests were made. A variation in the M_s of an alloy steel has been related to the changes in the substructure of austenite produced by altering the austenitizing treatment[11] and here too there promises to be significant correlation between M_s and the yield strength of the austenite.[12]

Since a macroscopic shear strain of about 0·2 is involved in the formation of a crystal of martensite in iron–nickel alloys and high-carbon steels, the austenite in the vicinity must suffer a plastic accommodation strain[13] as, of course, has been observed.[8,9] It follows that the stronger the matrix the greater the amount of work required to deform the matrix and the lower the temperature at which the crystal can grow. An additional effect may arise from a direct interaction of the matrix defect structure with the martensite/austenite interface, again leading to an increased difficulty of growth. On this basis, it is reasonable to ascribe stabilization to a strengthening of the austenite occurring during aging. If this is so, then the strengthening might be expected to be measurable.

Direct confirmation of true matrix strengthening on the alloy on which the stabilization experiments were made was precluded by the interference of strain-induced martensite. Tensile tests carried out by Rose[14] on more stable Fe–Ni–C alloys have revealed, however, a small but reproducible strain aging effect. The yield stress of a 32%Ni–0·12%C alloy, for example, strained 5% and aged at 90°C, increased from 52·5 to 53·75 lb/in² after 15 min, 55·25 lb/in² after 1 h, and 57·5 lb/in² after 168 h. Strain aging remained initially very rapid at room temperature and even below. Certain conclusions were drawn about the mechanism of strain aging from this work but for the present it may be noted that the presence of carbon (or presumably nitrogen) is essential and that there appears to be no increase in strength during aging unless the alloy has been plastically deformed.

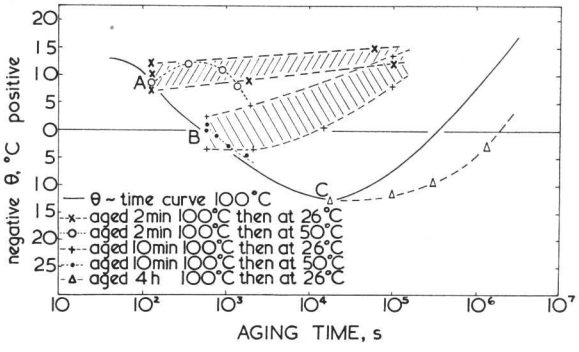

8 *Reversibility of the degree of stabilization*

These are, of course, just the conditions in which stabilization is observed, the deformation here being provided by plastic accommodation strain where the martensite plates form. Since the proximity of a martensite plate constitutes a favourable site for further transformation, it is in precisely these regions that the mechanical properties of the austenite will be of most significance in controlling the transformation. It would seem reasonable then to associate the increase in θ during the early stages of stabilization with the strain aging which is now known to occur in austenite. The eventual fall in θ with increased aging time then suggests a type of overaging which leads to a fall in the yield stress of the austenite. Closer examination of this point is required but there is already some supporting evidence. It has been noted that specimens aged to beyond the peak in the θ curve are more permanently stabilized than those with an identical θ value aged for less than the peak time. This could be due to actual precipitation in the austenite, the strengthening effect of which would persist after the austenite had been further deformed by the formation of fresh martensite at M_S. The tensile tests on the 32%Ni–0·12%C alloy showed that, for aging times beyond 15 min at 90°C, not only was the yield stress raised but also the flow stress at strains beyond the yield point extension. Presumably, as in the strain aging of ferrite, this signifies precipitation hardening, and it is reasonable that in the very high carbon steel used for the stabilization experiments overaging would rapidly follow. There is, in fact, microscopic evidence of precipitation at 100°C in this alloy and current work is aimed at studying it in detail. A further possibility is that the precipitation of carbide will deplete the matrix so locally raising the M_S through a purely chemical effect.

A dislocation-locking mechanism which could operate in an fcc structure containing interstitial solute is discussed elsewhere. It is plain from the kinetics of strain aging, however, that a dislocation atmosphere is formed and it is to be expected that the stability of the atmosphere will increase with decreasing temperature. Therefore, provided precipitation of the carbide has not progressed too far at the higher aging temperature, there may be a reversion on subsequent aging at lower temperature from the precipitation to the atmosphere condition.

To test this possibility, a group of specimens containing 30% martensite was aged at 100°C for a period of time such that their degree of stabilization would lie on that part of the θ–time curve between the maximum and minimum points. The degrees of stabilization of some of the group were then determined. The remaining specimens were aged for a series of times at a lower temperature and their subsequent degree of stabilization determined. The results of several such experiments are summarized in Figure 8. Specimens aged for 2 min at 100°C attained a degree of stabilization of about 9 degC, as represented by *A* in Figure 8. At this point θ has passed its maximum value and it is inferred that the postulated precipitation of a carbide phase has commenced. Further aging at 50°C caused θ to rise to a well defined maximum and then to fall more rapidly than for normal aging at 50°C. Aging at 26°C after the 100°C treatment also caused θ to increase, but at a lower rate thar at 50°C. Evidently stabilization is reversible from point *A* on the 100°C θ–time curve during subsequent aging at either 50°C or 26°C. Specimens which were aged for 10 min at 100°C to obtain nominally zero stabilization (point *B* in Figure 8) exhibited reversibility of stabilization upon further aging at 26°C, but not at 50°C. Reversibility did not occur at 26°C after aging to the minimum (point *C*) of the 100°C θ–time curve. In conclusion, then, reversion is observed provided the aging treatment has not been excessive; the further aging progresses at the upper temperature the greater must be the temperature drop to allow this reversion.

ACKNOWLEDGMENTS

This work was carried out in the Department of Physical Metallurgy, University of Birmingham, under the general direction of Professor G. V. Raynor, to whom grateful acknowledgment is made for the provision of facilities and for the encouragement of the research.

REFERENCES

1. J. Philibert: *Compt. Rend.*, 1955, **240,** 190–194
2. J. Philibert and C. Crussard: *JISI*, 1955, **180,** 39–48.
3. S. G. Glover: *ibid.*, 1962, **200,** 102–105.
4. B. Edmondson: *Acta Met.*, 1957, **5,** 208–215.
5. R. Priestner and S. G. Glover: *ibid.*, 1957, **5,** 536–537.
6. K. Hoselitz: 'Ferromagnetic properties of metals and alloys', 1952, O.U.P.
7. J. F. Breedis and W. D. Robertson: *Acta Met.*, 1963, **11,** 547–559.
8. G. Krauss: *ibid.*, 1963, **11,** 499–509.
9. B. Edmondson and T. Ko: *ibid.*, 1954, **2,** 235.
10. L. F. Porter and G. J. Dienes: *Trans. AIME*, 1959, **215,** 854–863.
11. A. S. Sastri and D. R. F. West: *JISI*, 1965, **203,** 138–145.
12. O. A. Ankara: quoted in reference 10.
13. B. A. Bilby and J. W. Christian: 'The mechanism of phase transformations in metals', 121–172; 1956, Institute of Metals Report no. 18.
14. K. S. B. Rose and S. G. Glover: To be published.

Discussion 2

Chairman: Professor R. W. K. Honeycombe (University of Sheffield)

Dr A. G. Crocker (Battersea College of Technology) said he could not help feeling that, as the strains involved in moving atoms from parent to product sites were certainly non-elastic, it might be more realistic to base a theory of martensite formation on flow stresses rather than on elastic moduli. Such a theory would of course be consistent with the description of the martensite interface in terms of an array of dislocations.

Professor W. D. Robertson (University of Yale) explained that he was working on the assumption that the characteristics of the transformation could be understood in terms of energy and, accordingly, elastic constants were required as a measure of the strain energy. The energy was a volume property and, if a correlation could be established, the appropriate volume properties could be more or less easily measured in any particular case.

Dr L. Kaufman (ManLabs Inc.), in answer to Dr Crocker, pointed out that the degree of undercooling or supercooling would be controlled by the nucleation barrier, which depended more on the elastic constants[1] than on the flow stress.

Mr J. A. Klostermann (Stichting voor Fundamenteel Onderzoek der Materie) asked if Dr Entwisle was sure that these transformations were so fast that the growth played no part. He thought that the growth for these materials could also be very slow and would still continue after hours or days.

Dr A. R. Entwisle (University of Sheffield) replied that Cech and Hollomon had produced, some years ago, a film of what went on on the surface of the kind of steel he was studying, and had made the observation that most of the growth was very rapid, although they implied that there was some small amount of rather slower growth.

In his work a number of microstructures at various stages in the transformation had been examined and it seemed that the shape of the plates was maintained constant. In the early stages the plates went right across the grain and these did not appear to thicken with time. Therefore, it was not thought that there was any significant amount of slow growth, although he pointed out that as long as the growth was not too slow it would not affect the theory provided that the time during which there was a significant increase in the size of a plate by isothermal growth was not long compared with the total time of the experiment. The curve would not be affected to any significant degree.

Dr J. W. Christian (University of Oxford) said that it was not obvious to him that the autocatalytic effect ought to depend on the volume of the plate transformed; why should it not depend on the thickness?

Dr Entwisle replied that it was not obvious to him, either. In fact, the volume had been tried first. They had also tried assumptions based on the fact, firstly, that it was the two regions round the ends of a plate that were significant, so that they tried to put in a parameter allowing for a constant number of new embryos per plate; this did not seem to work. It was perhaps the volume of the deformed material round the plate that was important, so they tried to put in a parameter which depended effectively on the surface area of the plate. Neither of these could cope with the grain size effect at all. It was only when they assumed that the number of embryos was proportional to the volume of the plate that they could cope with the grain size effect. Whereas he was worried that it could not be shown that it was the volume that was important, empirically this seemed to be so.

Mr Klostermann said that he wished to bring forward some facts that confirmed the opinion of Professor Robertson. Professor Robertson stated that the elastic constants entered the problem of martensite transformations in two ways, firstly as a measure of lattice instability and secondly to evaluate the restraint imposed on the transformation by the surrounding matrix, thereby providing a measure of the supercooling required for transformation to occur. He wished to point out that there was a third reason why more should be known about the elastic constants. If more were known about them (and one would like to know the anisotropic elastic constants of both phases and their temperature dependence) habit phenomenon and growth mechanisms would be better understood.

The work started by Professor Robertson was important and he wished to illustrate this with some experimental facts.

There appeared to form, on cooling single crystals of Fe–30%Ni, a martensite morphology, often with a 'butterfly' appearance, which had a midrib and formed on cube planes (Figures *A* and *B*(iii)). The cooling temperature was just above M_b.

A cut parallel to a cube plane just over a row of butterflies showed that there was a network of angle profiles which were lying in $<210>_\gamma$ directions (Figure *B*(i)). He assumed that the network formed by branching (Figure *C*), as was the case with surface martensite. The straight boundaries of the butterflies lay in $\{112\}_\gamma$ planes.

X-ray work with a texture goniometer showed that *one* particular habit variant $(2\bar{1}0)_\gamma$ (one system of angle profiles) was related to *two* orientations of the martensite lattice (Figure *D*). (The two systems of angle profiles $(2\bar{1}0)_\gamma$ and $(\bar{1}20)_\gamma$ had a mutual twin correspondence.)

When it was assumed that growth had started from the midrib region and that this region had an orientation of the martensite lattice intermediate between the two orientations found,

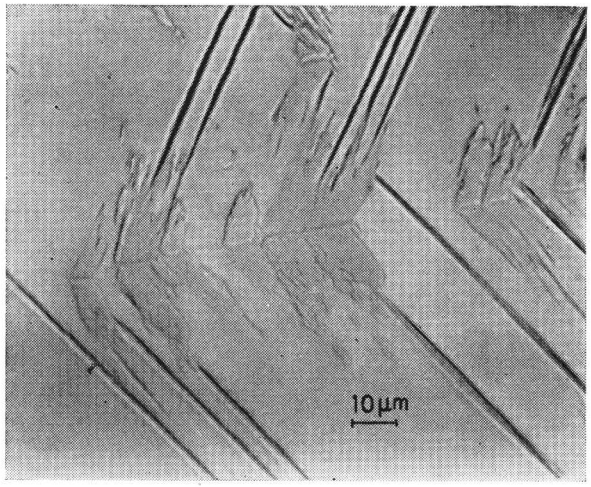

A *Angle profile martensite with midribs*

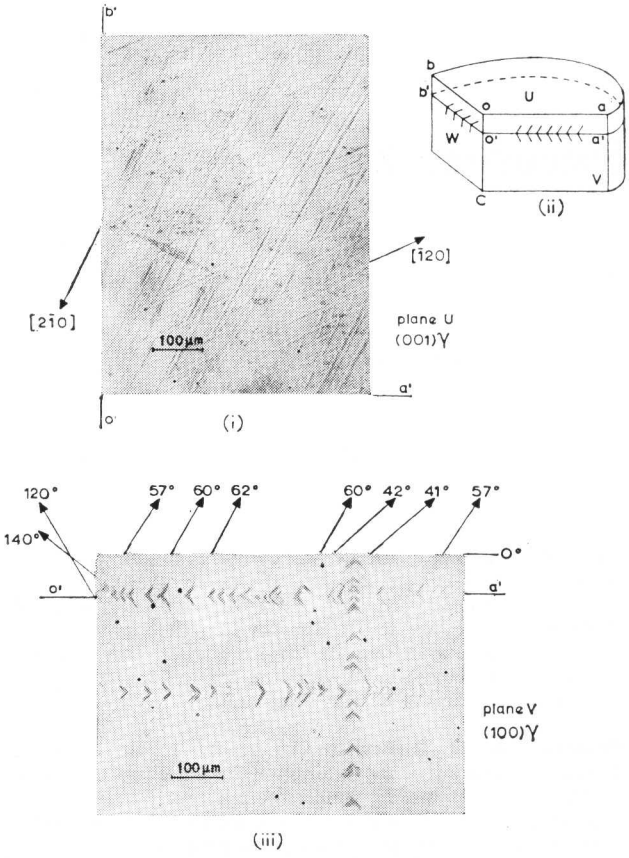

B *(i)–(iii) (i) Network apparent when the specimen (ii) was cut over a row of 'butterflies; (iii) the {100}γ habit of the angle profile martensite; the specimen surfaces U, V, and W are parallel to cube planes of the austenite*

then it followed that the growth of the wings of the butterflies was accompanied by an orientation rotation of about 10°.

It was remarkable now that if one considered only the volume expansion of the martensite, one would expect that it would form on the cube plane because the cube direction of the austenite had the lowest Young's modulus. If one considered the lattice deformation, then one would expect just those two variants of the three possible variants of the Bain correspondence which formed on the cube plane of the austenite, because they gave the smallest deformation in the cube direction perpendicular to this cube plane, while in this cube plane mutual compensation occurred.

The problems of the morphology were far from being solved. Of course dislocation mechanisms had also to be considered but he thought that knowledge of the elastic constants would be very important for doing this.

Dr Christian said that he agreed with Dr Kaufman's point about elastic constants in the nucleation stage, and providing there was some form of critical nucleus which had to be formed, it was the elastic constants one had to measure, not the flow stress. He was not at all convinced that elastic constants were relevant in the crystallographic problems, and conventional geometric matching theory did not involve elastic constants. The only way they could be brought in was by supposing that the constraints in the matrix forced a modification of the invariant plane strain conditions. He had once tried to explain the dilatation parameter in this way, using isotropic elasticity, but the calculations were difficult.

If the martensite nucleus had the form of a lenticular plate, the point of determining the elastic constants was to calculate the strain energy produced by the shape change of the plate. In the approximation of isotropic elasticity all the terms in the strain energy calculation depended on the shear modulus. Presumably this was the calculation that Professor Robertson was using. He thought he was correct in saying that a solution could not be obtained of the Eshelby equations in systems which had cubic anistropy, so he was not at all convinced that if one measured the single crystal elastic constants one could improve the calculation in this respect.

Before Professor Robertson actually made these difficult measurements, had he satisfied himself that he would be able to use the results in this way?

Professor Robertson replied that, quantitatively, the answer was no. He had not satisfied himself in the kind of detail that Dr Christian had raised. Further, he would like to have a good deal more information before deciding that it was indeed possible, because he was not quite sure that enough was known to determine just what calculations to make. He would like to have elastic constants from more systems to see whether there was some empirical correlation that would indicate how to make the calculations.

Dr Crocker said that he might have been wrong in emphasizing the flow stress. What he had wanted to do was to question the use of elastic constants because the displacements involved in the model put forward were very large. Perhaps what should be attempted was the use of atomic force laws to calculate the energy necessary for transforming one structure into another. In any case, it might be that the flow stress would give some useful information and it was not simply the elastic constants that were the controlling factor.

Professor J. Nutting (University of Leeds) said that his points referred to the paper by Priestner and Glover and the problems of stabilization. He found the simple arguments given somewhat difficult to believe in the sense that if precipitation occurred on the dislocations that were generated in the austenite, giving an increase in yield stress of the austenite and therefore making it more difficult to transform, then one could offset this by the fact that, as precipitation occurred, carbon would be taken out of solution from the austenite and this would raise the M_s temperature, i.e. have a negative stabilizing effect. Dr Glover put this forward as an explanation of the final rise of his curves. But if one thought about the way in which aging reactions occurred, solute depletion was usually most marked up to maximum hardness. When there was resolution and growth of precipitates, most of the solid solution depletion had already occurred and one felt therefore that it would be difficult to accept Dr Glover's

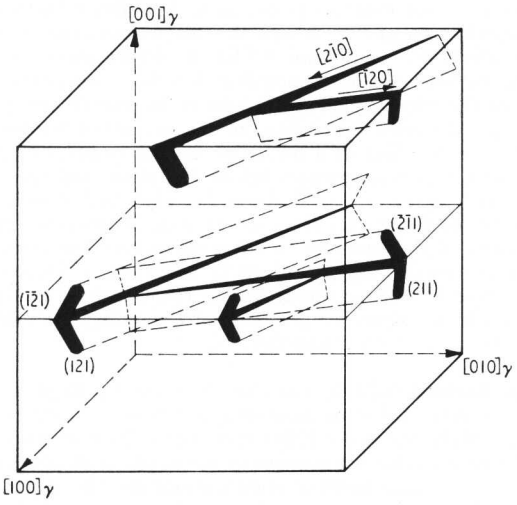

C *Angle profiles in [2$\bar{1}$0] directions forming branches in [$\bar{1}$20] directions which can again branch in [2$\bar{1}$0] directions; a cut more or less perpendicular to the network shows arrays of 'butterflies'*

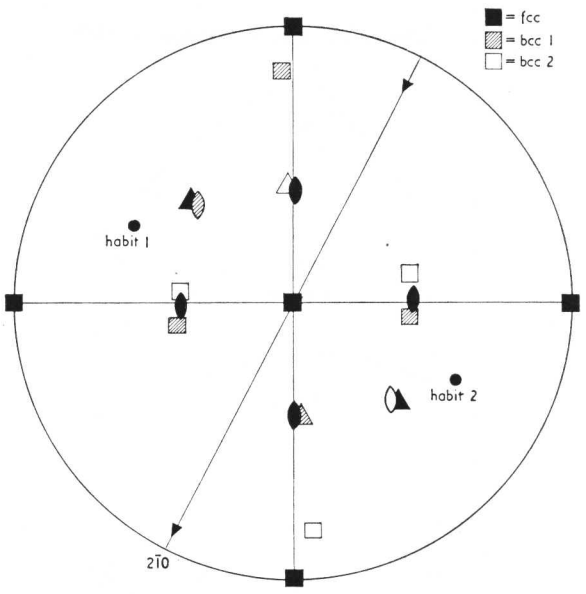

D *One system of angle profiles all lying in [2$\bar{1}$0] directions, related to two orientation relations of the martensite*

account for the curve going back upwards after prolonged treatments.

It would appear that more likely explanation of the stabilizing effect should be sought not in the distribution of dislocations and precipitates within the untransformed austenite but in the locking of the dislocations at the martensite/austenite interface.

Dr S. G. Glover (University of Birmingham) said that they had discussed the mechanism of aging of austenite only briefly because at this stage it was rather conjectural. If stabilization was attributable to a strengthening of the residual austenite by precipitation then, as Professor Nutting rightly asserted, one might expect to find the destabilizing effect of carbon depletion predominating in the early stages. This was, of course, contrary to what was observed.

Considering the aging mechanism in more detail, however, it was known that both stabilization and also strain aging in an austenitic iron–nickel–carbon alloy could occur at temperatures as low as 40°C, developing to measurable extents within a minute. This would appear from their calculations to be too rapid to be explained on the basis of the movement of carbon atoms over several atomic distances in austenite as would be necessary in forming a dislocation atmosphere or precipitate. What seemed more likely was that the initial hardening was due to Snoek ordering, the ordering unit here being probably a vacancy–carbon pair. This would have the effect of strengthening the austenite without depleting the matrix of carbon. It might also be added that results of the strain aging work suggested that further carbon–vacancy pairs were created by the movement of vacancies towards carbon atoms and that only after the more severe aging treatments was there a significant segregation of carbon.

On Professor Nutting's final point, it was fairly certain that it would be the dislocations in the neighbourhood of existing martensite plates which would be significant in determining further transformation. The fact that, after treatments producing negative stabilization, subsequent transformation started by the growth of rims on existing plates did, perhaps, point to the martensite–austenite boundary itself as the significant site.

A rather puzzling aspect of this, however, was that one would not expect austenite at or near the martensite boundary to become depleted in carbon. There was, in fact, evidence[2] that during low-temperature tempering a significant amount of carbon drained from the martensite into the surrounding austenite. This would, of course, be expected to lower the M_s not raise it as effectively happened in negative stabilization.

Dr Entwisle said that a good deal of work on stabilization was done on materials that had M_s temperatures just above room temperature, and these were alloys in which the crystallography was undecided. Such a steel did not really seem to know which crystallography it wanted to have. He wondered whether this was contributing to the complexity of the subject. He would like to urge those who were interested in the details of stabilization to work on an alloy with a rather low M_s (−50°, −60°, or −70°C), where the steel was quite certain what kind of plates it wanted to have and, to some extent, a little of the complexity might be removed.

On a structural point, in iron–nickel–carbon alloys with an M_s above or below room temperature, one often saw plates formed and, at a subsequent stage in the transformation, they were surrounded by small pairs of plates and, zoologically, he called these 'seagulls', not 'butterflies'. This was fairly clear evidence that something was going on in the deformed region round the plate. He wondered whether Dr Glover had noticed this kind of effect? Dr Glover spoke about martensite rims; did he see this effect? There were too many possibilities in these alloys where the crystallography was rather undecided, so he urged work on alloys where the alloy was quite clear what shape of plate it wanted to have.

Dr P. M. Kelly (University of Leeds) asked if Dr Glover was implying that the diffusion of vacancies occurred more rapidly than the diffusion of carbon at temperatures in the range 0°–200°C. This implication would appear to be incorrect.

Dr Glover said that Dr Entwisle was correct in emphasizing the significance of the crystallography and morphology of the martensite with respect to stabilization. They had observed plates forming in the way described by Dr Entwisle but what they had called rims were something quite different. As illustrated in reference 5 of the paper, these appeared to be formed by the resumed growth of the existing plate and not the initiation of fresh ones. In answer to Dr Kelly, he did not believe that carbon moved sufficiently quickly in austenite. The situation was very different from that in ferrite where it was accepted that carbon had a very high mobility.

If one extrapolated the high-temperature data for the diffusion of carbon in austenite to room temperature one arrived at a value for the diffusivity many orders of magnitude smaller than that

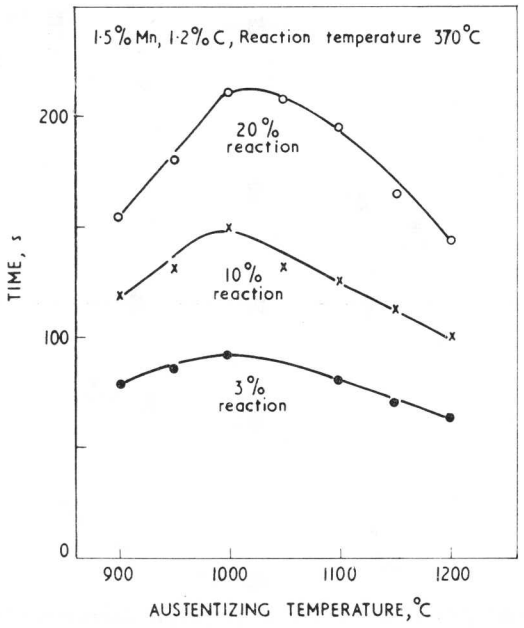

E *Effect of double austenitizing treatment on rate of bainite formation in Fe–C–Mn alloys*

for carbon in ferrite. Despite the uncertainties involved there, it seemed fairly certain that the initially very rapid rate of both stabilization and strain aging could not be ascribed to the movement of carbon. It was for this reason that they were forced to seek alternative mechanisms.

As to the determination of an activation energy, the stabilization process was so complex as to preclude a meaningful activation energy analysis and values which had been published could be given little credence.

Professor H. W. Paxton (Carnegie Institute of Technology) said that he had some comments on embryos but was not sure whether they were relevant to the present discussion. His department had been doing some experiments on deforming single crystals of transformable austenites at various temperatures to see the effect on the M_s temperature – more properly the burst temperature M_b. These were primarily steels which were in the maraging range of compositions.

The interesting experiment so far as the present discussion was concerned was that if one plastically deformed these single crystals, the M_b temperature was raised; this was not very surprising, but what was rather surprising was that the amount by which the M_b temperature was raised was independent of whether or not one deformed these crystals above or below T_0. If there were some sort of dislocation nuclei which one called embryos, one would think one should at least have a chance of readjusting these or sweeping them out by deforming above T_0.

Dr Kaufman said, firstly, that he agreed with Dr Kelly on the vacancy migration versus carbon diffusion. This question was settled ten years ago by Philibert and Crussard[3] who showed that stabilization disappeared when carbon and nitrogen were removed by treatment in moist hydrogen. In his view, the stabilization effect was clearly associated with the pinning of the interface dislocations. This was a critical product of the growth of the embryo to the stage where it could propagate, and if carbon atoms invaded the interface and pinned the dislocations that had to move, this could provide a strong barrier for nucleation.

As to the zoological configuration of martensite, M_d experiments on an iron–nickel alloy (which transformed normally at −150°) at 30°C yielded an extremely irregular structure associated with the deformation pattern.[4]

On Professor Paxton's point, he had published his views on the stabilization of the embryo and the temperatures at which these effects were significant.[5,6] Firstly, deformation above the M_s temperature was very complicated as the temperature range entered the effect. One could inhibit or increase the propensity for transformation depending on the amount of deformation. Moreover the effect of deformation on the embryo itself was not limited to temperatures below T_0, since embryos were stable at temperatures well above T_0. They had attempted to demonstrate this several years ago by using hydrostatic pressure treatment of the austenite to effect subsequent transformation in the martensite, and so, at least in their view, T_f the temperature where the embryo was 'frozen-in' rather than T_0 was critical as regards the nature or potencies of the embryo. The former could be substantially higher than T_0.

Dr J. Barford (CEGB) said that the paper by Raghavan and Entwisle presented some interesting results and a significant extension of the analysis of Fisher *et al.*[7] In the form presented, the results showed that the number of martensite embryos per unit volume was independent of grain size and that the embryos did not need the stimulus of a grain boundary in order to become active. However, it appeared that the data also showed an effect of austenitizing temperature upon the number of active embryos. On the basis of the authors' assumption that the straight lines in the $\tau_i^{-\frac{1}{3}}$ versus grain diameter plots (Figures 5–7) showed the true relationship, one might calculate the value of τ_i for specimens of constant grain size produced at different austenitizing temperatures.

The results of this exercise were given in Table 1 from which it could be seen that there was a consistent trend in increasing τ_i with increasing austenitizing temperature.

It was also apparent that this effect was more strongly observed on reaction at −66°C.

These results might be compared with some on the effect of austenitizing temperature on bainite kinetics obtained some time ago by Professor Owen and himself[8] and some on martensite kinetics in low-alloy steels recently published by Sastri and West.[9] Figure *E* showed the effect of a double austenitizing treatment on the rate of bainite formation at 370°C (upper bainite) in two iron–carbon–manganese alloys. Specimens were austenitized at the highest temperature in the range to fix the grain size, and then cooled to and held at some lower temperature in the range 900°–1150°C before quenching to 370°C. The rate of reaction clearly depended on the second austenitizing temperature. This was interpreted on the basis of the number and/or size distribution of active embryos being dependent on austenitizing temperature. The minimum reaction rate on quenching from about 1050°C was a reflection of the fact that the fcc phase was most stable at this temperature. Increasing or decreasing the temperatures brought the conditions nearer to a boundary containing the bcc phase, and thus increased the size and numbers of bcc embryos present in the γ-phase.

However, similar double austenitizing treatments failed to show any effect of the second austenitizing temperature on the kinetics of martensite formation in low-alloy steels.[9] In view of this behaviour, and, of course, the isothermal behaviour of the authors' alloys it might be that there was a closer connexion between iron–nickel martensite and 'normal' bainite than between the iron–nickel martensite and 'normal' athermal martensite in low-alloy steels.

It would be of interest to examine in more detail the effect of

TABLE 1 Values of τ_i in seconds

Austenitizing temperature, °C	d, mm 0·02		0·04		0·06	
	−66°C	−78·5°C	−66°C	−78·5 C	−66°C	−78·5°C
800	—	580	—	72	—	23
900	5720	1210	640	145	190	45
1000	13500	1810	1680	178	500	61

austenitizing temperature in the authors' alloys. One would predict on the basis of the austenite stability model and the iron–nickel phase diagram that a continually increasing τ_1 with increasing austenitizing temperature would be found.

Dr Entwisle replied that he and Dr Raghavan would certainly like to believe that there was an austenitizing temperature effect. They were rather uncertain and hoped to investigate this point further. There was a difficulty: if they heated their alloys for too long at high temperatures, they began to get a contamination effect, and this was the reason why they had not proceeded to any more exotic kinds of heat treatment. He would not like to commit himself on bainite or martensite in the same breath!

REFERENCES

1. L. KAUFMAN and M COHEN: 'Progress in metal physics', VII, 165; 1958, London, Pergamon.
2. S. J. MATAS and R. F. HEHEMANN: *Nature*, 1960, **187**, 685–686.
3. J. PHILIBERT and C. CRUSSARD: 'The mechanism of phase transformations in metals', 312; 1955, Institute of Metals.
4. L. KAUFMAN and M. COHEN: *Trans. AIME*, 1956, **206**, 1393–1401.
5. L. KAUFMAN *et al.*: *Acta Met.*, 1960, **8**, 270–272.
6. L. KAUFMAN *et al.*: 'Progress in very high pressure research', (ed. Bundy *et al.*), 90; 1960, New York, Wiley.
7. J. C. FISHER *et al.*: *Trans. AIME*, 1949, **185**, 691–700.
8. J. BARFORD and W. S. OWEN: *JISI*, 1961, **197**, 146–151.
9. A. S. SASTRI and D. R. F. WEST: *ibid.*, 1965, **203**, 138–145.

Thermodynamics of martensitic fcc ⇌ bcc and fcc ⇌ hcp transformations in the iron–ruthenium system

Larry Kaufman

SYNOPSIS

A thermodynamic analysis of the iron–ruthenium system has been performed on the basis of the regular solution model by approximating the lattice stability of hcp, fcc, and bcc ruthenium as being similar to non-magnetic iron. The analysis permits calculation of the entire phase diagram, the $T_0 - x$ *curves for diffusionless fcc⇌bcc and fcc⇌hcp reactions at one atmosphere and the compositional dependence of the fcc/bcc/hcp pressure–temperature triple points, all of which compare reasonably well with observation. The driving force for the martensitic fcc⇌bcc reaction is temperature dependent and similar to that observed for iron–nickel alloys. The driving force for the martensitic fcc⇌hcp reaction is about 50 cal/mole and, as expected from crystallographic considerations, is smaller than the corresponding fcc⇌bcc driving force.* 2613

INTRODUCTION

RECENT STUDIES of the phase transformations in iron–ruthenium alloys[1] and in iron[2,3] have confirmed the earlier suggestion[4] that hcp iron becomes a stable phase at high pressures. The observation of the temperature–pressure dependence of the fcc⇌hcp transition in iron–ruthenium alloys permitted calculation of the difference in free energy $\left(\Delta F_{\text{Fe}}^{\alpha\rightarrow\varepsilon}\right)$ between the hcp (ε) and bcc (α) forms of iron as a function of temperature and pressure.[1] These values, when combined with the earlier description of the free energy difference between the fcc (γ) and bcc forms of iron,[5] resulted in a calculation of the free energy difference $\Delta F_{\text{Fe}}^{\gamma\rightarrow\varepsilon}$ and its dependence on temperature and pressure. The availability of these free energy differences make possible the computation of the complete temperature–pressure diagram for iron.[1] Very recently, Bundy[6] has performed a complete experimental study of the triple point in iron. The comparison of his results shown in Figure 1 along with the computed version[1] shows reasonable agreement and offers support for the computed* $\Delta F_{\text{Fe}}^{\alpha\rightarrow\gamma}[T,P]$ and $\Delta F_{\text{Fe}}^{\alpha\rightarrow\varepsilon}[T,P]$ results.[1] Consequently, these values have been applied to compute the free energy relations in the iron–ruthenium system between the α, γ, and ε-phases as a function of temperature, composition, and pressure, in order to elucidate the driving force for the martensitic fcc⇌hcp reaction in this system.[7,8]

The author is with ManLabs Inc., Cambridge, Massachusetts. The research was sponsored by the Metallurgy Branch, Office of Naval Research, Washington D.C., under Contract Nonr 2600(00). (MG/Conf/75/65). UDC No.669.15'236: 669.112.227.342

THERMODYNAMIC ANALYSIS OF THE IRON-RUTHENIUM PHASE DIAGRAM

The iron–ruthenium phase diagram[9–11] is shown in Figure 2.

* Square brackets are used exclusively to denote functional relations. Thus $\Delta F_{\text{Fe}}^{\alpha\rightarrow\varepsilon}[T,P]$ is read as the free energy difference between bcc and hcp iron as a function of temperature and pressure.

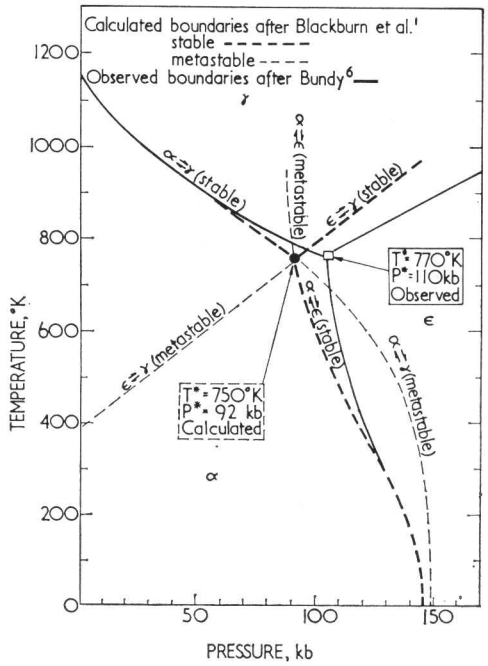

1 *Comparison of computed[1] and observed[6] T-P diagram for iron*

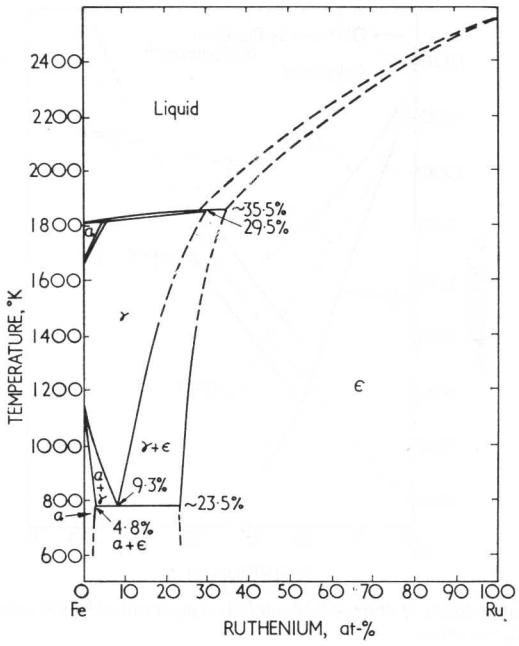

2 *Observed iron–ruthenium phase diagram*[9–11]

It exhibits a large hcp field based on ruthenium and the α and γ fields based on iron. Since very few thermodynamic data are available for this system, the regular solution approximation has been applied along the lines indicated earlier.[12] In particular (see equations (1), (2), (31), and (32) of reference 12) the excess free energies of mixing of the α, γ, ε, and liquid (L) phases have been assumed to be parabolic with composition and represented by the following, where x is the atomic fraction of ruthenium

$$F_E^{\alpha} = x(1-x)\ (1800-2{\cdot}5T) \text{ cal/mole} \quad \text{.....(1)}$$

$$F_E^{\gamma} = -x(1-x)\ 2000 \text{ cal/mole} \quad \text{.....(2)}$$

TABLE I Difference in free energy between the fcc and hcp forms of iron and ruthenium

T,°K	$\Delta F_{Fe}^{\gamma\rightarrow\varepsilon}$, cal/mole	$\Delta F_{Ru}^{\gamma\rightarrow\varepsilon}$, cal/mole
0	— 153	— 153
100	— 165	— 175
200	— 140	— 230
300	— 75	— 305
400	+ 20	— 385
500	+ 115	— 465
600	+ 235	— 550
700	+ 340	— 640
800	+ 445	— 725
900	+ 565	— 815
1000	+ 685	— 905
1100	+ 805	— 990
1200	+ 920	—1070
1300	+1035	—1150
1400	+1140	—1235
1500	+1240	—1320
1600	+1340	—1405
1700	+1430	—1485
1800	+1520	—1570

$$F_E^{\varepsilon} = -x(1-x)\ 3800 \text{ cal/mole} \quad \text{.....(3)}$$

$$F_E^{L} = -x(1-x)\ 1200 \text{ cal/mole} \quad \text{.....(4)}$$

Equation (1) is restricted to temperatures above 200°K to avoid violation of the 'third law'. The free energy differences between the α, γ, ε, and L forms of iron have been discussed earlier;[1] however, $\Delta F_{Fe}^{\gamma\rightarrow\varepsilon}$ is included for convenience in Table I.

The free energy differences between the α, γ, and L forms of iron are described by equations (5) and (6) for temperatures above 1 650°K

$$\Delta F_{Fe}^{\alpha\rightarrow L} = 3\,680-2{\cdot}03T \text{ cal/mole} \quad \text{.....(5)}$$

$$\Delta F_{Fe}^{\gamma\rightarrow L} = 3\,905-2{\cdot}165T \text{ cal/mole} \quad \text{.....(6)}$$

while the difference in free energy between the hcp and liquid form of iron[1] for temperatures above 1300°K is

$$\Delta F_{Fe}^{\varepsilon\rightarrow L} = 3\,680-3{\cdot}0T \text{ cal/mole} \quad \text{.....(7)}$$

The free energy differences between the α, γ, and ε forms of ruthenium were assumed to be identical to that of iron (which occupies the same column in the periodic system as ruthenium) *except* that the magnetic free energy of α-iron and the magnetic free energy due to the 'two spin state' population of γ-iron are omitted.[5] This permits direct numerical computation of $\Delta F_{Ru}^{\gamma\rightarrow\varepsilon}$ as shown in Table I. In iron, the difference in free energies between the α and γ forms is 1303 cal/mole at 0°K. If bcc iron were not ferromagnetic its free energy at 0°K would be increased by about 2300 cal/mole (i.e., by about 1·05 RT_{Curie}) so that γ-iron would be more stable than non-ferromagnetic α-iron by about 1000 cal/mole. Since the vibrational and electronic specific heat contributions to the free energies of α and γ-iron are equal, the free energy difference between these forms would be independent of temperature. In fact the loss of ferromagnetism and population of two spin states with increased temperature control[1] $\Delta F_{Fe}^{\alpha\rightarrow\gamma}[T]$. As a consequence of the assumption that such factors are absent in ruthenium

$$\Delta F_{Ru}^{\alpha\rightarrow\gamma} = -1000 \text{ cal/mole} \quad \text{.....(8)}$$

The free energy differences between the α, γ, ε, and L form of ruthenium are approximated from the melting point of ε-ruthenium[13] at 2 550°K, estimating the entropy of fusion of ε-ruthenium as 2·0 cal/mole.°K. Hence, for $T > 1000$°K

$$\Delta F_{Ru}^{\varepsilon\rightarrow L} = 5100-2{\cdot}0T \text{ cal/mole} \quad \text{.....(9)}$$

$$\Delta F_{Ru}^{\gamma\rightarrow L} = 4980-2{\cdot}8T \text{ cal/mole} \quad \text{.....(10)}$$

$$\Delta F_{Ru}^{\alpha\rightarrow L} = 3980-2{\cdot}8T \text{ cal/mole} \quad \text{.....(11)}$$

Equation (11) yields a melting point for bcc ruthenium at about 1 420°K, which is consistent with the molybdenum–ruthenium phase diagram.[14]

Equations (1-11) are sufficiently explicit to permit application of the rule of common tangents for calculation of the

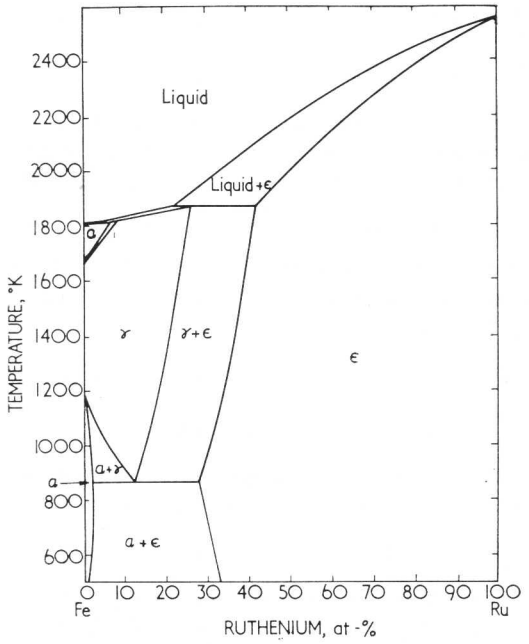

3 *Computed iron–ruthenium phase diagram*

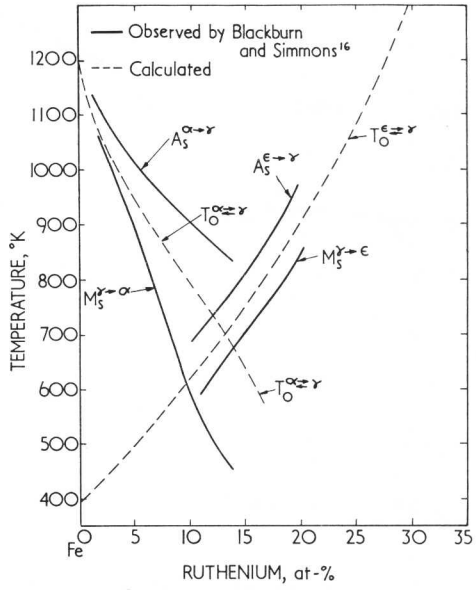

5 *Comparison of observed M_s and A_s temperatures[16] with calculated T_0—x curves*

phase diagram. In line with the development of equations (1)-(8) of reference 12, equilibration of the partial molar free energies of both iron and ruthenium across each of the two-phase fields permits calculation of the phase boundaries. For example, the present analogue to equations (7) and (8) or (33) and (34) of reference 12 at 1300°K are

$$\Delta F_{Fe}^{\gamma\rightarrow\varepsilon} + RT\ln\frac{1-x_\varepsilon}{1-x_\gamma} = x_\gamma^2\,(-2000) - x_\varepsilon^2\,(-3800) \quad \ldots(12)$$

$$\Delta F_{Ru}^{\gamma\rightarrow\varepsilon} + RT\ln\frac{x_\varepsilon}{x_\gamma} = (1-x_\gamma)^2(-2000) - (1-x_\varepsilon)^2(-3800) \quad \ldots(13)$$

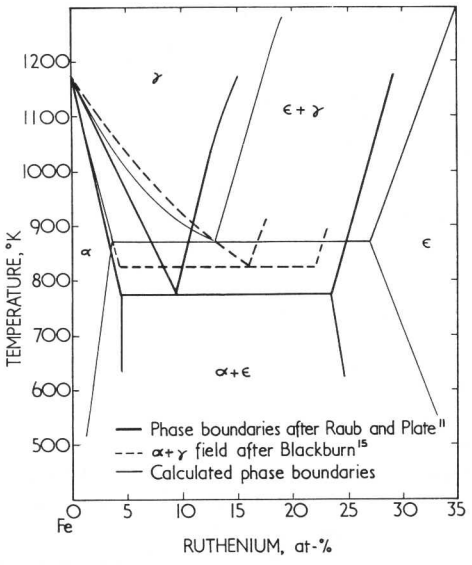

4 *Detailed comparison of experimental[11,15] and computed α, γ, and ε-phase fields at low temperatures*

where x_γ is the composition of the $\gamma/\varepsilon+\gamma$ phase boundary and x_ε is the composition of the $\varepsilon+\gamma/\varepsilon$ phase boundary at 1300°K. Equations (12) and (13), as well as similar equations for α/L, γ/L, ε/L, α/γ, and α/ε, can be solved for the corresponding phase boundaries as a function of temperature. The result is shown in Figures 3 and 4. In view of the simplicity of the models used for computing the entire phase diagram, the level of agreement is quite satisfactory. The major differences between the observed and computed versions are the widths of the $\varepsilon+\gamma$ and ε+L fields and the temperature of the $\gamma\rightarrow\alpha+\varepsilon$ eutectoid.

In addition to performing the phase diagram computation, it is possible to compute the locus of T_0-x curves for the $\gamma\rightleftharpoons\alpha$ and $\gamma\rightleftharpoons\varepsilon$ reactions. These are defined by equations (14) and (15) as

$$0 = (1-x_0)\Delta F_{Fe}^{\alpha\rightarrow\gamma}[T_0] + x_0\Delta F_{Ru}^{\alpha\rightarrow\gamma} - x_0(1-x_0)(3800-2{\cdot}5T) \quad \ldots(14)$$

for the $\gamma\rightleftharpoons\alpha$ reaction, and

$$0 = (1-x_0)\Delta F_{Fe}^{\varepsilon\rightarrow\gamma}[T_0] + x_0\Delta F_{Ru}^{\varepsilon\rightarrow\gamma}[T_0] + x_0(1-x_0)1800 \quad \ldots(15)$$

for the $\gamma\rightleftharpoons\varepsilon$ reaction. The T_0-x_0 curves satisfying equations (14) and (15) are shown in Figure 5. It should be pointed out that the definition of the T_0—x_0 or T_0—x curve[7,8] does not require, or even infer, that the subject reaction ($\gamma\rightleftharpoons\alpha$ or $\gamma\rightleftharpoons\varepsilon$) take place at T_0, but rather that the difference in free energy between the two phases at a fixed composition is zero. The computed T_0—x curves for the $\gamma\rightleftharpoons\varepsilon$ and $\gamma\rightleftharpoons\alpha$ cases are seen to lie between the appropriate $M_s^{\gamma\rightarrow\alpha}$, $A_s^{\alpha\rightarrow\gamma}$, $M_s^{\gamma\rightarrow\varepsilon}$, and $A_s^{\varepsilon\rightarrow\gamma}$ curves recently determined by Blackburn and Simmons.[16]

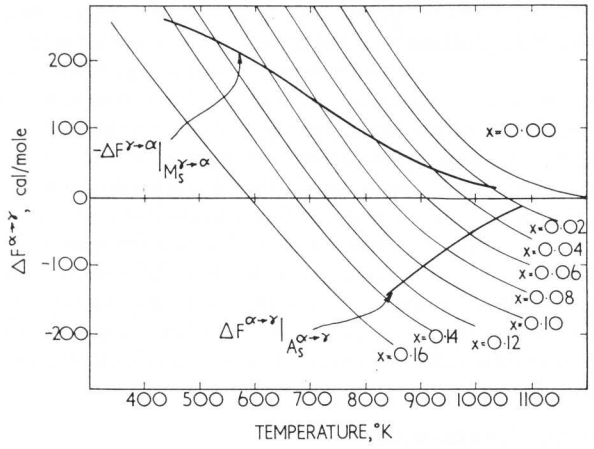

6 *Computation of the driving force at* $M_S{}^{\gamma\to\alpha}$ *and* $A_S{}^{\alpha\to\gamma}$ *for iron–ruthenium alloys as a function of composition*

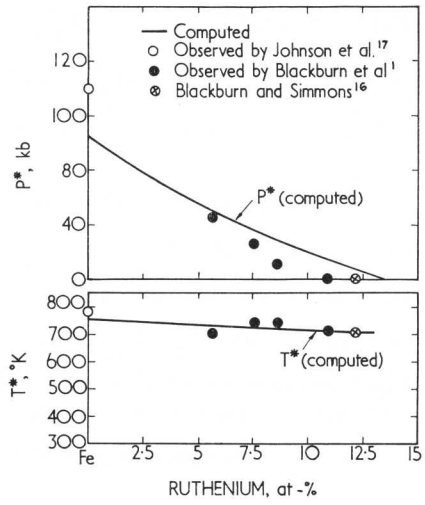

8 *Comparison of observed*[1,16,17] *and computed triple point pressures and temperatures in iron–ruthenium alloys.*

CALCULATION OF THE DRIVING FORCE FOR MARTENSITIC $\delta\rightleftharpoons\alpha$ AND $\delta\rightleftharpoons\epsilon$ REACTIONS

The driving force attending the $\gamma\rightleftharpoons\alpha$ and $\gamma\rightleftharpoons\varepsilon$ reactions can be computed by writing equations (14) and (15) for various x and T other than T_0 and x_0,[7,8,12] i.e.

$$\Delta F^{\alpha\to\gamma}[T,x]=(1-x)\Delta F_{Fe}^{\alpha\to\gamma}+x\Delta F_{Ru}^{\alpha\to\gamma}$$
$$-x(1-x)(3800-2{\cdot}5T)\ \text{cal/mole} \quad \ldots\ldots (16)$$

and*

$$\Delta F^{\varepsilon\to\gamma}[T,x]=(1-x)\Delta F_{Fe}^{\varepsilon\to\gamma}+x\Delta F_{Ru}^{\varepsilon\to\gamma}$$
$$+x(1-x)\,1800\ \text{cal/mole} \quad \ldots\ldots (17)$$

Substitution of various values of x and T into equation (16) yields the $\Delta F^{\alpha\to\gamma}[T,x]$ curves shown in Figure 6. When the appropriate $M_S{}^{\gamma\to\alpha}$ and $A_S{}^{\alpha\to\gamma}$ points (from Figure 5) are cross plotted, the driving force for the fcc⇌bcc reactions is obtained. These values are quite similar to those obtained earlier[7,8] from a similar analysis of the fcc⇌bcc reactions in iron–nickel alloys where the driving force at M_S was observed to increase with decreasing temperature, reaching 200 cal/mole at about 600°K. The driving force at A_S in the present case is somewhat smaller than in the iron–nickel case, where 260 cal/mole was computed at 835°K, as compared with 150 cal/mole at 835°K in the present instance. These discrepancies may be caused by the simplicity of the present thermodynamic model.

A similar procedure can be applied to compute the driving force for the $\gamma\rightleftharpoons\varepsilon$ reactions. Thus, equation (17) generates the $\Delta F^{\varepsilon\to\gamma}[x,\ T]$ curves shown in Figure 7. Cross plotting the appropriate $M_S{}^{\gamma\to\varepsilon}$ and $A_S{}^{\varepsilon\to\gamma}$ values indicates that the driving force for the $\gamma\rightleftharpoons\varepsilon$ reactions is about 50 cal/mole. This result is consistent with a closer lattice correspondence for the fcc⇌hcp reaction (requiring a smaller driving force) than for the fcc⇌bcc reaction, which requires a larger driving force.

* Equation (16) should not be applied below 200°K to avoid violating the 'third law'.

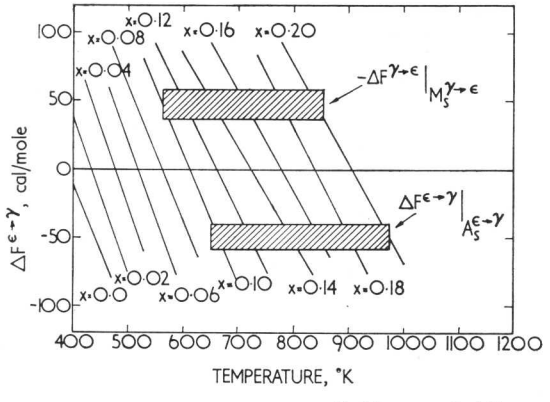

7 *Computation of the driving force at* $M_S{}^{\gamma\to\varepsilon}$ *and* $A_S{}^{\varepsilon\to\gamma}$ *for iron–ruthenium alloys as a function of composition*

CALCULATION OF THE COMPOSITIONAL DEPENDENCE OF TRIPLE POINT TEMPERATURES AND PRESSURES IN THE IRON-RUTHENIUM SYSTEM

Figure 1 shows the triple point T^*, P^* at which $\Delta F_{Fe}^{\alpha\to\gamma}[T^*,P^*]$ and $\Delta F_{Fe}^{\varepsilon\to\gamma}[T^*,\ P^*]$ are both equal to zero. Figure 5 shows the alloy analogue at one atmosphere. Thus at 700°K and about 13 at-% Ru, $\Delta F^{\alpha\to\gamma}=\Delta F^{\varepsilon\to\gamma}=0$. Calculation of the curve representing $T^*[x]$ and $P^*[x]$ can be performed by using the results of equations (15)–(18) and assuming that the difference in volume between the α, γ, and ε-phases is not affected by ruthenium in this composition range. Thus, by using the volume differences employed earlier,[1,5] the following conditions can be specified*

* Equation (19) corrects a typographical error appearing in equation (39) of reference 5 in which the pressure P was omitted.

$$\Delta F^{\alpha\rightarrow\gamma}[T,P,x]=(1-x)\Delta F_{Fe}^{\alpha\rightarrow\gamma}[T,P]+x\Delta F_{Ru}^{\alpha\rightarrow\gamma}$$
$$-x(1-x)\ (3\,800-2{\cdot}5T)+x23{\cdot}9P(\Delta V_{Fe}^{\alpha\rightarrow\gamma_0}[T]$$
$$+y[T,P]\Delta V_{Fe}^{\gamma_0\rightarrow\gamma_1}[T])\ \text{cal/mole} \quad \ldots\ldots(18)$$

where[5]

$$\Delta F_{Fe}^{\alpha\rightarrow\gamma}[T,P]=1\,303-F_{Fe}^{\alpha\mu}[T,P]+RT\ln(1-y[T,P])$$
$$+23{\cdot}9P\Delta V_{Fe}^{\alpha\rightarrow\gamma_0}[T]\ \text{cal/mole} \quad \ldots\ldots(19)$$

The values required for numerical computation of the magnetic free energy of α-iron ($F_{Fe}^{\alpha\mu}[T]$), the relative population ($y[T, P]$) of the low volume (γ_0) and high volume (γ_1) spin state in fcc iron, and the respective volume differences $\Delta V_{Fe}^{\alpha\rightarrow\gamma_0}[T]$ and $\Delta V_{Fe}^{\gamma_0\rightarrow\gamma_1}[T]$ have been presented earlier.[5] In addition

$$\Delta F^{\alpha\rightarrow\varepsilon}[T,P,x]=(1-x)\Delta F_{Fe}^{\alpha\rightarrow\varepsilon}[T]+x\Delta F_{Ru}^{\alpha\rightarrow\varepsilon}$$
$$-x\ (1-x)\ (5\,600-2{\cdot}5T)+23{\cdot}9P\Delta V_{Fe}^{\alpha\rightarrow\varepsilon}[T]\ \text{cal/mole} \quad (20)$$

where $\Delta V_{Fe}^{\alpha\rightarrow\varepsilon}[T]$ has been defined numerically.[5] If equations (18) and (20) are set equal to zero simultaneously for fixed values of x, then the $T^*[x]$ and $P^*[x]$ curves shown in Figure 8 result. The comparison between these computed curves and the values obtained experimentally are satisfactory in view of the present model.

CONCLUSIONS

Estimates of the thermodynamic properties of the α, γ, ε, and liquid phases of the iron–ruthenium system based on the regular solution model have been made. In addition, it has been assumed that the difference in free energy between the γ and ε and the α and γ forms of ruthenium are approximately the same as those for iron without magnetic contributions. These assumptions permit calculation of the entire iron–ruthenium phase diagram and the T_0—x curves for the martensitic $\gamma\rightleftharpoons\alpha$ and $\gamma\rightleftharpoons\varepsilon$ reactions in reasonable agreement with experimental observation. In addition, the compositional dependences of the triple point pressure and temperature in the iron–ruthenium system have been computed and compare favourably with experiments. The driving force for the diffusionless $\gamma\rightleftharpoons\alpha$ reaction was found to depend on temperature in a manner similar to that observed for iron–nickel alloys, while the driving force for the diffusionless $\gamma\rightleftharpoons\varepsilon$ reaction was computed to be approximately 50 cal/mole. The latter value is smaller than the driving force for the $\gamma\rightleftharpoons\alpha$ transformation as expected from crystallographic considerations.

ACKNOWLEDGMENT

The author is indebted to Dr L. D. Blackburn of the Air Force Materials Laboratory, Dayton, Ohio, for permission to cite research results prior to publication.

REFERENCES

1. L. D. Blackburn *et al.: Acta Met.*, 1965, **13,** 533–541.
2. R. L. Clendenon and H. G. Drickamer: *J. Phys. Chem. Solids*, 1964, **25,** 865.
3. T. Takahashi and W. A. Basset: *Science*, 1964, **145,** 483.
4. J. C. Jamieson and A. W. Lawson: *J. Appl. Phys.*, 1962, **33,** 776–780.
5. L. Kaufman *et al.: Acta Met.*, 1963, **11,** 323–335.
6. F. P. Bundy: *J. Appl. Phys.*, 1965, **36,** 616.
7. L. Kaufman and M. Cohen: *Trans. AIME*, 1956, **206,** 1393–1401.
8. L. Kaufman and M. Cohen:' Progress in metal physics', VII, 165–246; 1958, London, Pergamon.
9. W. S. Gibson and W. Hume-Rothery: *JISI*, 1958, **189,** 243–250.
10. W. Obrowski: *Naturwiss.*, 1959, **46,** 624.
11. E. Raub and W. Plate: *Z. Metallk.*, 1960, **51,** 477–481.
12. L. Kaufman: *Acta Met.*, 1959, **7,** 575–587.
13. W. Hume-Rothery: *J. Less Common Met.* 1964, **7,** 152.
14. E. Anderson and W. Hume-Rothery: *ibid.*, 1960, **2,** 443.
15. L. D. Blackburn: Private communication, to be published.
16. L. D. Blackburn and C. Simmons: Private communication (M. S. Thesis submitted May 1964 by C. Simmons to Air Force Institute of Technology), to be published.
17. P. C. Johnson *et al.: J. Appl. Phys.*, 1962, **33,** 557–561.

A note on massive structures

W. S. Owen and E. A. Wilson

SYNOPSIS

The microstructural constituents described as 'massive' in a variety of ferrous and non-ferrous alloys are discussed. In general they are of two types: those formed by a transformation involving short-range diffusion and those formed martensitically. Consequently, it is proposed that the use of the adjective 'massive' should be confined to descriptions of the microconstituent and that the use of the term 'massive transformation' should be discontinued. The influences of composition, annealing temperature, and cooling rate in deciding which of the two transformations occurs are discussed briefly. 2614

MICROCONSTITUENT

THE WORD 'massive' was applied first by Greninger[1] who, in 1939, used it to describe a microconstituent in a Cu–9·3%Al alloy quenched from 1020°C. Volumes of the α-phase which appeared in the microsection as shapeless areas with very jagged and irregular boundaries were described as areas of massive α (Figure 1). They were recognized to be very similar to a microconstituent in a Cu–38%Zn alloy quenched from 850°C, described some years earlier by Phillips[2] (1930) and again by Baker[3] (1931). Slower cooling of the brass from the β condition results in the separation of α by long-range diffusion and the formation of a two-phase (α+β) structure. By showing that the massive α constituent is formed only when the cooling rate is sufficient to prevent this separation, Phillips recognized at the outset that the massive constituent is formed by a transformation which does not involve long-range diffusion. He wrote 'The cooling rate must be rapid enough to prevent any change in composition'. A more detailed study of the transformation of β-brass was reported by Hull and Garwood[4] (1955). They also describe a microconstituent massive α, but in this case some of the areas of α to which the term was applied were less jagged than those illustrated in the earlier papers, although the interfaces were made up of numerous planar facets (Figure 2).

Many other examples of massive volumes of a low-temperature phase (often, but not always, a primary phase) formed from a high-temperature phase of the same composition have been reported. Massalski[5] examined the structures formed by the transformation of the β-phase to massive ξ in copper–gallium, copper–gallium–germanium, and copper–zinc–gallium alloys. The β-copper–gallium alloys have been studied also by Spencer and Mack[6] and more recently by Suburi and Wayman.[7] Since the Greninger paper,[1] copper–aluminium has been studied by Gawranek *et al.*[8] and Swann and Warlimont[9] and copper–aluminium–nickel by Hull and Garwood.[10] Microstructures containing an α-phase exactly similar in appearance to the massive α in copper alloys have been found in a wide range of iron alloys. These massive α constituents, sometimes called 'equiaxed α',[12] have also formed from a high-temperature phase (γ) without a change in composition.[13] Microstructures containing massive α have been found in fairly pure iron,[11] iron–carbon,[12] iron–nitrogen,[12] iron–nickel,[12–15] iron–chromium,[13] iron–silicon,[13] and iron–manganese[16] alloys. There is no doubt that analogous microstructures can be formed in other alloy systems, for example in silver–cadmium,[17] and that the phenomena involved are quite general.

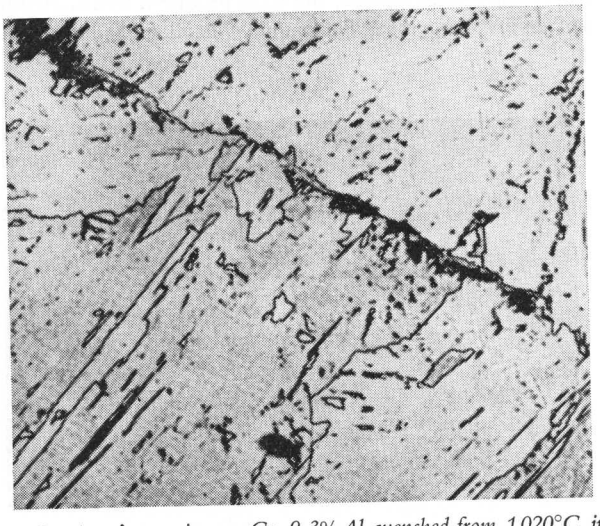

1 *Greninger's massive α; Cu–9·3%Al quenched from 1020°C in 10%NaOH; etched with $NH_4OH + H_2O_2$*[1] ×100

The authors are with the Department of Metallurgy, The University of Liverpool. (MG/Conf/76/65). UDC No.620.186.12

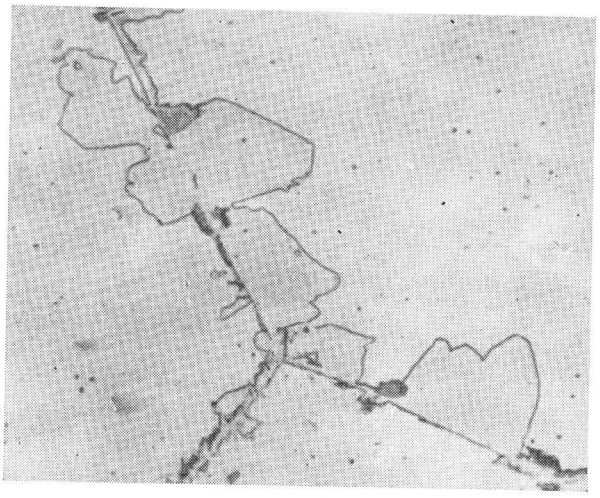

2 *Massive α in Cu–38·7%Zn quenched from 850°C into 10% NaOH at 0°C; etched in ammoniacal ammonium persulphate*[4] ×150

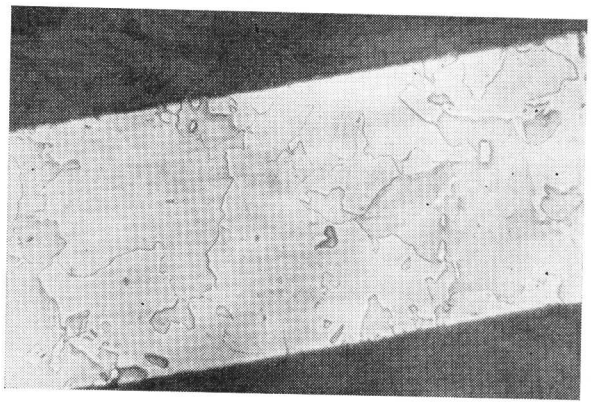

4 *Fe–6·0 at-%Ni quenched from 1100°C, etched in nital*[12] × 200

TRANSFORMATION

The word 'massive' has also been applied to classify a type of transformation. Following Massalski,[5] a massive transformation is defined in 'Perspectives in materials research'[18] as one which is essentially diffusionless but in which, unlike the martensite transformation, there is no shape change or surface relief. The word massive is a poor description of the transformation envisaged. It gives the impression of the *in situ* transformation of large volumes of the parent phase, whereas the atom transfer must occur across an interface which moves through each crystal separating the massive and parent phase. The wisest course would seem to be to confine the application of the word massive to descriptions of constituents of optical microstructures.

All microstructures containing a massive constituent do not form by the same transformation mechanism. Two extremes can be recognized: those formed by short-range diffusion across an incoherent, or possibly semi-coherent, interface with no resulting shape change, and those produced by a martensitic process involving shear. Kurdjumov[19] has described the former transformation as one of 'disorderly growth' but the term short-range diffusional (SRD) transformation is preferred. The massive grains grow by the movement of incoherent grain boundaries which are not restricted or impeded by the boundaries of the parent grains[5] through which they move. For example, Figure 5 shows the microstructure of an iron–nickel alloy annealed *in vacuo*, when the γ grain boundaries were thermally grooved, and then cooled to room temperature. The boundaries of the massive α have been revealed by etching and it is clear that these boundaries cross the γ boundaries without restriction. The boundaries of the parent phase can be seen also in Massalski's photomicrograph,[5] Figure 3, and clearly in this case also the massive constituent has grown across the original boundaries. The surface of specimens of iron–nickel transformed by SRD have been examined but no evidence of surface shears or other irregularities has been found.[12,13]

The other extreme, martensitic transformation, is represented by the transformation of iron–nickel alloys containing between 10 and 29·5%Ni.[12] Over a wide range of cooling rates these alloys transform from γ to α of the same composition. Alloys with the highest nickel content in this range do not transform completely and Figure 6 shows the appearance of masses of α in parent γ as revealed by etching a polished

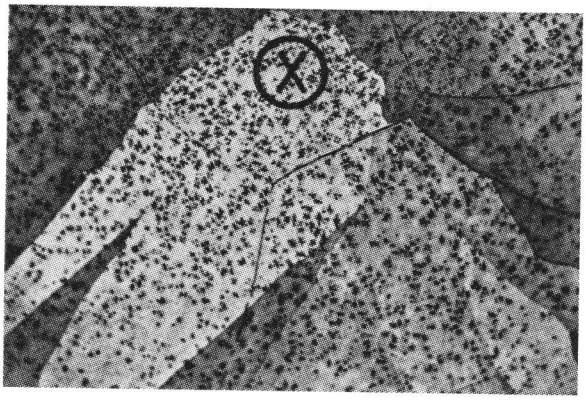

3 *Cu–18·4%Ga–5%Ge alloy quenched from 750°C, etched in alcoholic $FeCl_3$, polarized light*[5] ×150

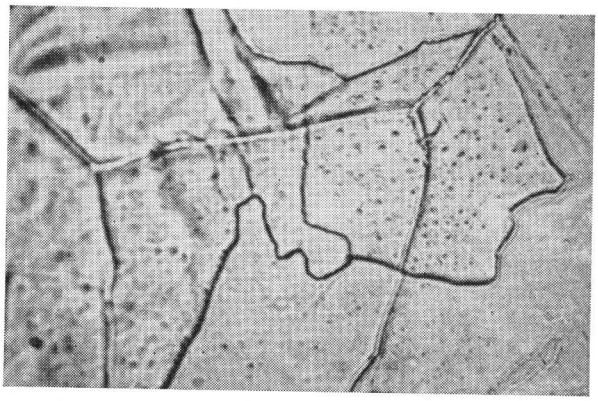

5 *Typical equiaxed α structure; Fe–4·0 at-%Ni; thermally etched to reveal austenite boundaries, quenched, and subsequently etched to reveal ferrite boundaries* ×880

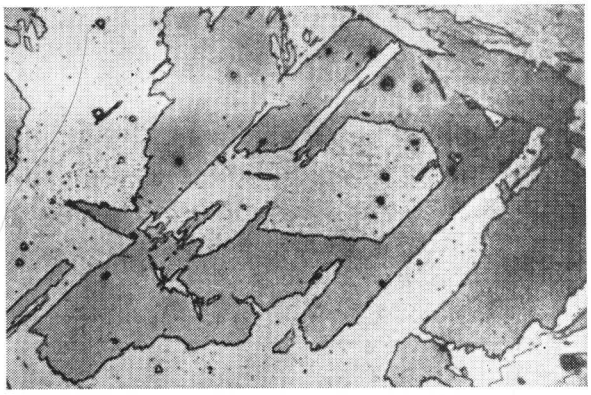

6 *Fe–28·8%Ni partially transformed by slow cooling to room temperature; etched in 10% aqueous ferric chloride followed by 30% aqueous sodium bisulphite*[15] ×500

surface.[15] With lower nickel contents all the γ is transformed and the massive α structure with jagged boundaries shown in Figure 7 is obtained. It is an important feature of this transformation that the change can go to completion and it does so, leaving no 'retained austenite', if the cooling is continued through the necessary temperature range. It is evident from the surface-relief structure that the masses of α are made up of packets each containing a large number of parallel, or in some places interlacing, shear plates[12,15] (Figure 8). Thus, the transformation is martensitic and the product could be designated massive α′. The shear plates do not cross the γ-phase grain boundaries (which in Figure 8 are revealed by thermal grooving) and the volumes of α are smaller than the volume of a γ-grain, but otherwise the masses of α are not related to the parent grain. Although there is little doubt that the masses of α′ are made up of shear plates, the individual plates cannot be revealed by the conventional etching techniques. This type of martensite is strikingly different in microstructural appearance from the more familiar acicular forms of martensite which consist of single or connected lenticular martensite plates

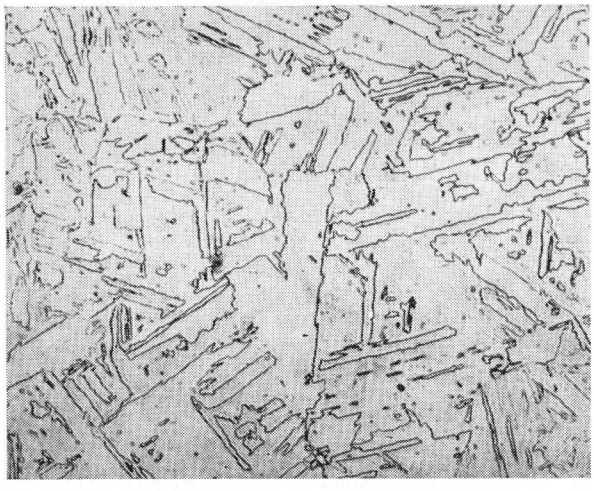

7 *Fe–23·8 at -%Ni quenched from 1100°C, etched in nital*[12] ×350

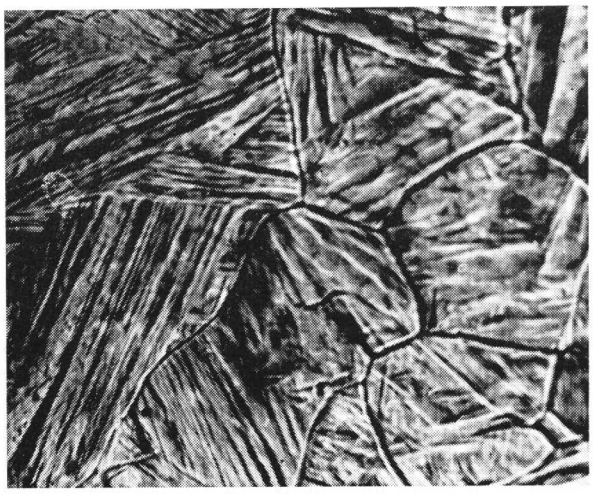

8 *Surface shears on pre-polished specimen of Fe–15%Ni transformed at 388°C* ×875

embedded in a matrix of retained parent phase. Since it is often convenient, and for some purposes important, to distinguish between the two general forms of martensite the terms massive martensite and acicular martensite have been introduced.[12]

However, identification of the type of transformation producing many of the massive microconstituents observed is not always so straightforward. Unfortunately, considerable experimental difficulties are often encountered when attempts are made to observe surface shears on specimens polished before transformation, and it is then necessary to resort to deductions from less direct evidence, such as that provided by optical examination of etched specimens or electron-transmission micrography of thin foils. In many structures short straight lengths of boundary are observed in optical microstructures. These suggest the possibility of the existence of a martensitic transformation by the movement of a planar semi-coherent interface, although the geometric arrangement of shear plates which could produce the shape of massive constituent observed is sometimes difficult to visualize. The first study of a planar boundary was made by Hull and Garwood,[4] who found that of the planar facets enclosing massive α grains grown in the β-phase of a Cu–39·0%Zn alloy (Figure 2) about 10% corresponded to $\{001\}_\beta$, 30% to $\{011\}_\beta$, and 40% to $\{112\}_\beta$. However, it was noticed that in some β-grains many of the traces of the boundary planes in the plane of polish were parallel to martensitic surface shear markings in the grains and, on reassessing the boundary traces, it was found that 40% of the trace normals intersected $\{115\}_\beta$, reducing to 20% the number of solutions of the $\{112\}_\beta$ type. It had been shown previously[20] that the martensite habit plane is close to $\{155\}_\beta$. From these observations it was suggested that a 'dislocation mode of growth' might operate during the growth of massive α. In the copper–gallium system massive ξ with straight boundary segments occurs in some alloys (Figure 3). Frequently, two parts of a crystal separated by a planar interface are twin-related[5] but Saburi and Wayman[7] found that more frequently many of the straight boundaries in microstructures

of massive ξ are traces of planes parallel to internal stacking faults in massive ξ. Bowles and Barrett[21] suggested that if the orientation relationship between the parent and the new phase is the same for both the diffusion-controlled and martensitic transformations, they may have grown from the same nucleus. Massalski[5] adopted this concept to explain some of his results and later Saburi and Wayman concluded that their observations also supported the idea that a martensitic lattice correspondence exists at the nucleation of the massive ξ. Very little information about the orientation relationships between a growing massive constituent and the parent phase is available but what there is[5] suggests that an unlimited number of orientations are possible. This, together with the observation that the stacking faults in massive ξ are of variable density and non-uniform spacing, caused Saburi and Wayman to discount the idea that there is a martensitic element in the *growth* of massive ξ. It seems most likely that the planar boundaries develop because, during the growth of the massive constituent, segments of low-energy, relatively immobile interface develop and become progressively more extensive simply because they move more slowly than the adjacent high-angle boundary. There is an analogy with the development of a twin interface during the growth of annealing twins. It is expected that such planar interfaces will be rational.

COMPETITION BETWEEN SRD AND MARTENSITIC TRANSFORMATION

Alloy systems are known in which either an SRD or a martensitic transformation to produce a massive microconstituent can occur, depending upon the composition of the parent phase, the annealing temperature (and hence the grain size of the high-temperature phase), and the cooling rate. Very little undercooling is required for the SRD transformation to occur in the copper–gallium alloys,[7] and in iron–nickel, iron–chromium, and iron–silicon alloys it has been shown[13] that the free-energy change accompanying the transformation is only 20–80 cal/mole (compared with about 300 cal/mole for the transformation to massive α′), so that the degree of undercooling below T_0 (the temperature at which the free-energy of the parent and product phases is equal) is very small. The SRD transformation is thermally activated and can be suppressed by rapid cooling. The range of composition in which a complete change in transformation mechanism can be effected by changing the cooling rate, within practical limits, is usually small. In the iron–nickel system, about 4–10%Ni either massive α or massive α′ can be obtained, but at lower nickel contents the product is always massive α and at high nickel contents massive α′. At 29·5%Ni or more a subzero transformation produces an acicular martensite. Recent experiments have shown that the annealing temperature can also influence the choice of transformation. An Fe–10%Ni alloy when annealed in the γ temperature range (austenitized) at any temperature between 700° and 1200°C and cooled at 50 deg C/s transformed at about 530°C to massive α. However, when the same series of experiments was repeated using a cooling rate of 300 deg C/s, the specimens austenitized below about 1050°C transformed at 530°C by SRD to massive α, but those austenitized between 1050° and 1200°C transformed martensitically at a much lower temperature (450°C) to give

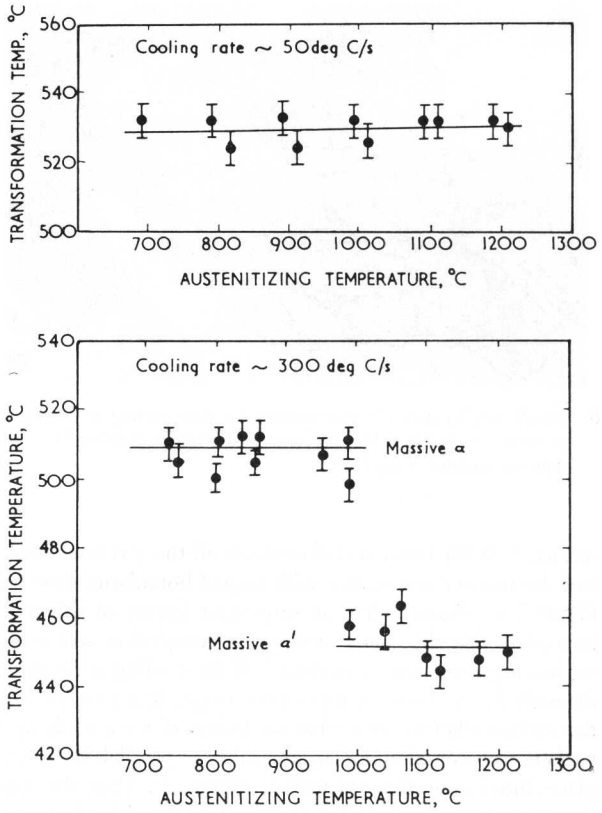

9 *Transformation temperatures of an Fe–10%Ni alloy as a function of austenitizing temperature*

massive α′. The experimental data are given in Figure 9. Increasing the austenitizing temperature produced an appreciable increase in the size of the γ-grains and thus a decrease in the grain-boundary area per unit volume. Thus, if it is assumed that massive α is nucleated at the boundaries of the γ-grains,

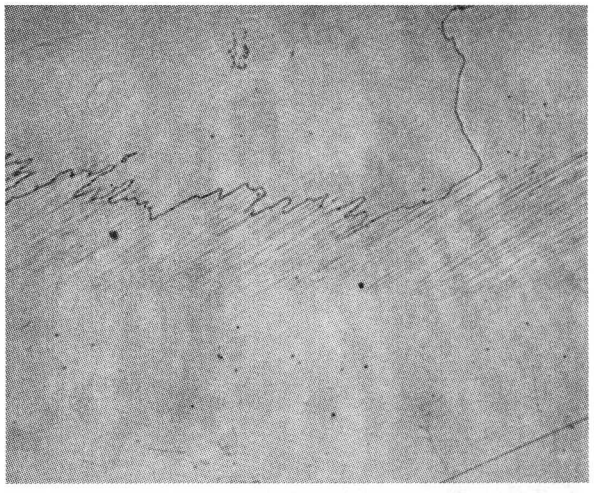

10 *Cu–23·86%Ga quenched in 10%NaOH from 750°C; etched in $NH_4OH + H_2O_2$, polarized light*[5] ×200

the effect of austenitizing temperature may be due simply to the change in grain size. There is a general impression, although no definitive experimental demonstration has been reported, that martensitic transformations are less affected by the grain size of the parent phase. The nucleation of massive α at the grain boundaries of the β-phase in a brass was demonstrated by Hull and Garwood[4] by the metallographic examination of partially transformed specimens (Figure 2).

Since the SRD transformation is isothermal, on continuous cooling a specimen may transform partially by this mechanism and then, at some low temperature, complete the transformation martensitically. An example, described by Massalski,[5] is illustrated in Figure 10. A Cu–23·86 at-%Ga alloy quenched relatively slowly from the β-phase to allow some separation of γ to occur on cooling through the $(\beta+\gamma)$ phase field, contains at room temperature both massive ξ and β' martensite. The jagged interface is formed by the interaction of these two structures in adjacent grains. It is probable that many of the jagged outlines of massive areas observed in optical micrographs are the result of the parent phase transforming partially by the formation of shear plates.

REFERENCES

1. A. B. Greninger: *Trans. AIME*, 1939, **133,** 204–227.
2. A. J. Phillips: *ibid.*, 1930, **89,** 194–202.
3. R. S. Baker: *Trans. ASM*, 1931, 159.
4. D. Hull and R. D. Garwood: Institute of Metals Monograph and Report Series No. 18, 219, 1955.
5. T. B. Massalski: *Acta Met.*, 1958, **6,** 243–253.
6. C. W. Spencer and D. J. Mack: *J. Inst. Metals*, 1955–56, **84,** 461–466, and in 'Decomposition of austenite by diffusional processes', (ed. V. F. Zackay and H. I. Aaronson), 549; 1962, Interscience.
7. T. Saburi and C. M. Wayman: Private communication.
8. V. Gawranek *et al.*: *Metallwirtschaft*, 1936, **15,** 370–371.
9. P. R. Swann and H. Warlimont: *Acta Met.*, 1963, **11,** 511–527.
10. D. Hull and R. D. Garwood: *J. Inst. Metals*, 1957–58, **86,** 485–492.
11. R. F. Mehl and D. W. Smith: *Trans. AIME*, 1934, **113,** 203–210.
12. W. S. Owen *et al.*: 'The structure and properties of quenched iron alloys'; Second International Materials Symposium, University of California, 1964.
13. A. Gilbert and W. S. Owen: *Acta Met.*, 1962, **10,** 45–54.
14. R. B. G. Yeo: *Trans. AIME*, 1962, **224,** 1222–1227.
15. R. B. G. Yeo: *Trans. ASM*, 1964, **57,** 48.
16. E. A. Wilson: unpublished work.
17. G. R. Speich and D. J. Mack: *Trans. AIME*, 1953, **197,** 548.
18. M. Cohen *et al.*: 'Perspectives in materials research', Office of Naval Research, US Navy, 1961, 315.
19. G. V. Kurdjumov: *Probe. met. fiz. met.*, 1952.
20. A. B. Greninger and V. G. Mooradian: *Trans. AIME*, 1938, **128,** 337–368.
21. J. S. Bowles and C. S. Barrett: 'Progress in metal physics', III, 1–41; 1952, London, Pergamon.

Microstructure, crystal structure, and mechanical properties of martensite phases in copper alloys

H. Warlimont

SYNOPSIS

Recent determinations of the microstructures and crystal structures of the martensitic phases in Cu–Al, Cu–Sn, Cu–Zn, and Cu–Ga–Zn alloys, mainly performed by transmission electron microscopy, are described. The mechanisms of nucleation and growth are discussed. The crystal structures and mechanical properties of the martensite phases are analysed in relation to the corresponding features of the stable phases. 2584

INTRODUCTION

The martensitic transformations of β-Cu alloys have been investigated intensively for a long time,[1] but details of the microstructures and some of the crystal structures of martensitic phases were detected and determined by transmission electron microscopy and selected area electron diffraction only recently.[2–7] The purpose of this paper is to survey these recent results rather than to review the entire field of martensitic transformations of β-Cu alloys. Furthermore, the presentation will essentially be restricted to martensite phases formed upon quenching. However, martensite phases arising from deformation will be treated briefly in the appropriate context.

Before describing the martensite phases, their formation and interrelation, it is useful to refer to the constitution of the relevant phase equilibria. The β-phase fields and related phase equilibria of the Cu–Al, Cu–Ga, Cu–Sn, and Cu–Zn systems are shown in the upper parts of Figures 1–4, together with some transformation temperatures and composition ranges of martensitic and ordered metastable phases in the lower sections of the figures. The bcc (A2) β-phase occurs in equilibrium with the fcc terminal α-phase in all cases. Depending on the system the phases at higher solute concentrations are: an ordered bcc ($L2_1$) phase, an ordered hcp ($DO_{19}S_{1/2}$) phase, or the γ-brass type ($D8_2$) phase. At lower temperatures an ordered bcc (B2) phase, an hcp (A3) phase, or a two-phase mixture of α and one of the phases mentioned are in equilibrium. From crystallographic considerations it would be expected that under suitable thermodynamic conditions the β-phase would transform martensitically into either fcc or hcp structures. A martensitic transition of the β-phase into the γ-brass type structure is not to be expected because of the atom distribution in the γ-brass unit cell which cannot be achieved by the shear and dilatational strains to which martensitic transformations are restricted. In comparing these considerations with the actual observations which are summarized in Table I it may be noticed that all martensite phases in the relevant systems may be ascribed to either the bcc→fcc or the bcc→hcp transition.

For the purpose of this paper the martensite phases are designated in such a way that phases of identical crystal structure (orthorhombic distortion of close-packed lattices being disregarded) are given a common symbol. Based mainly on usage in the past the following symbols are applied:

- β: bcc–fcc transition
- γ: bcc–hcp transition ($e/a=1{\cdot}5$)
- ε: bcc–hcp transition ($e/a=1{\cdot}75$)
- $_1$: derived from Fe_3Si ($L2_1$) type superlattice
- $_2$: derived from CsCl (B2) type superlattice
- ′: faulted or twinned
- ″: lamellar composite of two structures
- +: obtained by deformation.

When analysing the martensitic transformation products in detail it becomes evident that, in general, their crystal structures are more complex than indicated above. This is for two reasons:

(i) stacking faults present in the fcc martensites due to the 'inhomogeneous shear' or 'lattice invariant deformation'[8]★ occur in a statistically ordered array contributing to the crystal lattice an additional periodicity normal to the faulting planes; this applies to the β′, β'_1, β'_2, and β''_1 martensites

(ii) during quenching and before the martensitic transformations most alloys (except for copper-rich Cu–Al and Cu–Ga alloys) undergo an ordering transformation and

The author is at the Max-Planck-Institut für Metallforschung, Stuttgart, Germany.(MG/Conf/77/65). U.D.C. No. 669.15:669.112.227.34. 536.7

★The term 'inhomogeneous shear' is preferred to the term 'lattice invariant deformation' in this paper because the resulting lattice defects of some of the martensite phases are more appropriately treated as components of the crystal lattices.

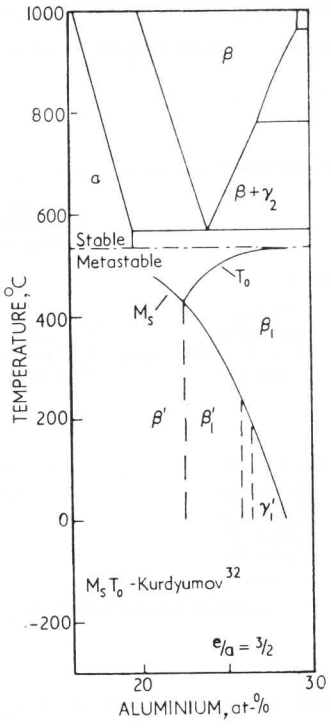

1 *Cu–Al*

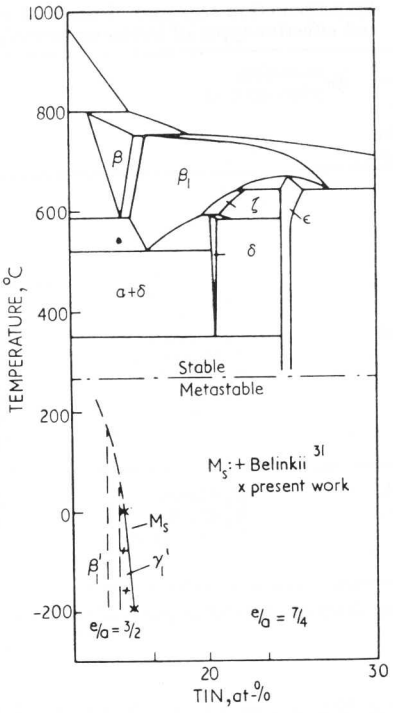

3 *Cu–Sn*

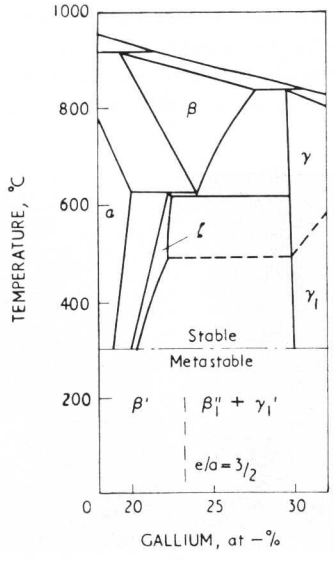

2 *Cu–Ga*

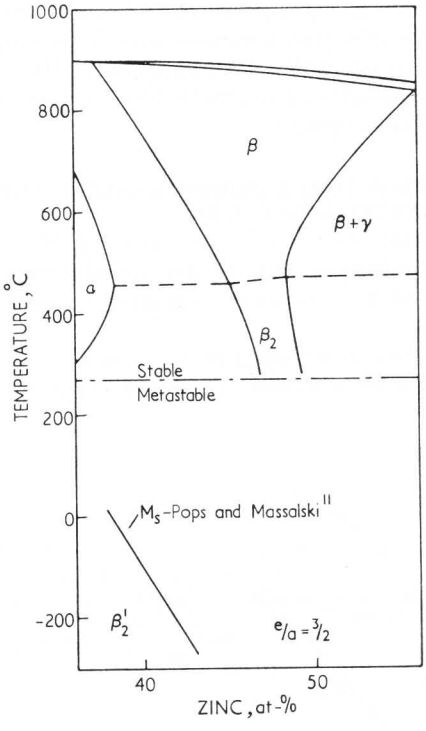

4 *Cu–Zn*

1–4 *Stable and metastable phases in relation to the β-phase of some copper alloys*

TABLE I Transformation sequence of the Cu-base Martensite phases, qualitative description of their resulting crystal structures and effective types of inhomogeneous shear

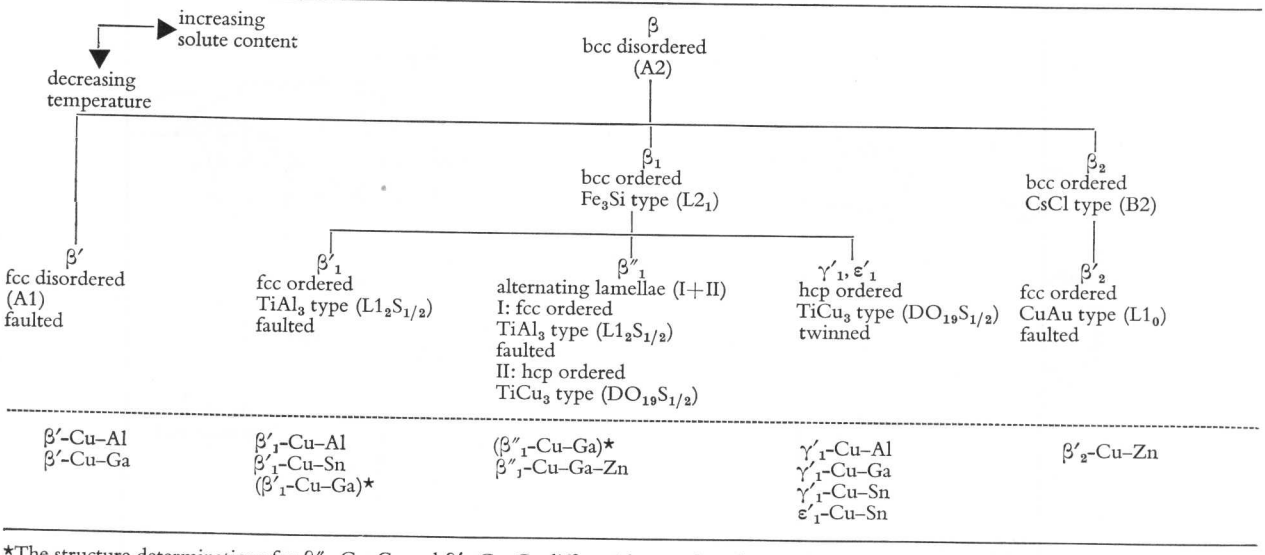

*The structure determinations for β''_1-Cu–Ga and β'_1-Cu–Ga differ with regard to the simultaneous presence of the $DO_{19}S_{1/2}$ structure.[6,7]

the resulting atomic order is incorporated in the martensite lattice; this applies to the β'_1, β'_2, β''_1, and γ'_1-martensites; the resulting unit cell is hexagonal for the β' and orthorhombic for all other martensites.

Before dealing with the structures in detail it is useful to note that the general basic transformation mechanism involved[9] is the transition of $(011)_{bcc}$ planes by appropriate shears $\pm[01\bar{1}]_{bcc}$ into the final stacking sequences of the respective crystal structures, and by appropriate distortions $\varphi_{bcc}=70°32' \rightarrow \varphi_{fcc}=\varphi_{hcp}=\varphi_{orthorhombic}\simeq 60°$ into close packed planes $(111)_{fcc}$, $(00.1)_{hcp}$, or $(001)_{orthorhombic}$, respectively. These elementary relations are illustrated in Figure 5.

MICROSTRUCTURES, INHOMOGENEOUS SHEARS, AND CRYSTAL STRUCTURES

In this section on the microstructures and inhomogeneous shears the ordering reactions are disregarded in order to clarify the effects of the inhomogeneous shears in the apparent crystal structures.

The essential contribution of transmission electron microscopy to the determination of martensitic structures is that it reveals the mode of the inhomogeneous shear operative in a diffusionless transformation. Thus, although all of the martensite phases which are discussed here exhibit essentially the same plate-like microstructure in the light microscope they differ markedly in appearance in the electron microscope.

Figures 6 and 7 show the microstructure characteristic of the interior of plates of the β', β'_1, and β'_2-martensites in two different orientations to the electron beam. They contain stacking faults which are seen 'on edge' in Figure 6 and somewhat inclined to the beam, exhibiting the typical contours, in Figure 7. Diffraction analysis of these martensites confirms that their formation is accompanied by the production of a profusion of stacking faults on one set of lattice planes and with a common Burgers vector. Since most of these faults are distributed uniformly throughout the volume of every plate, the resulting statistically periodic stacking sequence of close-packed planes may be described in first approximation in

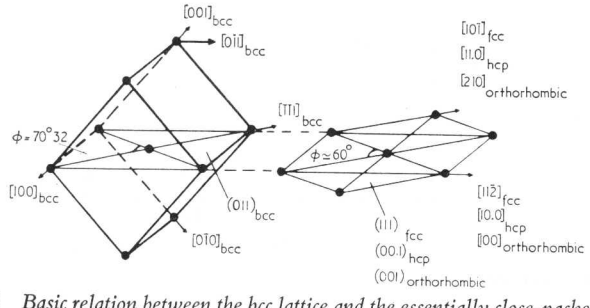

5 *Basic relation between the bcc lattice and the essentially close-packed structures resulting from martensitic transformation*

6 *Interior of a β'_1-martensite plate with striations due to stacking faults parallel to the electron beam; Cu–13·7 at-% Sn; transmission electron micrograph* ×70000

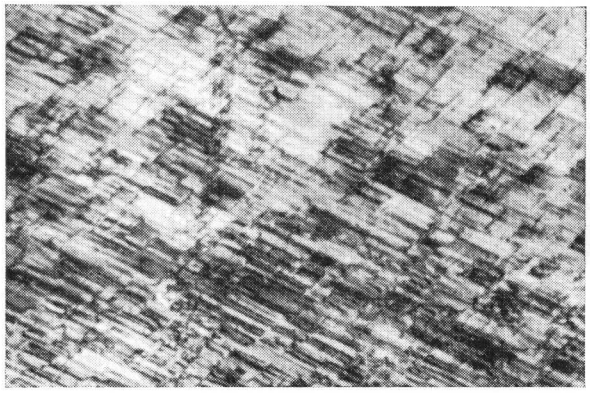

7 *Interior of a β'_1-martensite plate with stacking faults and partial dislocations inclined to the electron beam; Cu–13·7 at-%Sn; transmission electron micrograph* ×30000

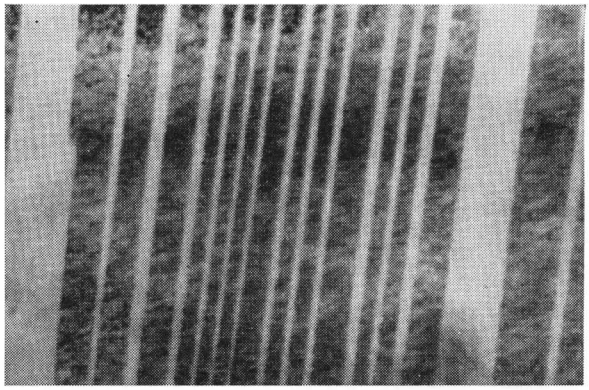

9 *Interior of a γ'_1-martensite plate with twin interfaces parallel to the electron beam; Cu–15·1 at-%Sn; transmission electron micrograph* ×80000

orthorhombic symmetry with the close-packed plane being taken as the *a–b* plane and with the identity period of the stacking sequence, or at least a whole-number ratio of faults per plane, determining the number of planes in the *c*-direction and hence the *c*-parameter of the 'unit cell'. An example of a pertinent diffraction pattern which is practically identical (except for orthorhombic distortion) for a $[\bar{2}10]$ orientation of the β', β'_1, and β'_2-martensites is shown in Figure 8. Three features of this diffraction pattern corroborate the proposed mode of inhomogeneous shear, by faulting, of these martensites:

(i) the main reflections are displaced to a position intermediate between the fcc and hcp reflections indicating some intermediate mode of stacking order[10]

(ii) the presence of additional reflections indicates the stacking sequence of the close-packed planes to be statistically ordered

(iii) the continuous streaking along the reciprocal lattice directions normal to the fault planes indicates that the stacking sequence remains to some extent random.

It ought to be realized that the stacking fault contrast in the microstructure arises only from random faults since the ordered 'faults' are part of the lattice periodicity and will, therefore, not be visible. Thus, although it can be inferred that the transformations into β', β'_1, and β'_2 are of the bcc–fcc type, the resulting apparent orthorhombic crystal structures reflect this transition only indirectly.

Turning to the γ'_1-martensite phases it may be seen from their characteristic microstructure in Figure 9, and from selected area diffraction patterns of appropriate crystal orientations such as that shown in Figure 10, that they consist basically of a twinned hexagonal structure. The twinning accounts for the inhomogeneous shear in this case. For all martensitic transformations in copper alloys analysed so far it could be shown that the density of the stacking faults and relative amount of the twins, respectively, account quantitatively for the amount of inhomogeneous shear involved in the particular transformation concerned.

A uniquely complex structure is obtained for the β''_1-martensite in Cu–Ga and Cu–Ga–Zn[6] alloys. The microstructure indicates a lamellar product (Figure 11). The diffraction patterns, as in Figure 12, show two crystal structures superimposed. One of these corresponds to the orthorhombic structure arising from a regularly faulted fcc lattice, similar to the β', β'_1, and β'_2 crystal structures. The other is an hcp structure (disregarding the superlattice) like that of the γ'_1-phase. These two different crystal structures, arranged in alternating lamellae, form the β''_1-martensite. From assessing the 'fault' density of the 'faulted fcc' component and measuring the relative lamellar thicknesses of both components the composite inhomogeneous shear amounts to the shear which may be derived from the theory of martensite crystallography within the accuracy of measurements.

The structural data of the martensite phases described in this section are summarized in Table II. In referring to the stacking sequences and *c*-parameters of the β-type martensites it should

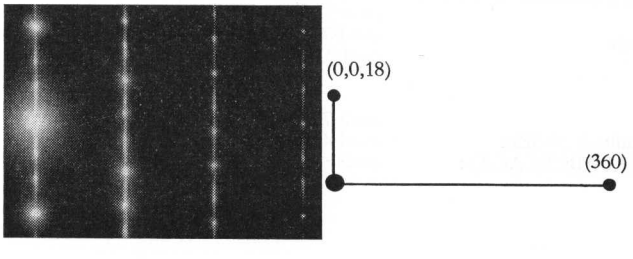

8 *Electron diffraction pattern of β'_1-martensite, zone $[\bar{2}10]$; Cu–13·7 at-%Sn*

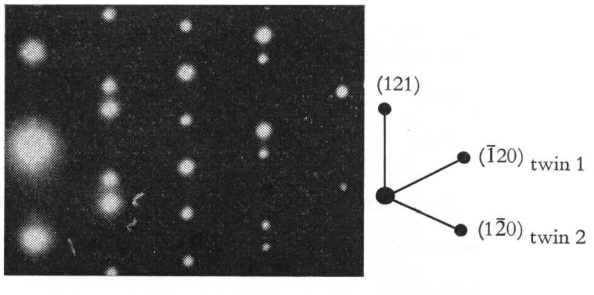

10 *Electron diffraction pattern of γ'_1-martensite zone $[21\bar{4}]$; Cu–15·1 at-%Sn*

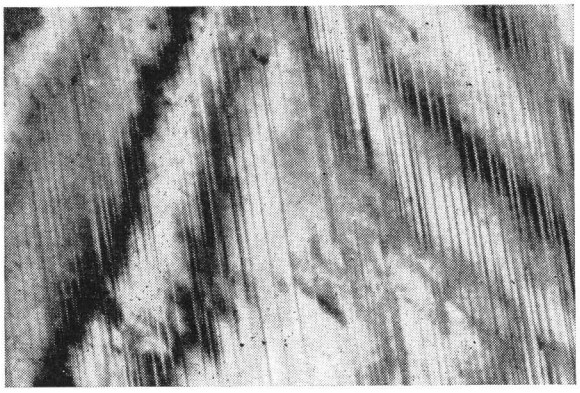

11 *Interior of a β''_1-martensite plate with interfaces of the lamellae parallel to the electron beam; Cu–12·6 at-% Ga–19·2 at-%Zn; transmission electron micrograph* ×70000

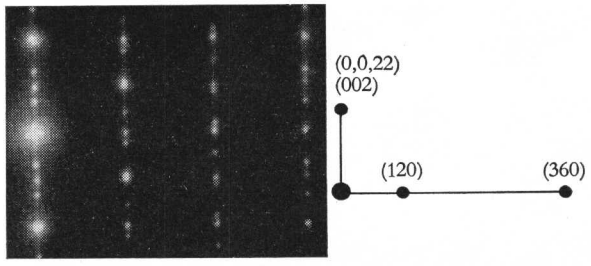

12 *Electron diffraction pattern of β''_1-martensite showing the reflections of a faulted and ordered fcc and an ordered hcp structure superimposed; zones* [$\bar{2}$10] *(orthorhombic unit cells); Cu–12·6 at-%Ga–19·2 at-%Zn*

be remembered that these represent only a best-fit approximation of the stacking order and do not have the same meaning as in the description of phases in stable equilibrium. This may also explain some of the uncertainties[24] remaining in a recent meticulous crystallographic analysis of X-ray data of Cu–Zn martensite.[47]

RELATIONS BETWEEN METASTABLE AND STABLE PHASES

All metastable ordered and martensitic crystal structures correspond to stable phases occurring in quasi-homologous systems.

The occurrence of the superlattice of the β_1-phase in Cu–Sn alloys is mainly due to the difference in atomic size of the components, as may be seen by comparison with the data for the Cu–Sb system in Table III. The metastable occurrence of β_1-phases in Cu–Al and Cu–Ga alloys where the size factor is less

TABLE II Crystallographic data of martensite phases formed from β-Cu phases*

Alloy system	Martensite phase and composition range, at -%	Martensite structure <stacking sequence>	Lattice parameters	References
Cu–Al	β'	hexagonal ($\triangle$A1, faulted)		2,4
	20–22·5 Al	⟨BABCBCACABA⟩		
	β'_1	orthorhombic ($\triangle L1_2S_{1/2}$, faulted)		3,4
	22·5–26·5 Al	24·38 Al: ⟨ABCBCACABAB⟩;	a=4·494 Å, b/a=2/$\sqrt{3}$,	4
		or	c/a=22$\sqrt{2}$/3	
		23·8 Al: ⟨ABCBCACAB⟩	a=4·49 Å, b/a= 2/$\sqrt{3}$,	3
			c/a=18$\sqrt{2}$/3	
	γ'_1	orthorhombic $DO_{19}S_{1/2}$	a=4·51 Å, b=5·20 Å,	20
	26–28 Al	(twinned)	c=4·22 Å	
Cu–Ga	β'	A1, faulted		7
	22·7 Ga			
	β''_1	lamellar composite of orthorhombic		6
	23·7 Ga	($\triangle L1_2S_{1/2}$, faulted) and orthorhombic $DO_{19}S_{1/2}$		
	γ'_1	orthorhombic $DO_{19}S_{1/2}$ (twinned)		6
Cu–Ga–Zn	β''_1	lamellar composite of orthorhombic		6
	12·6Ga, 19·2Zn	($\triangle L1_2S_{1/2}$, faulted approx.: ⟨ABCBCACABABCBCACA⟩) and orthorhombic ($\triangle DO_{19}S_{1/2}$)	a=4·45 Å; b=5·35 Å; c=72·4 Å	
Cu–Sn	β'_1	orthorhombic ($\triangle L1_2S_{1/2}$, faulted) 13·7Sn:		5
	13·1–14·8 Sn	⟨BABCBCACABA⟩	a=4·46 Å, b/a= 2/$\sqrt{3}$,	
			c/a=22$\sqrt{2}$/3	
	γ'_1	orthorhombic $DO_{19}S_{1/2}$ (twinned) 15·5 Sn	a=4·55 Å, b=5·36 Å,	21,5
	14·5–16·3 Sn		c=4·31 Å	
	ε'_1	orthorhombic $DO_{19}S_{1/2}$	a=4·772 Å, b=5·514 Å,	22
	25 Sn		c=4·335 Å	
	ε^+			5
	25 Sn			
Cu–Zn	α^+_1	fct ($L1_0$) 38·0Zn:	a=3·775, c/a=0·943	23
	β'_2	orthorhombic ($L1_0$, faulted) 39·5Zn:	a=4·417 Å, b=2·665 Å,	6,24
	38–41·5 Zn	approx. ⟨ABCBCACABABCBCACA⟩:	c=36·29 Å	
	$\beta^+_{(2)}$	fcc (faulted)		33
	~39–49 Zn			
	$\gamma^+_{(2)}$	hcp (faulted)		33
	~44–52 Zn			

*Details concerning the atomic order of some structures have been omitted from this table.

TABLE III Factors governing superlattice formation in β-Cu alloys

System	Volume size factor,* $\frac{\Omega_x - \Omega_{Cu}}{\Omega_{Cu}}$, %	Difference in (Pauling's) electro-negativity	Superlattice structure and stability
Cu–Al	+20·3	0·4	$L2_1$, metastable
Cu–Ga	+24·6	0·3	$L2_1$, metastable
Cu–Sb	+89·0	0·0	$L2_1$, stable
Cu–Sn	+85·6	0·1	$L2_1$, stable
Cu–Zn	+19·9	0·3	B2, stable

*Ω_x: mean vol/atom of the solute obtained by extrapolation from the values in Cu-rich phases to 100% solute; Ω_{Cu}: vol/atom of Cu; data taken from Massalski and King.[12]

favourable may be ascribed to the appreciable electrochemical factor involved as listed in the third column of Table III. This conclusion is supported by the correspondingly high value of the electrochemical factor for Cu–Zn alloys which suffices in that case to stabilize the superlattice of the β_2-phase.

Turning to the martensitic phases, it may be noted first, referring to Figures 1–4, that the fcc β-type martensites are forming as a metastable extension of the α solid solution in accordance with the phase equilibria, the β′-martensite phases being 'pure' examples. The atomic order of the β-type martensite phases corresponds to a general occurrence of stable superlattice structures in α-brass type alloys. Thus the $TiAl_3$ type ($L1_2S_{1/2}$) structure of β'_1-martensite (disregarding the stacking faults) occurring at $e/a \approx 1{\cdot}4$—$1{\cdot}5$ is characteristic of this range of electron concentration[13–15]; similarly the Cu Au type ($L1_0$) structure of β'_2-martensite (again disregarding the stacking faults) at $e/a \approx 1{\cdot}0$ is characteristic of that range.[13,15]

Regarding the hcp martensite phases the occurrence of electron compounds in this family of alloys (at $e/a = 1{\cdot}5$ and $1{\cdot}75$ respectively) exerts a remarkable influence. The formation of two nearly hcp martensite phases (γ'_1 and ε′) in Cu–Sn alloys which are isotypical to the stable ε-phase (disregarding the 'shift' periodicity[13,15] of the ε-structure) is a characteristic example of this influence. The Cu–Sn system constitutes a unique case because the β_1 high-temperature phase extends from 13 to 27 at-% Sn ($e/a = 1{\cdot}39$–$1{\cdot}81$) and may, therefore, transform martensitically into the γ'_1 as well as into the ε_1-phase at 15–16 at-% ($e/a = 1{\cdot}45$–$1{\cdot}48$) and at ≈ 25 at-% ($e/a \approx 1{\cdot}75$), respectively, with no martensitic transformation (at least down to about —200°C) at intermediate compositions. Usually, the concentration range of the β (β_1) phase is limited so that it does not extend up to the electron concentration $e/a = 1{\cdot}75$. Since, normally, only one hcp phase occurs in stable equilibrium in any one system, the observations in most of the alloys considered in this paper show that both electron concentrations concerned may give rise to hcp lattices if conditions to form metastable phases are provided. This applies, also, to the formation of a hexagonal martensite phase γ^+ in Cu–Zn alloys by deformation[33] in a concentration range where no martensite occurs on quenching but where the electron concentration is about 1·5. Hardly anything needs to be said about γ'_1-Cu–Ga: subsequent to the ordering transformation, the hcp substructure is the expected result of the martensitic transformation. With γ'_1-Cu–Al ($e/a = 1{\cdot}4$–$1{\cdot}5$) the electron concentration rules for the hcp structure may be invoked once again and similar conclusions may be drawn as for γ'_1-Cu–Sn.

An interesting observation was made regarding the relations between the concentration dependence of the stacking fault energy of the α-phase and the relative stability of the β'_1 and γ'_1 martensites[2]: in accordance with corresponding measurements in Co–Ni alloys the stacking fault energy of the fcc phase goes to zero in the $\beta_1' + \gamma_1'$ two-phase field. Similarly, the solute concentration at which a stable or metastable hcp phase occurs may be derived from the variations of the stacking fault probability with solute concentration in the fcc phase and its extrapolation to 0·5. Recent observations on copper and silver alloys based on extensive X-ray line shift measurements have corroborated this interrelation.[48]

Finally the stacking faults of the β-type martensites should be discussed with respect to their density and ordered distribution, since it has been argued[4] that they may arise through the strain requirements of the martensitic transformation as well as through structure chemical requirements. Regarding their origin in terms of the mechanism of martensitic transformation the ordered array of stacking faults can be interpreted as an optimally uniform distribution to minimize strain energy. This interpretation is supported by the good agreement of the theoretically computed and experimentally observed stacking density parameters.[2–7] However, it has also been considered[4] that stacking fault densities and distributions of the β-martensite structures at respective electron concentrations occur corresponding to those in stable phases of related alloy systems, e.g. in Au–Cd–In alloys.[16] (The lack of microstructural observations and the kind of heat treatments employed in the cited work do not exclude the possibility that metastable states may have been assumed to be at stable equilibrium.) Whether or not this correspondence is coincidental may best be checked by investigating martensitic structures which have not been formed in bulk material by quenching but under conditions of altered constraints, e.g. in thin foils or by the straining of single crystals. Such experiments have been performed,[17,23] and for the martensitic transformation of β-brass in thin foils[17] it has been found that an inhomogeneous shear occurs either by twinning or not at all, depending on the thickness of the foil. Likewise, straining of β_1-Cu–Zn single crystals to form martensite[23] results in an essentially perfect AuCu ($L1_0$) type structure, i.e. without an appreciable amount of faulting. In these experiments the colour was observed to change from the yellowish β-brass into the pink α-brass variant during transformation. These examples suggest strongly that the density and distribution of stacking faults in the β-type martensites formed by quenching in bulk material are due to the response of the new phase to the constraints imposed by the matrix rather than to structure chemical influences.

ORIENTATION RELATIONSHIPS AND HABIT PLANES

The geometrical theories of martensite transformations[25–27] provide a means to link and countercheck the determinations of martensite structures, orientation relationships, and habit planes, and the assumptions about the lattice correspondences involved. As applied to the martensite transformations in copper alloys they have corroborated the crystallographic and

TABLE IV Orientation relationships, habit planes, and inhomogeneous shear data*

Martensite phase	Alloy system	Orientation relationship		Habit plane		Stacking fault density α		Ratio of twin thickness, $\frac{x}{1-x}$		References
		theoretical	observed	theoretical	observed	theoretical	observed	theoretical	observed	
β', β'_1	Cu–Al		{001} β', 4° ∢{001}β corresponding pole figures corresponding to Cu–Al	~°3 ∢{133}β	~2° ∢{133}β	0·355	0·364	—	—	23, 2, 4 18
	Cu–Sn			~{133}β	~{133}β	0·355	0·36	—	—	18, 5, 30
γ'_1	Cu–Al	(011)γ', 4° ∢(011)β	(001)γ', 4° ∢(0$\bar{1}$1)β	~{133}β	~{122}β	—	—	3·5	1·3–3·3	29, 19, 2
		[110]γ'_1, 5° ∢(111)β	[110]γ'_1~ ||[11$\bar{1}$]							
	Cu–Sn	corresponding to Cu–Al	(001)γ'_1, 2° ∢(011)β			—	—	—	1·2–2·0	21, 5

* Most orientation and habit plane data have been simplified for clarity and brevity.

13 *Parts of two β''_1-martensite plates containing stacking faults on a slip plane different from that of the main martensitic inhomogeneous shear; Cu–12·6 at-%Ga–19·2 at-%Zn; transmission electron micrograph* ×30 000

microstructural observations. The results may be compared in Table IV. The amounts of inhomogeneous shear which are represented by the stacking fault density and ratio of twin thicknesses, respectively, have been listed as an additional parameter for comparison since the fault density can be derived from X-ray diffraction observations and the twin thicknesses can be measured directly on electron micrographs. It ought to be realized that, apart from the limitations in accuracy of such observations, the martensite plates are never perfect: the inhomogeneous shear by slip will produce numerous random stacking faults on the main slip system as shown in Figures 6 and 7, and additional faults may be found on a different plane from the main slip system as shown in Figure 13; the inhomogeneous shear by twinning may produce twin lamellae on different systems within one martensite plate, as shown in Figure 14, and further secondary twinning and slip.[2] These are only trivial imperfections since the impingement of subsequent onto previously formed martensite plates and more complicated interactions during growth of the plates cause secondary slip and twinning and a wide variety of lattice defects of considerable complexity. These imperfections and defects impose an inherent limit on the accuracy of measurements and hence on

14 *Interior of a γ'_1-martensite plate with twins on different twin systems; Cu–15·1 at-% Sn* ×50 000

the applicability of the geometrical theories as far as crystallographic and mathematical refinements are concerned.

NUCLEATION

The nucleation of copper-based martensite phases is most probably based on the principal shear mechanism of the transformation mentioned in the first section of this paper and illustrated in Figure 5. To the author's knowledge, the nucleation process has not yet been observed directly, but there are several experimental indications and theoretical reasons why a (011) $[01\bar{1}]$ shear of the bcc lattice should initiate the transformation.

The decreasing stability of the β-phase with decreasing temperature, which has been correlated with the anomalies of the elastic anisotropy of the bcc lattice in copper alloys,[34] may first be considered. Firstly, the shear elastic coefficient $(C_{11}-C_{12})/2$ of β-brass (and probably of most other β-Cu alloys) has an anomalously low value ($0{\cdot}093\times10^{12}$ ergs/cm^3). Thus the lattice exerts little resistance to a (011) $[01\bar{1}]$ shear. Secondly, the temperature variation of the shear coefficient $(C_{11}-C_{12})/2$ is positive, i.e. the resistance to a (011) $[01\bar{1}]$ shear decreases with decreasing temperature. Hence both anomalies favour the martensitic transformation to be nucleated by (011) $[01\bar{1}]$ shears of the bcc lattice.

The dislocation reaction required to supply the initial amount of transformation shear has been discussed in terms of partial dislocations on the {011} planes of the bcc lattice.[35] If the dissociation

$$\frac{a}{2}[\bar{1}11] \rightarrow \frac{a}{8}[011] + \frac{a}{4}[\bar{2}11] + \frac{a}{8}[011]$$

is considered it is easily recognized that the first partial dislocation $\frac{a}{8}[011]$ gives rise to a fault in the bcc lattice which results in atom positions very similar to those of close-packed lattices. The Burgers vector of the transformation dislocation is more closely represented by $a/6$ [011]. The transformation is complete when additional dilation in [011] and contraction in [100] perfect the close packing within the planes. If this shear occurs on all successive planes of one slip system it produces an fcc structure, whereas occurring on every other plane it produces an hcp structure.

Further information may be derived from observations of the precipitation of the α-phase from β_1-phase in Cu–Zn alloys on aging in the two-phase field. It has been found that this precipitation process has characteristics similar to those of the bainite transformation in steels[36]: diffusion-controlled kinetics and martensite-like crystallographic features. An electron microscope study of the precipitation process[28] has shown that, in the very early stages, extremely thin quasi-two-dimensional lamellae are formed which are parallel to $\{011\}_{bcc}$. In later stages the precipitate exhibits the microstructural and crystallographic characteristics of martensite. Therefore the lamellae on $\{011\}_{bcc}$ are likely to be not only the nuclei for the precipitation process but, also, to indicate the most probable shape and orientation of nuclei of the martensitic transformation.

Finally the nucleation of single interface martensitic transformation induced by the straining of β-Cu–Zn single crystals[23] exhibits an orientation dependence such that a certain minimum deviation of the wire axis from the $<110>$ direction (at least 10–15° in the cited case[23]) is required for the single interface transformation to be nucleated without prior necking of the crystal.

These observations supplement each other well and it is suggested that the indicated mechanism is the most likely to occur.

Since it has been observed that Cu–Zn alloys exhibit two temperatures of martensite formation,[11] namely an upper one M_S where single thin thermoelastic plates form, and a lower one M_B where numerous parallelepiped-shape plates form in a 'burst', it is probable that the former martensite is nucleated at sites of high energy and suitable imperfection already present in the matrix and the latter is the result of an autocatalytic process, the strains round earlier plates serving to produce shears suitable for subsequent nucleation.

The different amount of supercooling required to initiate the martensite transformation in different alloys, which may be seen in Figures 1–4, and the temperature and composition dependence of the rate of isothermal martensite formation,[37] are not discussed in this context because thermodynamic considerations are not treated in this paper.

GROWTH

The internal structure of martensite plates in Cu-based alloys is, in general, uniform throughout any one plate, i.e. the inhomogeneous shear by faulting or twinning extends from one interface to the other. This is less so in Fe-based alloys, where martensite plates have been found to contain a twinned core and a slipped outer region up to the interface.[38] The difference between Cu- and Fe-based alloys in this respect is probably due to a difference in crystallographic properties of the habit plane. The habit planes of most martensite phases in copper alloys lie near $(122)_\beta$ and $(133)_\beta$, respectively, i.e. close to the great circle in stereographic projection which passes through the $(011)_\beta$ and $(1\bar{1}1)_\beta$ poles. This is shown in Figure 15 and it should be noted that [011] partial dislocations of almost pure screw character may be incorporated in the interface rendering it essentially glissile.[39] (From crystallographic theory[29] it can be deduced that small changes in axial ratio, e.g. by alloying, may produce habit planes exactly at 90° to the $[0\bar{1}1]$ pole, which can be perfectly glissile interfaces.) A glissile interphase boundary can move conservatively: all lattice points in the matrix lattice are

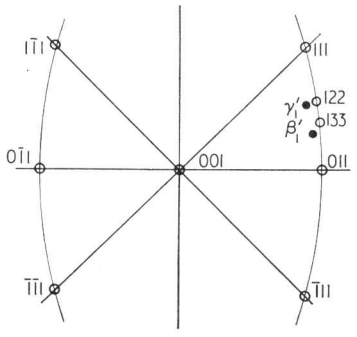

15 *Stereographic projection indicating the habit planes and possible Burgers vectors of interface dislocations in the bcc lattice for* β'_1 *and* γ'_1 *Cu–Al martensite*

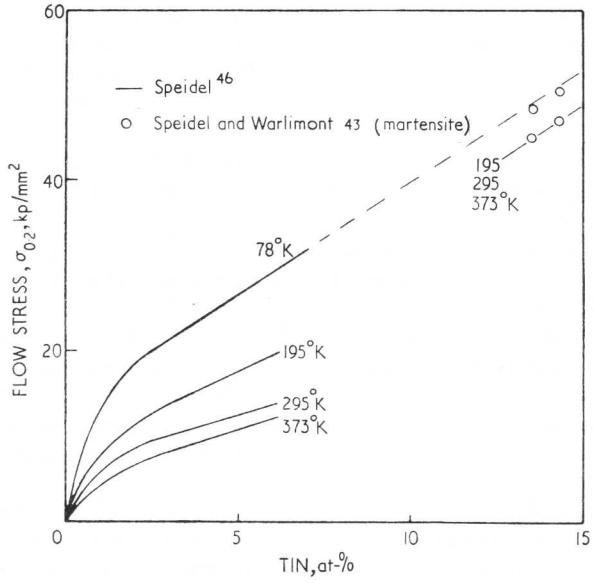

16 *Concentration dependence of the flow stress of the α solid solution[46] and β′$_1$-martensite[43] in Cu–Sn alloys*

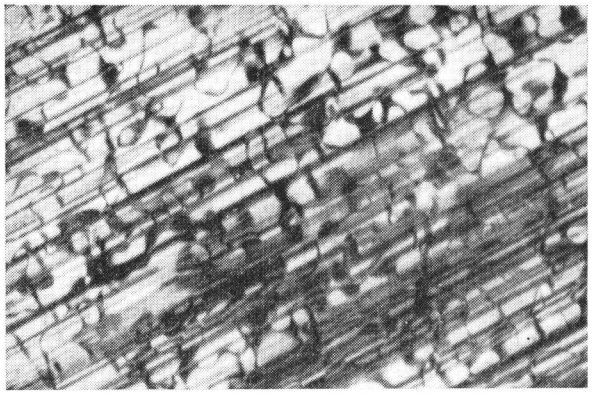

18 *Network of antiphase domain boundaries in β″$_1$-martensite in dark field contrast; Cu–12·6 at-%Ga–19·2 at-%Zn; transmission electron micrograph* ×50000

incorporated in the new lattice and vice versa, depending on the direction of motion.

This general property of martensite interfaces in copper alloys, whose degree of perfection will vary with each particular composition and transformation concerned, is in keeping with the microscopic observation of a rather uniform distribution of the inhomogeneous shear and with several other growth phenomena. Thus, the reversibility of the transformation, its low rate at low temperatures,[31,40] its small temperature hysteresis in certain alloys,[11] the occurrence of thermoelastic equilibrium (i.e. a case of balance of the chemical driving force against the coherency stresses due to the shape change),[41] the prevalence of plane interphase boundaries, and some recent electron microscopic observations of the interface structure by the author (unpublished), can only be accounted for by an essentially glissile interphase boundary.

MECHANICAL PROPERTIES

The metastable extension of the α solid solution of copper alloys to higher solute concentrations by the β-type martensitic phases is reflected by their mechanical properties.

For Cu–Sn alloys, where solid solution hardening is pronounced, the flow stress of β′$_1$-martensite has been shown[43] to lie on the extrapolation of the solid solution data[46] as illustrated in Figure 16. The apparent temperature independence of $\sigma_{0.2}$ between 195° and 373°K is probably due to compensation of the decreasing solid solution hardness by the increasing effect of atomic order with increasing temperature.[44] Young's modulus has also been measured for the stable phases in equilibrium[45] and for the β′$_1$-martensite phase.[43] These data are shown in Figure 17 and indicate that the values for the martensitic phase lie on the extension of the curve for the solid solution rather than following the composition dependence of the data for the intermetallic compounds.

Another dominant contribution to martensite strength in most copper alloys is due to ordering. Figure 18 shows a dark field image of the network of antiphase boundaries in a Cu–12·6 at-%Ga–19·2 at-%Zn alloy, characteristic of all ordered martensite phases discussed in this paper. In Cu–Al alloys, whose

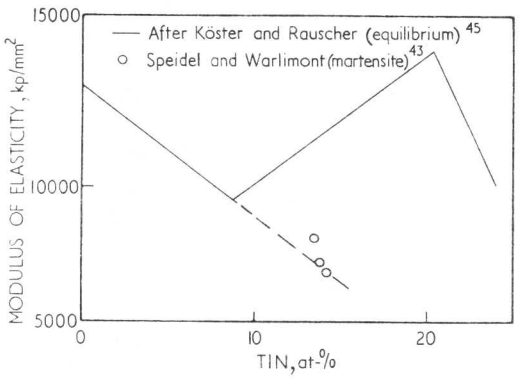

17 *Concentration dependence of Young's modulus of the α solid solution,[45] intermetallic phases,[45] and β′$_1$-martensite[43] in Cu–Sn alloys*

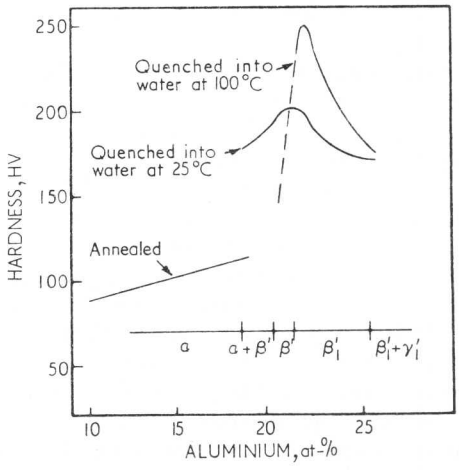

19 *Concentration dependence of the hardness of the α solid solution[42] and martensite phases[2] after quenching at different rates in Cu–Al alloys*

solid solution hardening is small, hardness measurements show distinctly the effect of ordering, as illustrated in Figure 19. The level of hardness in all martensitic specimens is higher than the extension of the curve of solid solution hardness. The effects of small variations in quenching rate, which alter the degree of order but do not influence the martensitic transformation, confirm that superlattice hardening contributes most to the apparent hardness of Cu–Al martensite. Quenching at a lower rate (into water at 100°C), which allows more complete ordering to occur than quenching at a higher rate (into water at 25°C) produces a higher hardness. The difference between the low hardness value at 20·7 at-% Al and the maximum value at about 22 at-% Al indicates the difference in hardness between the disordered martensite β' and the ordered martensite β'_1. (It is difficult to assess the remaining hardness increment of β' over the hardness of the α solid solution: point defects introduced by quenching and the effect of the stacking faults caused by the inhomogeneous shear may both contribute.) The variation of hardness within the composition range of ordered β'_1 reflects the influence of deviation from the ideal composition of the ordered phase.

Thus, the effects of solid solution hardening and of superlattice hardening appear to supersede the effect of work hardening (due to the martensitic inhomogeneous shear) in the martensite phases of these alloys.

CONCLUSIONS

The recent progress in experimental techniques, particularly in electron microscopy, has served to analyse the structure of martensite phases in copper alloys to a greater extent and accuracy than previously possible. The interrelations of the martensite phases in different alloy systems could be recognized, the observed phase changes correlated with the phase equilibria and the rules for the stability of electron compounds, and the modes of inhomogeneous shear analysed.

These observations have also served to reveal certain crystallographic features of the nucleation and growth phenomena, although the exact mechanism of transition of a quasi-two-dimensional nucleus into a plate and the atom motion during further growth are yet to be determined in detail. Measurements of mechanical properties have elucidated the effects of the prevailing sources of hardening in these martensite phases.

Several aspects of the martensite transformation in copper alloys, and of related phenomena such as the thermodynamics of nucleation and growth, the bainitic transformation, the precipitation process during tempering, the massive type transformation, and the equivalent martensite transformations in silver and gold alloys have not been discussed. But it is surmised that the present survey may serve to clarify some of the pertinent crystallographic features.

ACKNOWLEDGMENTS

I am grateful to Dr T. B. Massalski and Professor C. M. Wayman and their co-workers for making available some of their recent unpublished results and to Dipl.-Ing. L. Delaey and Dr M. Speidel for agreeing to the incorporation in this paper of some micrographs and results of current work.

REFERENCES

1. G. V. KURDYUMOV: *J. Techn. Phys. USSR*, 1948, **18,** 999–1025.
2. P. R. SWANN and H. WARLIMONT: *Acta Met.*, 1963, **11,** 511–527.
3. Z. NISHIYAMA and S. KAJIWARA: *Jap. J. Appl. Phys.*, 1963, **2,** 478–486.
4. H. WARLIMONT and M. WILKENS: *Z. Metallk.*, 1964, **55,** 382–387.
5. H. WARLIMONT and D. HÄRTER: to be published.
6. L. DELAEY and H. WARLIMONT: *Phys. Stat. Sol.* 1965, **4,** *K*121.
7. T. SABURI and C. M. WAYMAN: AIME Fall Meeting, 1964.
8. B. A. BILBY and J. W. CHRISTIAN: *JISI*, 1961, **197,** 122–131.
9. W. G. BURGERS: *Physica*, 1934, **1,** 561–586.
10. M. S. PATERSON: *J. Appl. Phys.*, 1952, **23,** 805–811.
11. H. POPS and T. B. MASSALSKI: 1964 Report of the Mellon Institute, USA, Pittsburgh.
12. T. B. MASSALSKI and H. W. KING: *Prog. Mat. Science*, 1961, **10,** 1–78.
13. K. SCHUBERT *et al.*: *Z. Metallk.*, 1955, **46,** 692–715.
14. M. WILKENS and K. SCHUBERT: *Z. Metallk.*, 1957, **48,** 550–557.
15. K. SCHUBERT: 'Kristallstrukturen zweikomponentiger Phasen'; 1964, Berlin-Göttingen-Heidelberg, Springer-Verlag.
16. J. WEGST and K. SCHUBERT: *Z. Metallk.*, 1958, **49,** 533–544.
17. D. HULL: *Phil. Mag.*, 1962, **7,** 537–550.
18. N. AGEEV and G. V. KURDYUMOV: *Metallurg*, 1932, **7,** 3–21.
19. A. B. GRENINGER: *Trans. AIME*, 1939, **133,** 204–221.
20. G. V. KURDYUMOV *et al.*: *Zhur. Tekhn. Fiz.. USSR*, 1938, **8,** 1959.
21. J. V. ISAITCHEV: *ibid.*: 1947, **17,** 829–834.
22. H. KNÖDLER: *Acta Cryst.*, 1957, **10,** 86–87.
23. E. HORNBOGEN *et al.*: *Z. Metallk.*, 1957, **48,** 379–384.
24. D. B. MASON and R. K. GOVILA: *ibid.*: 1963, **54,** 293–295.
25. M. S. WECHSLER *et al.*: *Trans. AIME*, 1953, **197,** 1503–1515.
26. J. S. BOWLES and J. K. MACKENZIE: *Acta Met.*, 1954, **2,** 129–137.
27. J. K. MACKENZIE and J. S. BOWLES: *ibid.*, 138–147.
28. E. HORNBOGEN and H. WARLIMONT: unpublished work.
29. J. K. MACKENZIE and J. S. BOWLES: *Acta Met.*, 1957, **5,** 137–149.
30. A. B. GRENINGER and V. G. MOORADIAN: *Trans. AIME*, 1938, **128,** 337–368.
31. A. L. BELINKII: *Metalloved. Term. Obra. Met.*, 1961, **3,** 25–27.
32. G. V. KURDYUMOV: *Byull. AN USSR, Ser. Khim.*, 1936, **2,** 271.
33. T. B. MASSALSKI and C. S. BARRETT: *Trans. AIME*, 1957, **209,** 455–461.
34. C. ZENER: *Phys. Rev.*, 1947, **71,** 846–851.
35. J. B. COHEN *et al.*: *Acta Met.*, 1962, **10,** 894–895.
36. R. D. GARWOOD: *J. Inst. Metals*, 1954–55, **83,** 64–68.
37. G. V. KURDYUMOV and L. G. KHANDROS: *J. Techn. Phys. USSR*, 1949, **19,** 761–768.
38. H. WARLIMONT: Proc. 5th Int. Congr. Electron Microscopy, 1962, HH–6, New York, Academic Press.
39. J. W. CHRISTIAN: in 'Decomposition of austenite by diffusional processes', Symposium Proceedings, 371–386; 1962, New York–London, Interscience.
40. G. V. KURDYUMOV and O. P. MAKSIMOVA: *Problems of metallography and metal physics*, 1948, **61,** 64–97.
41. G. V. KURDYUMOV and L. G. KHANDROS: *Doklady AN SSSR*, 1949, **66,** 211–214.
42. 'Metals Handbook' 8 edn.; 1961, Novelty, Ohio, USA, ASM.
43. M. SPEIDEL and H. WARLIMONT: unpublished work.
44. N. BROWN: in 'Mechanical properties of intermetallic compounds', Symposium Proceedings, 177–191; 1960, New York–London, Wiley
45. W. KÖSTER and W. RAUSCHER: *Z. Metallk.*, 1948, **39,** 111–120.
46. M. SPEIDEL: D.Sc. thesis, 1964, T.H. Stuttgart.
47. G. KUNZE: *Z. Metallk.*, 1962, **53,** 329–341, 396–402, 565–576.
48. L. DELÉHOUZÉ: Ph.D. thesis, Leuven University, to be published.

Discussion 3

Chairman: Professor R. W. K. Honeycombe (University of Sheffield)

Mr H. Warlimont (Max-Planck-Institut für Metallforschung), in presenting his paper, said that the β_1''-martensite observed in copper–zinc–gallium alloys was recently obtained also in copper–aluminium alloys[1] which had previously been quite thoroughly investigated (Figure *A*). If a specimen was transformed at 30 kb, i.e. heated under this pressure, quenched under pressure, and the pressure released and the thin foils were looked at, the banded structure was seen and the diffraction patterns showed the same crystal structure.

Dr F. G. Wilson (The United Steel Cos. Ltd) said that at Swinden Laboratories work was currently being carried out on maraging steels. As part of this programme they had been examining the shear transformations observed during cooling pre-polished specimens of an Fe–18%Ni alloy.

While basically confirming the conclusions reached by Professor Owen regarding the morphology of the massive martensite, careful examination of the fully transformed alloy revealed isolated plates which showed internal twinning.

Figure *B* showed a transformed region examined under polarized light with a Nomarski interference attachment. Although the general structure was typical of massive martensite, the region illustrated revealed what appeared to be internally twinned plates.

A polished and etched structure of this alloy (Figure *C*) showed the typical massive strutcure. The internal plate boundaries were well defined as were the original austenite grain boundaries. Although thin-foil examination revealed only plates with a high dislocation density (Figure *D*) the absence of twinned plates was not surprising since the number of twinned plates was low at the nickel content examined.

However, the work, which was still in progress, suggested that there might not be a sharp transition from massive martensite to twinned martensite at about 30%Ni, although a full investigation over a range of compositions had not yet been carried out. However, by analogy with plain carbon steels, it would not be surprising if the transition from massive martensite to twinned martensite were gradual, taking place over a wide range of nickel contents.

Dr G. P. Miller (International Nickel Ltd) said that his company had done similar work on these 18%Ni maraging steels and found a similar dislocated internal structure. If the nickel content was increased to 23% a twinned acicular martensite was obtained. This was with the normal alloying additions of the 18%Ni maraging steel, 7%Co, 5%Mo, and 0·4%Ti.

Professor H. W. Paxton (Carnegie Institute of Technology) said, on the same topic, with the maraging steels he had mentioned earlier, with 25%Ni, observations showed that there was some twinning but most of the plates appeared to be formed by slip.

Mr F. B. Pickering (The United Steel Cos. Ltd) said that in the slide shown by Professor Owen of Fe–23%Ni, which showed the surface relief effects after transformation, there appeared to be some striations across the plates. Were these indicative of twins?, because Professor Wayman in Figure 16 of his paper showed such striations in a 33%Ni alloy and indicated that they were twins.

Dr Miller suggested that he observed a twinned martensite in 23%Ni–7%Co–5%Mo alloy. The presence of the alloying elements appeared therefore to decrease the nickel content at which twinned martensite was observed. Was this due to some carbon in the alloy or did Dr Miller think that a depression of the M_s temperature brought about by the 5%Mo helped to form twinned martensite? Did the hardness of the martensite as well as the M_s temperature affect the formation of twins?

Professor W. S. Owen (University of Liverpool) said that he had no information about the origin of the markings on the plates in the transformed Fe–23%Ni.

Dr Miller, in reply to Mr Pickering, said that while the alloys examined by them contained more carbon (approximately 0·02%) than the very pure materials mentioned by Professor Owen, he thought that the lowering of the M_s temperature by the molybdenum addition was the major factor in the change to twinned martensite. In fact the 23%Ni, 7%Co, 5%Mo alloy had approximately the same M_s temperature as an Fe–28·5%Ni alloy.

There was no significant difference between the hardness of the twinned and untwinned martensites in these alloys.

Mr J. A. Klostermann (Stichting voor Fundamenteel Onderzoek der Materie) said he thought the markings were not twins; they were perhaps deformation bands that also formed in surface martensite.

Commenting on the paper by Owen and Wilson, he said that Professor Owen had stated that the geometric arrangement of shear plates which could produce the shape of massive constituents observed was sometimes difficult to visualize. He thought that they were related in the same way as angle profile martensite and surface martensite, having the same crystallographic boundaries. He was not convinced that there was no relation between the orientation of the equiaxed α, respectively 'massivemartensite' structures, and the matrix in iron–nickel alloys.

He reminded those present of the work of Mehl[2] who found that the Widmanstätten structure in pure iron had a Kurdjumov and Sachs orientation relationship.

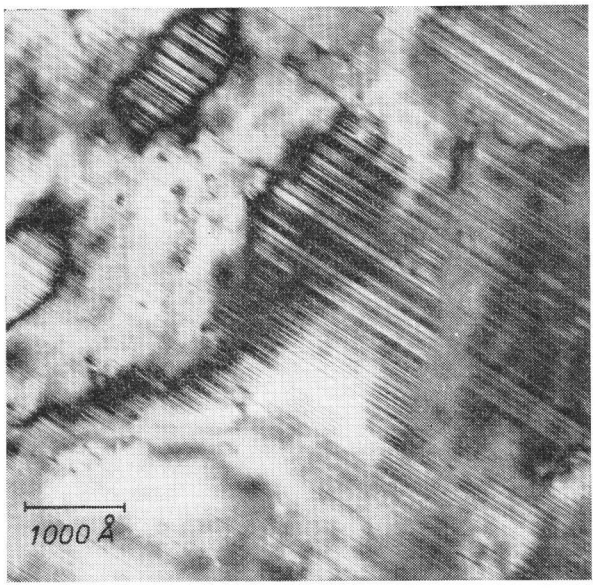

A *β_1''-martensite formed in a copper 25·0 at-% aluminium alloy at 30 kb pressure on quenching from 600°C to room temperature*

Dr T. Boniszewski (BWRA) said that, to get the record straight, he must insist that one could see substructure within the blocks of what Professor Owen called massive martensite. It was true that this substructure was difficult to reveal on metallographic sections, but the success lay in departing from nital etching and trying more exotic reagents. At least the substructure could be revealed within the blocks in 18%Ni–Co–Mo steel after etching in a reagent comprising 10 g $FeCl_3$, 100 ml conc. HCl, and 100 ml alcohol. It was shown in Figures *E* and *F* of Discussion 1 (p 22).

In reply to the Chairman's questions he said that he did not imply that the substructure within the blocks was equivalent to twinning. This substructure represented the elongated (acicular) crystals aligned in sheaves. Since, according to Wayman's paper, surface observations were suspect, it was worth the effort to reveal metallographically whether or not various blocky structures, referred to as massive, were composed of finer units.

Dr P. M. Kelly (University of Leeds) referred to Professor Owen's comment that the change from the so-called 'massive' martensite to twinned martensite occurred over a very narrow range of composition in carbon-free iron–nickel alloys and

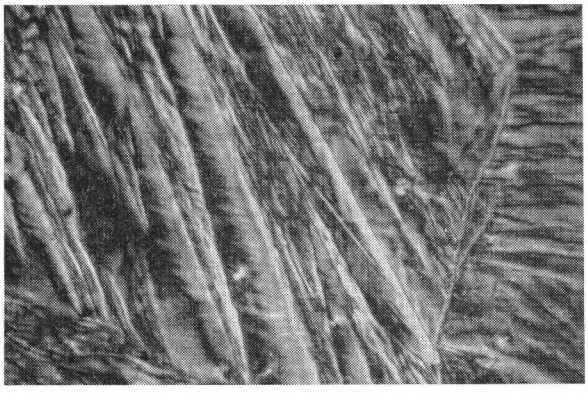

B *Fe–18%Ni alloy, pre-polished and transformed in vacuum to massive martensite* ×750

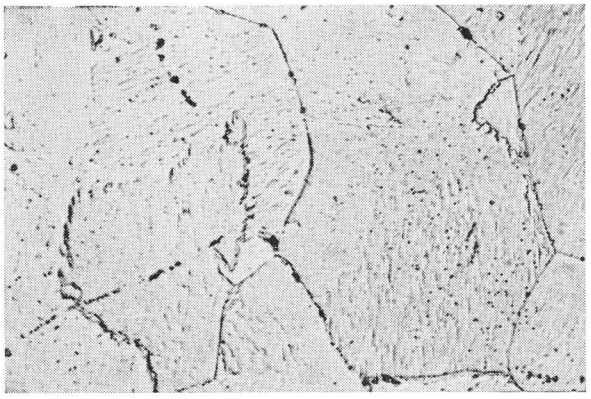

C *Fe–18% Ni alloy, transformed to massive martensite; polished and etched* ×750

pointed out that in the presence of carbon this composition range broadened considerably.

Professor Owen said that he agreed and the matter had been discussed at great length last year in California.

Professor C. M. Wayman (University of Illinois) said that the findings of Mr Patterson in his laboratory were in good agreement with those of Professor Owen and colleagues concerning the transition from untwinned to twinned martensite in iron–nickel alloys. Professor Owen had said it was 28·5 wt-%Ni whereas Professor Wayman reported it to be between 28 and 29%.

He then discussed aspects of the massive transformation in Cu–Ga alloys (β to ζ) where masses of ζ crystals resulted in no change of shape of the transformed region. He stated that the mechanisms of the massive and martensitic transformations appeared to be distinct and separable, according to the work of his former student Mr Saburi. At a certain quenching rate both the martensite and massive ζ could be formed in the same specimen. The massive phase stopped growing abruptly, and at a lower temperature the martensite formed in the untransformed

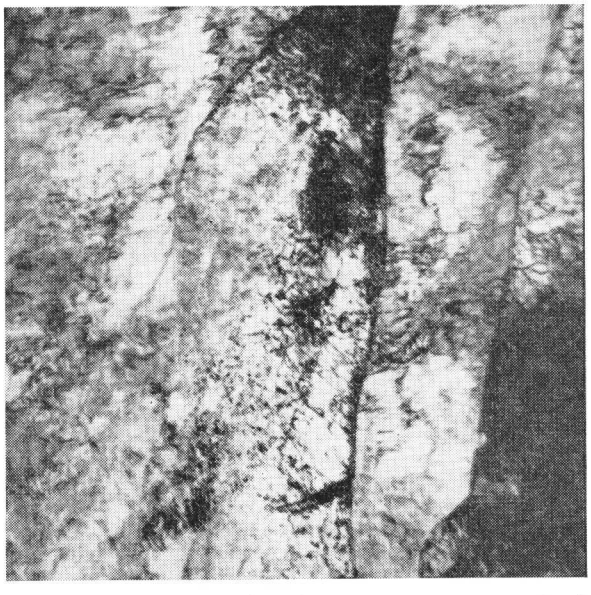

D *Fe–18%Ni alloy, transformed to massive martensite; thin-foil electron micrograph* ×60000

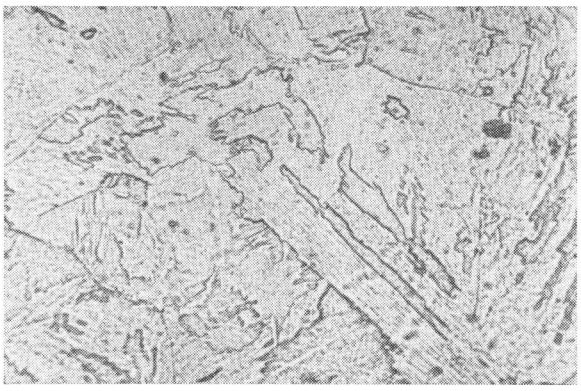

E *Massive martensite in 6%Cr–0·045%C steel quenched at 1000 deg C/s; transformation start temperature 546°C*

parent. The boundary delineating the stopping point of massive crystals was abrupt and sharp, resembling a high-angle grain boundary. The martensite plates in the untransformed region stopped at this boundary. There was no blending of the two structures (massive ζ and martensite) at all, as had been suggested.

He noted that the martensitic transformation in some β-copper–aluminium alloys was apparently a bcc→fcc transformation, although the fcc martensite by and large lost its identity because of the profuse faulting (second shear of the crystallographic theories). Diffraction patterns were complicated by the faults. If the transformation was indeed basically a bcc→fcc transformation, then the usual Bain correspondence (knowing the lattice parameters of the two phases) suggested that one of the principal strains was 1·25 (i.e. a 25% distortion). This was to be contrasted with steels, usually considered to be a large strain transformation, where the largest distortion was about 20%.

Dr C. Bodsworth (Richard Thomas & Baldwins Ltd) said that he wished to report some work which he did on the massive martensite reaction with Dr T. M. F. Ronald at Liverpool University. A series of steels, containing 6·25%Cr and varying

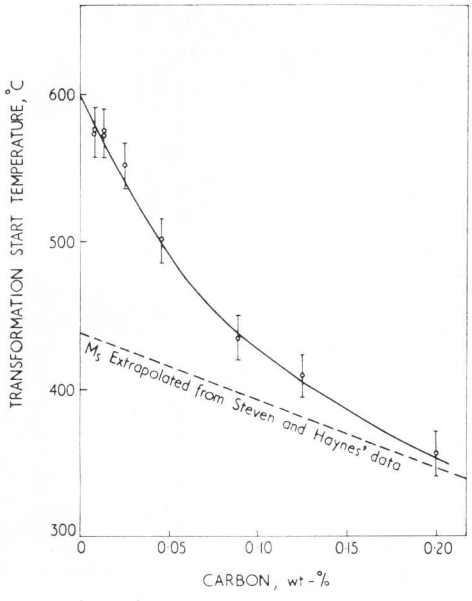

F *Variation of transformation start temperature with carbon content for Fe–6·25%Cr steel; cooling rate 7000 degC/s*

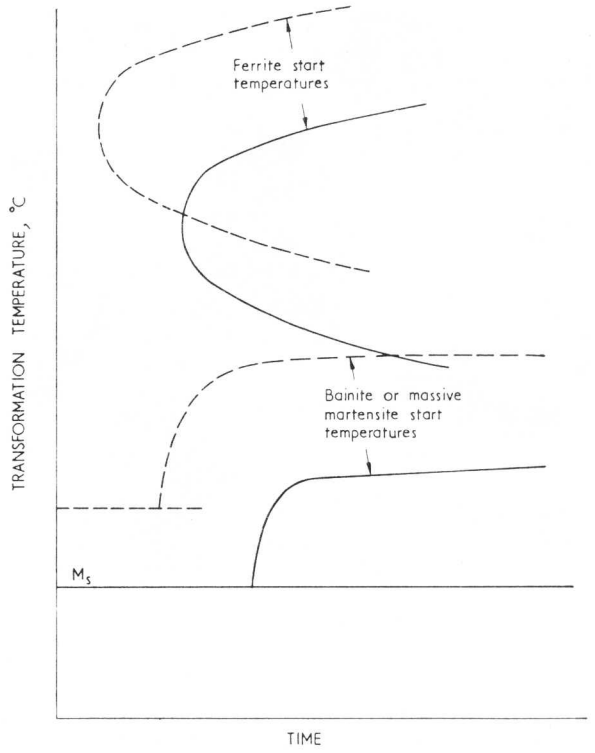

G *Schematic TTT diagram for 6%Cr steel containing 0·2%C (solid lines) and 0·05%C (dotted lines)*

amounts of carbon, were austenitized at 1050°C and the transformation behaviour was studied during quenching in the high-speed quenching apparatus used by Mr Wilson to obtain the results quoted in his paper.

With $\geqslant$0·2%C normal bainitic or martensitic structures were obtained. At lower carbon contents (0·008–0·14%) the product was equiaxed or massive ferrite on cooling at 100–1000 degC/s or, with cooling rates in the range 1500–7000 degC/s, massive martensite was found. For a constant carbon content, the transformation start temperature was dependent on cooling rate in the upper range, but independent of cooling rate in the lower temperature range. Similar behaviour had been reported by Owen and Gilbert[3] for a 6·3%Cr, 0·008%C steel.

Pre-polished specimens transformed at the faster quenching rates showed surface shears but, when the surface was removed by etching, no correlation was found with the underlying structure. Deep etching of the massive blocks of transformed material revealed a substructure comprising rows of parallel plates (Figure *E*), the preferential attack probably being caused by carbon diffusion to the plate interfaces. Microscopic and electrical resistivity measurements indicated that little or no carbide had separated during the quench.

Figure *F* illustrated the relation between the transformation start temperature and the carbon content for the massive martensite reaction. The broken line represented the M_s temperatures calculated from Steven and Haynes[4] equation (2). At a carbon content of 0·2% the measured M_s agreed, within the limits of experimental error, with the calculated temperature. At lower carbon contents the measured start temperature was above the calculated M_s, the difference increasing with decreasing carbon content. At 0·008%C (the lowest carbon content examined) the transformation started at 565°C, whereas the interpolated M_s temperature was 440°C for a chromium steel of the same composition quenched at a higher rate to form acicular martensite.[3]

A possible interpretation of the transformation behaviour of these steels was shown in Figure *G*. The start temperature of the

equiaxed ferrite transformation was dependent on cooling rate, and was probably represented by a *C* curve. The start temperature of the massive martensite reaction was constant, but with a sufficiently drastic quench it had been reported[5] that the reaction could be suppressed and normal martensitic structures obtained. This suggested that the *C* curve for the massive martensite reaction was flat-topped. No TTT curves for very low-carbon, 6%Cr alloys had been found in a literature search, but with small additions of molybdenum or other alloys the TTT diagram was often of the form shown in Figure *C*, where the low-temperature, flat-topped *C* curve was the bainitic reaction. In the experiments reported, a bainitic product was obtained at moderate quenching rates with the 0·2%C steel, the bainite start temperature being about 20–50 degC above the M_S temperature. It was possible, therefore, that in the steels examined the massive martensite reaction was a type of bainite reaction in which there was insufficient driving force for carbide separation during transformation, the bainitic *C* curve changing to the massive martensite *C* curve as it moved to higher temperatures and shorter times with decreasing carbon content.

Professor Owen said he would like to have Dr Kaufman's views about $\Delta F^{\alpha\rightarrow\gamma}$ in the iron alloys. Did he think it was about 300 cal/mole? He had reasons to doubt this figure and thought perhaps it was too low.

Dr L. Kaufman (ManLabs Inc.) said that, to start with, he did not think that ΔF at M_S had to be constant. Historically this idea arose in Zener's paper[6] and in the paper by Cohen *et al.*[7] In both cases the 'best' calculations possible at that time were performed and when the numbers came out to be 300 cal/mole independent of composition the implication of a constant ΔF was seized upon as being absolute. In his view there was no reason why ΔF at M_S should be a constant and if one considered all of the compositional and temperature dependent factors such as elastic constants, crystallography, and nucleation there was no reason to expect that ΔF at M_S was a constant. In fact some ten years ago he and Morris Cohen had shown that in the iron–nickel system ΔF at M_S varied with temperature[8]. Similar results were apparent for the iron–ruthenium system. Surprisingly, Parr and co-workers[9–13] had criticized the 'athermal theory' of martensite formation. They alleged that the latter theory *required* a constant driving force, thus ignoring the variable ΔF at M_S[8,14] computations presented in the iron–nickel case. Parr's position seemed to have changed frequently[9–13,15,16] during the past twenty years. His most recent[11] was that fcc iron should transform to bcc at the Curie point of bcc iron. This would appear to disregard the known thermodynamic properties of iron.[17]

During the past twenty years, thermodynamic information on the properties of bcc and fcc iron and its solid solutions had improved and would continue to improve. As a consequence, calculations of ΔF at M_S and A_S should become more accurate. Present results should be in error by no more than 20%.

The measurements done by Scheil and his co-workers of the enthalpy change attending the transformation in iron–nickel alloys[18,19] compared favourably with computations, considering the regular solution approximation. In some cases there were discrepancies, and in the iron–nickel system he thought the most recent measurements, those of Scheil and Seftig,[19] produced lower values of ΔF at M_S than his calculation. The discrepancy might have been as much as 70 cal, his calculation being about 300 in an Fe–30%Ni alloy and Scheil's value being 230 cal/mole.

There had not been any measurement of the enthalpy change in pure iron–carbon alloys. In other systems where the supercooling was larger there might be larger driving forces.[20] In any case, 300 cal was not claimed as a magic number.

The other support he and his colleagues had for their thermodynamics as regards direct observations were the high-pressure measurements which had now been done on a number of systems – iron–silicon,[21] iron–aluminium,[22] iron–vanadium,[23] chromium,[22,24] carbon,[22,25,26] nickel[22] – and there again, the pressure shifts of the M_S temperature, pressure shifts of the iron–carbon eutectoid and the phase boundaries were materially in keeping with the calculations. In summary, therefore, he would say that he did not believe ΔF at M_S need be a constant. He thought the calculations were reliable to within 15–20%, although it would not shock him if they were out by 25%.

This was something that would improve as time went on. Moreover in certain instances it was possible that physical reasons could be deduced for the larger driving force required.

Professor J. Gordon Parr (University of Windsor, Ontario) wrote in reply that he was glad that Dr Kaufman realized that his views about martensite had changed during the past twenty years: in the light of a growing body of information, he would not wish to be guilty of a stubborn inflexibility.

However, he had never suggested, as Kaufman imputed, that fcc iron should transform to bcc at the Curie point of iron. The comment they made[11] was simply: 'This temperature (750°C) is sufficiently close to the quoted Curie temperature for iron (770°C) to remind one of Zener's contention that fcc iron should transform to the bcc structure at the Curie temperature. However, we are not certain of the precise value of the Curie temperature for high-purity iron; and we are more intrigued by the approximate extrapolation of M_S at low carbon values to zero carbon, for it appears that M_S for pure iron (with substantially zero carbon) would lie between 800° and 900°C.'

It appeared that Dr Kaufman did not really appreciate the main point of that paper, which was that, accepting for the moment the thermodynamic approach, the approximate figure of 300 cal/mole for ΔF was associated with M_S in iron of 540°C. However, M_S in pure iron was *not* 540°C but above 750°C. A qualitative assessment of these figures implied that ΔF of pure iron, then was about 100 cal/mole.

The sharp change in the behaviour of iron as a function of an initial carbon addition, and manifested by M_S, was vitally important; and more attention might be paid to this than to an interpretation of an opinion that they had not, in fact, expressed.

Dr A. R. Entwisle (University of Sheffield) wished to reinforce the view that the constant driving force at M_S was not sacred. He thought one saw this immediately one looked at alloys showing substantial isothermal transformation. In some iron–nickel–manganese alloys there was a range of isothermal transformation between −50° and −120°C, but if one plunged the specimen into liquid nitrogen, one could audibly hear it burst, so clearly here was an alloy in which one did not know what the M_S was. If one took the burst as the M_S, it was around −150°C, but if one took the first trace of transformation in the specimen one might say that the M_S was −50°C. There was clear ambiguity here about what was meant by M_S. He agreed that the idea of a constant driving force at M_S was one that must be abandoned.

Dr A. G. Crocker (Battersea College of Technology) commented on the paper by Dr Warlimont. First, he said there appeared to be considerable confusion about the structure of the γ_1' phase. Thus in the text of Dr Warlimont's paper the structure was referred to as twinned-hexagonal whereas in Table II it was labelled orthorhombic. Indeed using the quoted orthorhombic lattice parameters it did not appear possible to refer the structure to a hexagonal basis. Secondly he did not think that $\{10\bar{1}1\}$ twinning occurred in preference to $\{10\bar{1}2\}$ twinning because of a superlattice effect. The inhomogeneous shear mode giving rise to a martensite product twinned on $\{10\bar{1}1\}$ was not the same as the reported deformation twinning mode with this composition plane,[27] the shear directions for the two cases being quite different. The reason for the appearance of the $\{10\bar{1}1\}$ twins seemed to be that in martensite both twin components were formed directly from the parent phase and no deformation twinning of the product was involved.[28] This process should perhaps be called *transformation twinning* rather than deformation twinning. Finally, in Table IV, the ratio of the twin thicknesses in the copper–aluminium and copper–tin martensites were quite different, there being about twice as much twinned material in the former.

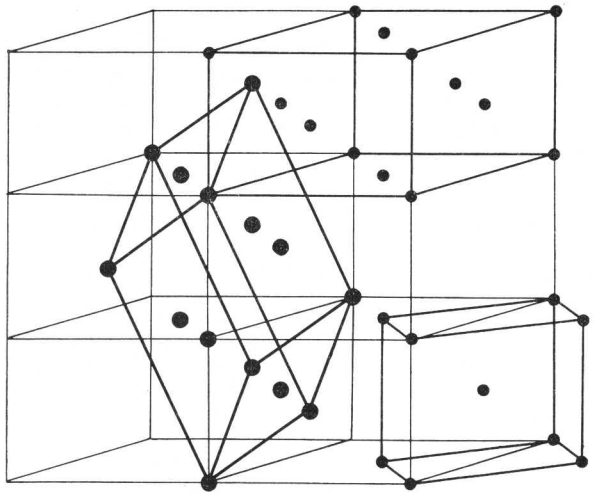

H *Three different cells which can be used to describe a bcc structure*

This seemed strange as the lattice parameters of the two alloys were similar.

Returning to Professor Wayman's point about the Bain correspondence being the only satisfactory means of relating the fcc and bcc structures, he showed a slide illustrating the second best correspondence between these structures (Figure *H*). It showed three different cells each of which could be used to describe a bcc structure. These were outlined in a group of six tetragonal cells of axial ratio $2^{-\frac{1}{2}}$. The cells were:

(i) the usual bcc cell at the bottom right
(ii) a face-centred tetragonal cell of axial ratio $2^{-\frac{1}{2}}$ at the top right,
(iii) a face-centred triclinic cell indicated in bold lines.

Referred to these cells the Bain correspondence related cell (ii) to an fcc cell; the next best correspondence related cell (iii) to an fcc cell. This second correspondence clearly had much lower symmetry than the Bain correspondence and thus, if used with the crystallographic theories, would give a host of different predictions. However, the strains involved were also much larger and it seemed most unlikely that this correspondence could operate in practice. It was thus necessary to rely on the Bain correspondence when considering transformations in steels.

Dr Warlimont said that he too was worried about the confusion on the structures. There were two ways in which the structures could be looked at. One way was as he liked to do it at present, where all these results were rather new, to emphasize the way that the transformation went, namely from bcc to fcc in one case, and bcc to hch in the other case, whereas, strictly crystallographically speaking, one had much more complicated and larger unit cells. He had used a certain kind of stenography in the tables and realized now, since he had been in Scarborough, that much of this could be misinterpreted, so he would try in the future to find a better way of describing these structures, particularly because it had been found by his department recently that for the copper–zinc–gallium alloy system which had been investigated quite intensively, there was a continuous change in the orthorhombic distortion with composition of the martensite lattices. The dependence was linear if the composition was taken in at-%. Perhaps, therefore, the last word had not been said about how to describe these structures.

He would also mention that there was still controversy about the question whether the ordered arrays of stacking faults had a chemical reason or whether they arose only from the mode of transformation.

He would not like to comment further on the twinning mode. This had to be looked into a little more. Perhaps he had not been quite aware of the implications mentioned by Dr Crocker.

About the twin ratio discrepancy, he stated that his measurements and those of a student of his who had done the main work on copper–tin had not coincided. He had not yet looked at the values in terms of the phenomenological theory. What Dr Crocker had said was quite right; a discrepancy should not exist if the lattice parameters were similar; the actual value probably lay somewhat above the theoretical value and this was expected to be true also for copper–tin.

The Chairman asked whether Dr Warlimont had paid any attention to what was basically a simpler case of the fcc going to the cph as one got in the supersaturated α solid solutions with copper–germanium, copper–silicon, etc.

Dr Warlimont replied that he had not done any work on this problem.

The Chairman said that this basically should be structurally simpler. In fact, it looked simpler.

Dr Warlimont said that it did not appear to be very much simpler. In fact, all those who were working with cobalt alloys were rather distressed about the variety of effects they observed in the electron microscope. It was very difficult to distinguish between the effects of deformation which accompanied the transformation and the transformation itself, and from his recent observations on the effects of thinning and further preparation of foils he was also very critical about any stacking fault structures in these low stacking fault energy materials. It had been noticed that they were extremely sensitive to mechanical deformation in the thinned condition and that many stacking faults might be introduced in addition to those formed in the bulk during the transformation.

The Chairman agreed but said that one could get a transformation by aging in an isothermal process and in this case the structure was fairly reliable.

Dr Warlimont said that he had not done any work on this transformation.

Professor D. Hull (University of Liverpool) asked Dr Warlimont and Professor Wayman what their views were of the massive transformations in copper alloys. Did they in fact see this transformation? Could they see anything in the substructures? He also asked Professor Wayman about the distinct break he had reported in the transformation behaviour in copper–gallium alloys. Did he observe it because of a change in the surface structure or in studies of sectioned specimens?

Professor Wayman replied that the surfaces had been looked at, but the distinct break was determined by means of a well defined and 'non-diffuse' boundary (transmission electron microscopy) between the massive crystals and the martensite plates.

Professor Hull asked if there was a change in surface structure with the massive transformation. Was there a surface tilt with the massive transformation?

Professor Wayman said that the massively formed ζ-phase in the copper–gallium system did not result in a crystallographic shape change as was usually observed in martensitic transformations. There were, however, slip markings which could be seen in unetched (massively transformed) specimens. These were parallel to the straight boundaries of the massive ζ crystals.

The transmission microscopy specimens of the massively formed ζ-phase showed numerous internal stacking faults of variable density. These were parallel to the straight boundaries and presumably to the surface slip markings. The fault density was very non-uniform within a given ζ crystal, in contrast to the faults in martensite plates (Cu–Ga) which were due to the 'second shear' of the crystallographic theories.